

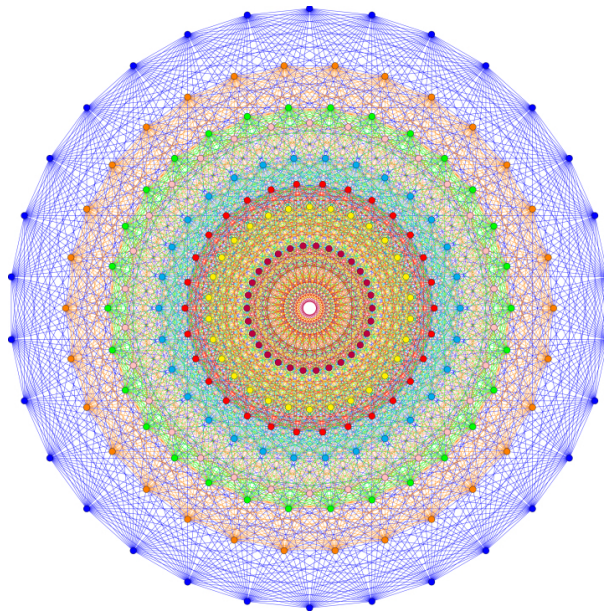
UNIVERSITY OF AMSTERDAM  
INSTITUTE FOR THEORETICAL PHYSICS

---

$E_8$  Symmetry Structures  
in the Ising model

---

*A master's thesis by*  
Abel Jansma



*Supervisor*

prof. dr. Bernard NIENHUIS

*Second examiner*

prof. dr. C.J.M. SCHOUTENS



August 6, 2018

---

*Cercavo la grande bellezza, ma non l'ho trovata.*

Jep Gambardella

## Abstract

This thesis presents an overview of the ways in which the Lie algebra/group  $E_8$  appears in different descriptions of a  $\sigma^z$  perturbed critical 1D transverse Ising model. We first review work by Alexander Zamolodchikov who established the link by looking at the integrals of motion and the conserved charge bootstrap equations. We then construct some field theories that contain  $E_8$  as an algebra, group, or lattice and lead us to the conformal field theory associated to the critical Ising model. After this, our attention turns towards discrete lattice models. The so-called dilute  $A_3$  model contains the  $E_8$  particles in its scattering matrix, and we have a description of these particles in terms of its thermodynamic Bethe Ansatz. Our goal is to express these Bethe Ansatz solutions in terms of simple fermion occupation quantum numbers, but we first practice this translation in the simpler case of the critical  $q$ -state Potts model. After this, we extend the mapping to the case of the dilute  $A_3$  model and provide a way to express its  $E_8$  particles in terms of free fermions. While we indeed get a consistent free fermion description, we don't find enough solutions to the Bethe Ansatz equations to make a full identification between the  $E_8$  particles and free fermions.

---

## Dankwoord

*Writing a theoretical physics master's thesis is a solitary occupation. Therefore, one cannot do it alone.* - Evita Verheijden, 2018 [31]

Deze scriptie is het resultaat van vele jaren praten, rekenen, schrijven, lachen, en wanhopen met de mensen om mij heen die onderweg hebben geholpen.

Allereerst wil ik mijn begeleider bedanken: professor Bernard Nienhuis. Niet alleen voor de uitstekende, gulle, en hartelijke begeleiding bij dit onderzoek, maar ook voor de vele dwaalsporen in onze wekelijkse gesprekken die mij altijd inspirerende nieuwe dingen lieten zien. Het was een eer om zo'n bijzondere tak van de mathematische en statistische fysica te leren van iemand die zo dicht bij de oorsprong ervan staat. Ook zijn visuele manier van denken en redeneren bewonder ik erg en hoop ik enigszins mijn eigen gemaakt te hebben. Mijn aantekeningen staan in ieder geval al vol met pijltjes en lussen. Daarnaast wil ik ook mijn tweede corrector Kareljan Schoutens bedanken voor zijn moeite, en interesse in dit onderzoek.

Verder wil natuurlijk ook mijn hele familie bedanken voor hun onuitputtelijke steun en interesse in een tumultueus jaar. In het bijzonder mijn vader Rein. Voor zijn vragen, ideeën, en liefde. Voor de wiskunde op het tafelkleed in Café-Restaurant Amsterdam. Ook Oekie's verhalen over wiskunde, puzzels, en dingen van Arie hebben er aan bijgedragen dat ik al op vroege leeftijd kon proeven van wiskunde en geometrie. Toen ik toch even van het wetenschappelijke pad af geraakte was daar tante Caro. Met haar kennis van mij en de academische wereld kan zij altijd goed advies geven, en gaf ze mij de moed om uiteindelijk de stap naar natuurkunde te maken.

Ook tijdens mijn studie heb ik veel mensen ontmoet die ik wil bedanken voor hun hulp. Hulp bij huiswerk, eten koken, en het inrichten van een grotemensen leven. In het bijzonder hebben Evita, David, Sander en Roshell mij geholpen om gedurende mijn studietijd mens te blijven, onzekerheden te omarmen, en kritisch te blijven op de wereld.

And lastly, my love Julia. You have seen me in many states over the last year, but supported me through all of them and made great effort to be there for me when I needed it. Only your warmth can turn me into a human again when I leave the library as a robot.

Finishing this thesis also means leaving theoretical physics behind me. This is not out of disillusion with the field, but rather a consequence of my discovery of yet another horizon:

---

biology. I am grateful to Bernard for bringing the PhD position to my attention, but no less also to the supervisor of my Bachelors thesis: dr. Greg Stephens, who introduced me into the wondrous world of biophysics.

Thank you all.

# Contents

<b>1</b>	<b>Introduction</b>	<b>6</b>
<b>2</b>	<b>The Ising Model as a CFT</b>	<b>11</b>
<b>3</b>	<b>Zamolodchikov's Conjecture</b>	<b>19</b>
3.1	Perturbations . . . . .	19
3.2	S-matrix theory . . . . .	25
<b>4</b>	<b>Affine Lie Algebraic Descriptions</b>	<b>31</b>
4.1	Lie algebras . . . . .	31
4.2	Affine extensions . . . . .	35
4.3	WZW models and the coset construction . . . . .	37
4.4	Toda field theory . . . . .	44
4.5	Hidden geometry . . . . .	46
<b>5</b>	<b>Back to Lattice Models</b>	<b>52</b>
5.1	Transfer matrix spectrum of a diagonal Ising model . . . . .	53
5.2	From spin models to loop- and vertex-models . . . . .	56
5.3	The twisted algebraic Bethe Ansatz . . . . .	70
<b>6</b>	<b>A Path Forward</b>	<b>80</b>
6.1	The dilute $A_3$ model . . . . .	80
6.2	Free fermions in the critical dilute $A_3$ model . . . . .	85
6.3	Next steps . . . . .	89
<b>7</b>	<b>Conclusion</b>	<b>90</b>
<b>A</b>	<b>Appendix</b>	<b>97</b>
A.1	The Experiment . . . . .	97
A.2	Coxeter orbit code . . . . .	101
A.3	Commutator of diagonal transfer matrix and 1D quantum Ising Hamiltonian	102
A.4	The diagonal Ising transfer matrix in fermion basis. . . . .	105
A.5	Wolff-Zittartz eigenvalues . . . . .	109

## CONTENTS

---

A.6 Derivation of the twisted Bethe equations . . . . .	110
---	-----

# 1

## Introduction

As the title of this thesis reveals, the central model that we study in this thesis is the Ising model. It was introduced in 1920 as a model of ferromagnetism by Wilhelm Lenz, then at the University of Rostock. The quantum mechanical nature of reality was just starting to show itself, and Lenz was thinking about the magnetic moments of molecules in a crystal. This moment might become quantised by interactions with the crystal lattice, he argued<sup>1</sup>, making the molecules polar. In his own words:

*”In a quantum treatment certain angles  $\alpha$  will be distinguished, among them in any case  $\alpha = 0$  and  $\alpha = \pi$ . If the potential energy  $W$  has large values in the intermediate positions, as one must assume taking account of the crystal structure, then the positions will be very seldom occupied, Umklapp processes will therefore occur very rarely, and the magnet will find itself almost exclusively in the two distinguished positions, and indeed on the average will be in each one equally long.”*[24]

Ernst Ising joined Lenz in Hamburg as his doctoral student in 1922 and worked with him on this model of ferromagnetism, summarising his final dissertation on the subject in an article published in 1925 with the title *Beitrag zur Theorie des Ferromagnetismus* [16]. Most famously, Ising (correctly) showed that when the molecules are arranged in a one dimensional configuration, the system as a whole cannot undergo a phase transition, and he then (incorrectly) extended this finding to higher dimensions. Since phase transitions

---

<sup>1</sup>In fact, he introduced the model only two years before the famous Stern-Gerlach experiment would conclusively show the quantum mechanical nature of these magnetic moments.

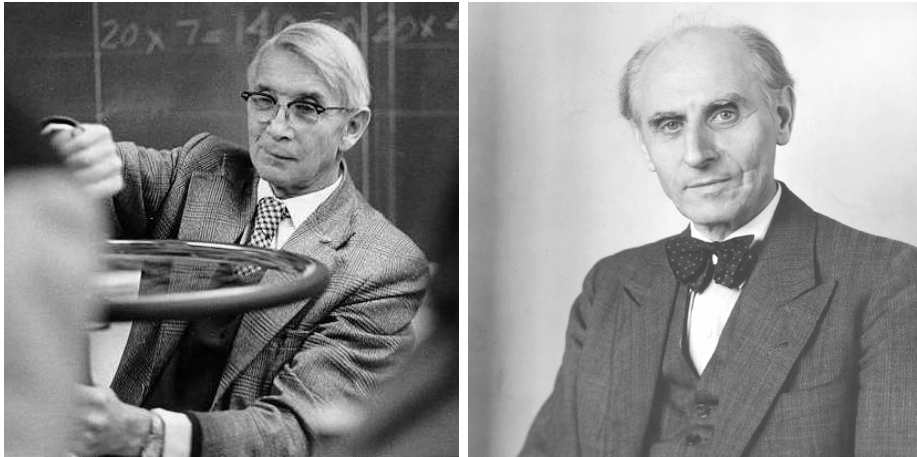


Figure 1.1: Ernst Ising (left) and Wilhelm Lenz (right)

were observed to be fundamental phenomena when talking about magnetism, the community quickly left the Lenz-Ising Model for what it was, and moved on to more complicated models to explain ferromagnetism (which started the investigation into what we now refer to as Heisenberg models). After obtaining his doctorate, Ising left academia, but quickly quit his new job to become a teacher at a German school, only to be barred from teaching by the upcoming Nazi-regime. During the War, Ising worked as a shepherd and a railroad worker, and it was only in 1947 that he emigrated to the United States and was able to find work at a university again.

**It Took a Chemist** What Ising didn't know was that while he had been isolated from the scientific community, a discovery by Rudolf Peierls in 1936 had made Ising's model world-famous. Contrary to what Ising had assumed, Peierls showed that in dimensions higher than one, the Ising model actually does contain phase transitions, and its dynamics turn out to be extremely rich. In fact, not only is it a powerful model to describe magnetism, but it actually turned out to describe many phenomena in wildly different fields, focusing a lot of attention on finding its solution (e.g. its free energy and magnetisation as a function of temperature and coupling strengths). Proving too difficult for physicists and mathematicians, it took a chemist to find the mathematical solution, and in 1944, three years before Ising reentered academia, Lars Onsager solved the anisotropic two-dimensional Ising model on a square lattice.

Nowadays, the Ising model is one of physics' most famous and beloved models and ubiq-

uitous in all statistical fields. A look at its Hamiltonian elucidates why:

$$\mathcal{H}_{\text{Ising}} = - \sum_{\langle i,j \rangle} J_{ij} \sigma_i \sigma_j - \mu \sum_i h_i \sigma_i \quad (1.1)$$

It describes objects  $i$  and  $j$ , in states  $\sigma_i$  and  $\sigma_j$ , interacting with interaction strength  $J_{ij}$ , as long as the as of yet undefined sum over  $\langle i, j \rangle$  includes them, and an interaction  $h_i$  that involves only one object  $i$ .

Originally, it was formulated to have the objects be molecules, the states  $\sigma$  the dipole orientations,  $\mu$  the molecular magnetic moment, and  $h$  an external magnetic field, resulting in the model that Lenz had in mind. However, we now see why the model could become so wildly applicable, since its components may refer to wildly different things. First of all, the Hamiltonian makes no mention of a lattice, so it can be defined on any ordered or disordered graph (which is how it can be used to describe e.g. amorphous glasses). The sum over  $\langle i, j \rangle$  specifies no support, so while Onsager solved it for nearest neighbours only, it could in general contain all possible combinations. The states  $\sigma$  also don't have to be binary numbers, and could take on values in any domain. In fact, making them take values in representations of a certain Lie algebra results in the quantum mechanical version of the Ising model which we will encounter later on in this thesis.

As such, Ising models are being used to describe and understand the dynamics of social interactions [30], networks of gene regulation [20], flocks of birds [4], networks of neurons in the brain [1], etc. Looked at in full generality, the Ising model is thus a *model of interactions on a graph*, its scope only limited by the fact that only terms with one or two nodes appear.

**CFTs** That last remark, about no higher interactions appearing, actually brings us to another fundamental remark to make in this introduction that will bring the Ising model into a language more familiar to modern physicists. The theory that explains why so many very complex (e.g. a flock of  $10^5$  birds or network of  $10^9$  neurons) models can be captured by a model only coupling two nodes at a time, was developed in the second half of the 20th century and goes under the name of Renormalisation Group (RG) theory. It is usually formulated in the language of quantum field theory, where the partition function is a path integral over field configurations of some action that contains all possible interactions. However, by integrating out high (UV) degrees of freedom, or equivalently, coarse

graining the underlying spacetime, the action can be rewritten with the the same fields, but with fewer interactions and adjusted coupling parameters, resulting in effective field theories. Each time we coarse grain, we arrive at a new theory, and we are lead to study the behaviour of theories under the repeated application of this RG process, generating a type of flow through theory-space. It turns out that this flow can have certain fixed points: theories that stay the same when coarse graining the spacetime. Looking at the theory at different scales then shows identical physics, and we are led to conclude that there is no characteristic scale present in the theory. In fact, the fixed points of this flow are invariant under a wide class of symmetries called conformal symmetries that includes more than simple scale transformations. These theories are aptly called *Conformal Field Theories* (CFTs) and have been omnipresent in physics ever since.

One of the reasons these CFTs became so popular is the fact that in two dimensions the symmetries alone can allow you to calculate many, if not all, interesting things. Finding a theory with this intricate set of symmetries might seem rare, but it was observed that some models actually started showing a lack of scale around their critical points, enabling this powerful framework to be applied to solve the model.

**Eight Particles** However, a natural question arises: By leaving the critical point, we might break the full conformal symmetry to some smaller subgroup, but are there cases in which even this lower symmetry is constraining enough to fix the theory? If so, then even off-critical theories could be solvable, an alluring thought... This question was also on Alexander Zamolodchikov's mind in 1989, when he perturbed the CFT associated to the critical Ising model. He found two deformations that preserved integrability<sup>2</sup>: a thermal one, and a magnetic one. Making some natural assumptions, he was able to write down the full scattering matrix of this theory, and discovered that this theory contained eight particles. He noticed that this spectrum contained some intriguing numbers, that all seemed to be related to properties of the largest semisimple Lie algebra  $E_8$ ; the masses of the particles are related to each other through its Cartan matrix, and the conserved quantities are characterised by numbers that coincide with the exponents of  $E_8$ , modulo 30, its Coxeter number. On top of that, there are  $\text{rank}(E_8) = 8$  particles. All of this, in combination with his personal communication with Fateev, lead Zamolodchikov to his

---

<sup>2</sup>We have not defined the concept of integrability yet, but will come back to this later. For now, it can be taken to mean the same as solvability.

conjecture:

*"By the way this  $E_8$  structure strongly suggests that particular [lattice models] associated to the weights of  $E_8$  can be constructed whose scaling limit would describe the universality class of the critical Ising model in a magnetic field."*[37]

This ‘coincidence’, and the mythical status of  $E_8$  throughout physics and mathematics, motivated a significant amount of research into the relationship between CFTs and Lie groups/algebras, which is most explicit in Wess-Zumino-Witten models and Toda field theory (as we will see later in this thesis). Deep connections became visible between some Lie algebras and the CFTs describing physical systems, but research eventually took off in different directions and many parts of these connections were left unexplained. Then in 2010, an experiment was able to reproduce the system Zamolodchikov originally investigated (a kind of 1-dimensional magnet), and found two particles that have a mass-ratio as predicted by the original paper from ’89. A quick review of this experiment is presented in the appendix A.1. This discovery sparked new interest in the problem, and inspired this thesis.

In the next chapter, we will first develop an understanding of the Ising model, which is originally a discrete lattice model, as a field theory. We will then follow and reproduce Zamolodchikov’s reasoning that lead him to his conjecture about the link to  $E_8$ . To motivate the existence of this link, we will further explore some Lie algebraic field theories, and the way they link  $E_8$  to the Ising CFT, before moving on to explicit lattice models. We don’t have an exact solution to the magnetic Ising model, but we will study a model that lies in its universality class, and has been shown to possess the same excitation spectrum in its thermodynamic limit[3]. It is a type of spin-one Ising model, called the dilute  $A_3$  model. We can solve it with a Bethe Ansatz approach, but also study its free fermion structure, and we set out to link the two descriptions to each other, in the hope that we can understand the  $E_8$  particles in terms of elementary excitations on the lattice. We first practice such a translation in terms of the simpler critical Ising model, and then pave the way to do the same for the dilute  $A_3$  model.

That’s a lot to cover, so let’s begin.

# 2

## The Ising Model as a CFT

Physicists can be notoriously ambiguous and paradoxical in their terminology. I will most likely continue this tradition throughout this thesis, but hope to eliminate as much confusion as possible by sometimes pointing out where I will be imprecise. In the following chapters:

- I will use the word Ising model a lot. This will sometimes refer to the classical version from the introduction, where spins take binary scalar values, but might also refer to the corresponding quantum chain where the spins take values in  $SU(2)$  algebra representations. When unspecified, I rely on the context to clear things up.
- When I say Ising model, it might also be unclear sometimes whether I mean the version with or without an external magnetic field. As a rule of thumb: 2D classical Ising models have their external fields turned off, while 1D quantum Ising models have a term in their Hamiltonian with a magnetic field along the transverse  $x$ -direction. When there are additional longitudinal fields present (those breaking the  $\mathbb{Z}_2$  symmetry of the ground state), I will use the term *magnetic* Ising models.
- I will also talk about dimensions a lot, and whenever I describe the number of dimensions, I will always, unless emphatically stated otherwise, refer to *spatial* dimensions. So when I say 2D, I mean 2(+1)D.
- When writing down Boltzmann weights for statistical ensembles, I will generally absorb the inverse temperature into the coupling constants without mentioning this fact explicitly.

- $\hbar = 1$ .
- Finally, I will vary with my summation notation. Where space allows it or clarification is necessary, I will use explicit sums, but other times I might imply Einstein summation by repeated indices.

**QC Mapping** With that out of the way, let's talk about statistical models. Recall first from elementary quantum field theory that any partition function can be written as a kind of discrete, Euclidean path integral over intermediate states:

$$Z = \sum_x \sum_{x_1, x_2, \dots, x_N} \langle x | e^{-H_d \delta t} | x_1 \rangle \langle x_1 | (\dots) | x_N \rangle \langle x_N | e^{-H_d \delta t} | x \rangle \quad (2.1)$$

Where the set  $\{|x_i\rangle\}$  is a complete set of eigenstates of the Hermitian Hamiltonian  $H_d$  of the d-dimensional quantum system, making  $|x_i\rangle \langle x_i|$  simply a resolution of the identity. It is then easily seen that (2.1) is just  $\text{Tr}(e^{-H_d N \delta t})$ , and it becomes the continuous quantum path integral when  $\delta t$  goes to zero while keeping  $N \delta t$  fixed.

Now note that this partition function can also be written as  $\text{Tr}[(e^{-H_d \delta t})^N]$ , which is actually precisely the partition function of a (d+1)-dimensional classical system composed of N copies along the (d+1)th direction of d-dimensional units, each with transfer matrix  $e^{-H_d \delta t}$ . This surprising correspondence between d-dimensional quantum systems and (d+1)-dimensional classical systems is known as the quantum to classical (QC) mapping. This QC mapping can be used to show that a 2D classical Ising model can be related to a 1D quantum Ising model. More precisely, the partition functions of systems described by the following two Hamiltonians are the same [27]:

$$H_{\text{classical}} = - \sum_{i,j} J_h \sigma_{i,j} \sigma_{i+1,j} + J_v \sigma_{i,j} \sigma_{i,j+1} \quad (2.2)$$

$$\hat{H}_{\text{quantum}} = -\beta \sum_i \hat{\sigma}_i^z \hat{\sigma}_{i+1}^z - \gamma \sum_i \hat{\sigma}_i^x \quad (2.3)$$

Where:

- The classical Hamiltonian is defined on a 2D lattice, the quantum one on a 1D lattice.

- $J_h$  and  $J_v$  are respectively the horizontal and vertical couplings between sites on the 2D lattice.
- The classical sites take the values  $\pm 1$ , while the quantum sites are described by the Pauli matrices  $\sigma^i$ .
- I introduced hats to emphasise quantum operators (but from now on will leave them implicit).
- $\beta = J_h/T$  and  $\gamma = e^{-2J_v/T}$

**Fermions** As mentioned in the introduction, we want to develop an understanding of these two equivalent lattice models in terms of a field theory. The seminal paper by Schultz, Mattis and Lieb [28] presented a way to transform the Ising model into a model of fermions, and a nice way to turn this model into a continuous field theory can be found in [38]. They start by defining the usual ladder operators on the quantum 1D Ising chain:

$$\sigma_i^+ = \frac{1}{2}(\sigma_i^x + i\sigma_i^y) \quad (2.4)$$

$$\sigma_i^- = \frac{1}{2}(\sigma_i^x - i\sigma_i^y) \quad (2.5)$$

These represent respectively spin raising/lowering operators along our quantisation axis, and it is tempting to look at them as creation operators of some quasi-particle that we'll refer to as a Paulion, and identify  $c_i^{(\dagger)} = \sigma_i^{-(+)}$ . On a single site, we can write these Paulion operators as

$$\sigma^+ = \begin{pmatrix} 0 & 1 \\ 0 & 0 \end{pmatrix} \quad (2.6)$$

$$\sigma^- = \begin{pmatrix} 0 & 0 \\ 1 & 0 \end{pmatrix} \quad (2.7)$$

Which indeed gives the usual fermionic anticommutator  $\{\sigma^+, \sigma^-\} = 1$ . So far so good. However, things turn messy once we start to look at the behaviour of these operators on the whole chain. Fermionic operators should anticommute when evaluated on different sites

of the lattice, but a quick inspection yields  $[\sigma_i^+, \sigma_j^-] = 0$  for  $i \neq j$ : our Paulion operators commute. This problem of mixed commutation relations can be solved by a Jordan-Wigner transformation, yielding proper fermions, and a writing their Fourier transform in Bogoliubov basis results in a remarkably simple version of our Hamiltonian (see e.g. [28], [38] or [21]), which can then be made continuous around the critical point to arrive at the field theory of a massive free fermion.

**Disorder Operators** Here, however, we will use another way to arrive at the same field theory. Following Mussardo [23], we will study the algebraic properties of so-called disorder operators on an infinite 1D lattice. Define the following operators  $\mu_r^i$  on the lattice dual to our original Ising lattice:

$$\mu_{r+1/2}^3 := \prod_{i=-\infty}^r \sigma_i^x \quad (2.8)$$

$$\mu_{r+1/2}^1 = \sigma_r^z \sigma_{r+1}^z \quad (2.9)$$

Where index  $r + 1/2$  refers to the node on the dual lattice that is between position  $r$  and  $r + 1$  of our original lattice. Note that  $\mu_{r+1/2}^3$  flips all spins to the left of  $r + 1$ , effectively creating a kink along the chain. In doing so, it affects the boundary condition on the leftmost edge, which is why they are defined on the infinite lattice to avoid inconsistencies. Like our original spin operators, they are involutory:  $(\mu^i)^2 = 1$ , and they obey the same commutation relations. A quick check verifies the following identities:

$$\left[ \mu_{r+1/2}^1, \mu_{r'+1/2}^3 \right] = 2\delta_{r,r'} \quad (2.10)$$

$$\left[ \mu_{r+1/2}^3, \mu_{r'+1/2}^3 \right] = 0 \quad (2.11)$$

$$\left[ \mu_{r+1/2}^3, \sigma_{r'}^x \right] = 0 \quad (2.12)$$

$$\mu_{r-1/2}^3 \mu_{r+1/2}^3 = \sigma_r^x \quad (2.13)$$

Remarkably, when we take our original Hamiltonian (2.3) to be on an infinite 1D lattice:

$$\mathcal{H}(\sigma, \lambda) = - \sum_{i=-\infty}^{\infty} (\lambda \sigma_i^z \sigma_{i+1}^z + \sigma_i^x) \quad (2.14)$$

We see that it can be written in terms of disorder operators as:

$$\mathcal{H}(\mu, \lambda) = -\lambda \sum_{r=-\infty}^{\infty} \left( \lambda^{-1} \mu_{r-1/2}^3 \mu_{r+1/2}^3 + \mu_{r+1/2}^1 \right) \quad (2.15)$$

That is, the order and disorder Hamiltonians are related by:

$$\mathcal{H}(\sigma, \lambda) = \lambda \mathcal{H}(\mu, \lambda^{-1}) \quad (2.16)$$

This remarkable fact thus links a description in terms of order operators at coupling  $\lambda$  to a description in terms of disorder operators at coupling  $1/\lambda$ . Since both describe the exact same system, when the ordered description becomes critical at coupling  $\lambda_c$ , the disordered description must be critical at  $1/\lambda_c$ . If we now add some physical intuition and demand that there be only one critical point in the Ising model, we can immediately conclude that the critical point must be at  $\lambda_c = 1$ .

Now to get to the equations of motion, let's establish ourselves in the Heisenberg picture of quantum mechanics, and make our operators time dependent. Denote by  $\partial_\tau$  the derivative with respect to imaginary time, we have for a general operator  $\mathcal{O}$  then that  $\partial_\tau \mathcal{O}(\tau) = [\mathcal{H}, \mathcal{O}]$ . The time dependence of our operators then follows immediately from their algebraic properties.

Defining the following operators<sup>1</sup>:

$$\psi_1(r) = \sigma_r^3 \mu_{r+1/2}^3 \quad (2.17)$$

$$\psi_2(r) = \sigma_r^3 \mu_{r-1/2}^3 \quad (2.18)$$

We get the equations of motion[23]:

---

<sup>1</sup>Note that we have switched our notation from position as an index to full functional dependence on position: a sign of things to come.

$$\partial_\tau \psi_1(r) = -\psi_2(r) + \lambda \psi_2(r+1) \quad (2.19)$$

$$\partial_\tau \psi_2(r) = -\psi_1(r) + \lambda \psi_1(r-1) \quad (2.20)$$

**The Scaling Limit** If we now want to take the limit to continuous space, we should look at the limit where  $r+1$  becomes  $r+\epsilon$ , and  $\epsilon \rightarrow 0$ . To get rid of the ambiguity around what to make of  $\psi_i(r+1)$ , we note the following, which is true only in exactly this limit:

$$\partial_r \psi_2(r) = (\psi_2(r+\epsilon) - \psi_2(r))/\epsilon \quad (2.21)$$

$$\implies \lambda \psi_2(r+\epsilon) = \lambda \epsilon \partial_r \psi_2(r) + \lambda \psi_2(r) \quad (2.22)$$

So that we can write the equation of motion for  $\psi_1(r)$  as:

$$\partial_\tau \psi_1(r) = -(1-\lambda)\psi_2(r) + \lambda \epsilon \partial_r \psi_2(r) \quad (2.23)$$

And similarly for  $\psi_2(r)$ :

$$\partial_\tau \psi_2(r) = -(1-\lambda)\psi_1(r) - \lambda \epsilon \partial_r \psi_1(r) \quad (2.24)$$

We are now finally able to completely let  $\epsilon$  go to zero and arrive at a continuous theory with the following equations of motion:

$$(\gamma^0 \partial_t + \lambda \gamma^3 \partial_r + m)\psi = 0 \quad (2.25)$$

Where we have defined the following things:

- The spinor field  $\psi(r) = \begin{pmatrix} \psi_1(r) \\ \psi_2(r) \end{pmatrix}$
- $t = \epsilon \tau$
- $m = \frac{1-\lambda}{\epsilon}$

- The Clifford  $\gamma$ -matrices:  $\gamma^0 = \sigma^x$  and  $\gamma^3 = \sigma^z$

We have accomplished our first goal: a field theory describing the scaling limit of the Ising model. But the real power of this formalism lies at the critical point  $\lambda = 1$ . There, the mass vanishes, and we get a free fermion theory whose equations of motion follow from the action:

$$S = \int d^2x \psi \gamma^0 \gamma^\mu \partial_\mu \psi \quad (2.26)$$

To rewrite this action into a language that is more familiar in the context of conformal field theory, we define new, complex light-cone coordinates:

$$z = t + ix \quad (2.27)$$

$$\bar{z} = t - ix \quad (2.28)$$

So that

$$\partial := \frac{\partial}{\partial z} = \frac{1}{2} \left( \frac{\partial}{\partial x} \frac{\partial x}{\partial z} + \frac{\partial}{\partial y} \frac{\partial y}{\partial z} \right) = \partial_x - i\partial_y \quad (2.29)$$

$$\bar{\partial} := \frac{\partial}{\partial \bar{z}} = \partial_x + i\partial_y \quad (2.30)$$

And new fermion fields

$$\psi = \frac{\psi_1 + i\psi_2}{\sqrt{2}} \quad (2.31)$$

$$\bar{\psi} = \frac{\psi_1 - i\psi_2}{\sqrt{2}} \quad (2.32)$$

In these new coordinates, our critical action reduces to

$$S = \int dz d\bar{z} (\psi \bar{\partial} \psi + \bar{\psi} \partial \bar{\psi}) \quad (2.33)$$

Our equations of motion are now easily seen to be the Cauchy-Riemann equations, making  $\psi$  and  $\bar{\psi}$  resp. holomorphic and antiholomorphic functions. This action is the famous  $c = \frac{1}{2}$

conformally invariant free fermion action, and extensively studied in all CFT literature.

# 3

## Zamolodchikov's Conjecture

### 3.1 Perturbations

Noether's theorem is arguably physics' most loved theorem. It relates symmetries to conserved quantities. If a system contains a conserved quantity, then one can impose the conservation of this quantity to solutions of the equations of motion to restrict the possibilities, and help solve for trajectories. Similarly, conformal symmetry can constrain the correlation functions, and in doing so make the theory solvable. Remarkably however, there are perturbations of CFTs that break conformal symmetry, but leave the theory solvable.

**Deformations** This lead Zamolodchikov to look at deformations of the  $c = \frac{1}{2}$  Ising CFT in his now famous paper [37]. This CFT contains two nontrivial primary operators (or fields),  $\epsilon = \Phi_{1,3}$  and  $\sigma = \Phi_{1,2}$ , where the notation  $\Phi_{r,s}$  refers to the field at position  $(r, s)$  in the corresponding Kac-table of the minimal model. The first corresponds to a  $\mathbb{Z}_2$ -even thermal perturbation, but the second corresponds to the more interesting magnetic perturbation. The three primaries ( $\sigma, \epsilon$  and the identity  $\mathbb{1}$ ) define three holomorphic highest weight modules by repeated action on them by the Virasoro modes  $L_n$  for  $n < 0$  (And three antiholomorphic ones by repeated action of the antiholomorphic  $\bar{L}_n$ ). Through the operator-state correspondence, these primary operators correspond to highest weight states, and their Verma modules are not only a nice way to generate all the operators, but they actually generate the full Hilbert space associated to our Ising CFT in a highest weight representation.

When perturbing this CFT, we thus have the choice of inserting  $\mathbb{Z}_2$  symmetric operators

( $\epsilon$  and  $\mathbb{1}$ ) or the  $\mathbb{Z}_2$  odd operator  $\sigma$ . Zamolodchikov chose the latter. Introducing the parameter  $h$  to control the strength of this perturbation, we get the new action:

$$S_{\frac{1}{2}}^{\sigma} = S_{\frac{1}{2}} + h \int \sigma(z, \bar{z}) dz d\bar{z} \quad (3.1)$$

Where  $S_{\frac{1}{2}}$  is the action corresponding to the original  $c = \frac{1}{2}$  CFT. Since the original  $S_{\frac{1}{2}}$  had total dimension  $(0, 0)$ , the perturbation must also have dimensions  $(0, 0)$ , and we can conclude the following:

$$[h \int \sigma(z, \bar{z}) dz d\bar{z}] = (0, 0) \quad (3.2)$$

$$[h] + [\sigma(z, \bar{z})] + [dz d\bar{z}] = (0, 0) \quad (3.3)$$

$$[h] + \left(\frac{1}{16}, \frac{1}{16}\right) + (-1, -1) = (0, 0) \quad (3.4)$$

$$\implies [h] = \left(\frac{15}{16}, \frac{15}{16}\right) \quad (3.5)$$

This perturbation thus results in a few (related) things:

- It introduces a dimensionful quantity  $h$ .
- It introduces a typical scale for the theory.
- Conformal invariance is broken.
- Fields are no longer purely (anti)holomorphic functions.

We will especially focus on this last point. All holomorphic fields  $\Phi$  in the CFT are by definition conserved along the antiholomorphic coordinate (and the other way around), i.e.

$$\partial_{\bar{z}} \Phi = 0 \quad (3.6)$$

However, when the perturbation destroys this holomorphicity, we should allow for a nonzero r.h.s. of equation (3.6).

To study this in detail, let's look at the space  $\Lambda$  of holomorphic descendants of the identity. It is generated by applying the Virasoro generators  $L_n$  ( $n < -1$ ) to  $\mathbb{1}$ . They are thus combinations of the holomorphic stress-energy tensor  $T(z)$  and its  $z$ -derivatives. In fact,

$\Lambda$  also contains fields which are a total z-derivative, which we don't want to consider<sup>1</sup>, so let's set them to zero by looking at the quotient space  $\hat{\Lambda} := \Lambda/(L_{-1}\Lambda)$  instead. With the  $L_0$  operator, we can separate this space into spin-sectors  $\hat{\Lambda}_s$ . Its eigenvalues in different subspaces of  $\hat{\Lambda}$  provides the following decomposition:

$$\hat{\Lambda} = \bigoplus_s \hat{\Lambda}_s \quad (3.7)$$

$$L_0 \lambda_s = s \lambda_s \quad \lambda_s \in \hat{\Lambda}_s \quad (3.8)$$

Each of these spin-subspaces  $\hat{\Lambda}_s$  contains a basis of fields  $T_s^{(k)}$ ,  $k = 1, \dots, \dim(\Lambda_s)$ . As a result of the perturbation, these operators will in general satisfy a modified version of equation (3.6):

$$\partial_{\bar{z}} T_s^{(k)} = \sum_n h^n R_{s'}^{(k,n)} \quad (3.9)$$

With  $R_{s'}^{(k,n)}$  some arbitrary spin- $s'$  operator. Comparing dimensions, we can get those of  $R_{s'}^{(k,n)}$ :

$$(0, 1) + (s, 0) = n \left( \frac{15}{16}, \frac{15}{16} \right) + [R_{(s')}^{(k,n)}] \quad (3.10)$$

$$\implies [R_{(s')}^{(k,n)}] = \left( s - n \frac{15}{16}, 1 - n \frac{15}{16} \right) \quad (3.11)$$

$$\implies s' = s - 1 \quad (3.12)$$

Where in the last line we used that an operator's spin is defined as the difference between it's holomorphic and antiholomorphic dimensions. Furthermore, we now see that higher powers of  $h$  result in operators with negative dimensions, which don't appear in a unitary theory, so we can just take the linear term and write:

$$\partial_{\bar{z}} T_s^{(k)} = h R_{s-1}^{(k)} \quad (3.13)$$

---

<sup>1</sup>Integrating them over our base space manifold gives, by partial integration, just a constant shift by their value on our manifold boundary.

with

$$[R_{s-1}^{(k)}] = \left(s - \frac{15}{16}, \frac{1}{16}\right) \quad (3.14)$$

**Integrability** Knowing its conformal dimensions, we have a lot of information about these fields  $R_{s-1}^{(k)}$ . To identify them further, we have to compare its dimensions to fields we know. Zamolodchikov noticed that, if we decompose the space  $\Omega$  of  $\sigma$ -descendants in a similar way as we did with the  $\mathbb{1}$ -descendants, we get the following construction:

$$\Omega = \bigoplus_s \Omega_s \quad (3.15)$$

$$L_0 \omega_s = \left(\frac{1}{16} + s\right)\omega_s \quad \omega_s \in \Omega_s \quad (3.16)$$

$$\bar{L}_0 \omega_s = \left(\frac{1}{16}\right)\omega_s \quad (3.17)$$

From equations (3.16) and (3.17), we can see that the dimensions of  $R_{s-1}^{(k)}$  exactly coincide with those of the fields in  $\Omega_{s-1}$ . Since these dimensions fully determine the field, we can conclude  $R_{s-1}^{(k)} \in \Omega_{s-1}$ . We can therefore look at equation 3.13 as defining a map:

$$(\partial_{\bar{z}})_s : \hat{\Lambda}_s \rightarrow \Omega_{s-1} \quad (3.18)$$

This is where Zamolodchikov made a clever observation. Say we can find that for certain values of  $s$ , the r.h.s. of (3.13) is actually a total holomorphic derivative of a spin  $s - 2$  field, then we get the identity (leaving the index  $k$  implicit):

$$\partial_{\bar{z}} T_{s+1} = \partial_z \Theta_{s-1} \quad (3.19)$$

Which is a complex continuity equation from which we can construct integrals of motion  $P_s$  [37]:

$$P_s = \int (T_{s+1} dz + \Theta_{s-1} d\bar{z}) \quad (3.20)$$

Demanding the r.h.s. of (3.13) to be of this shape might sound like a tall order, but if we define the following quotient space:

$$\hat{\Omega}_s = \Omega_s / (L_{-1}\Omega_s) \quad (3.21)$$

Then the fields we are interested in, the total  $z$ -derivatives, are set to zero. This might seem counterproductive, but consider the following projection operator:  $\Pi_s : \Omega_s \rightarrow \hat{\Omega}_s$ . It induces a map between the quotient spaces:

$$B_s = \Pi_{s-1}(\partial_{\bar{z}})_s : \hat{\Lambda}_s \rightarrow \hat{\Omega}_{s-1} \quad (3.22)$$

The operator  $B_{s+1}$  has an interesting property. Whenever it sends a field  $T_{s+1}$  to zero, we get the following:

$$B_{s+1}T_{s+1} = 0 \quad (3.23)$$

$$\implies \Pi_s(\partial_{\bar{z}}T_{s+1}) = 0 \quad (3.24)$$

$$\implies \partial_{\bar{z}}T_{s+1} \in L_{-1}\Omega_s \quad (3.25)$$

But this space  $L_{-1}\Omega_s$  is precisely made up of fields  $\partial_{\bar{z}}\Theta_{s-1}$ . We therefore find that fields of spin  $s + 1$  that are in the kernel of  $B_{s+1}$  obey an complex continuity equation and we get integrals of motion whenever our  $B_{s+1}$  has nontrivial kernel. Given the rank-nullity theorem for a general linear map between vector spaces  $T : V \rightarrow W$ :

$$\dim(\text{im}(T)) + \dim(\text{ker}(T)) = \dim(V) \quad (3.26)$$

We see that the dimension of the kernel of  $B_{s+1}$  obeys

$$\dim(\hat{\Omega}_s) + \dim(\ker(B_{s+1})) = \dim(\hat{\Lambda}_{s+1}) \quad (3.27)$$

So that we get nontrivial integrals of motion whenever the dimension of  $\hat{\Lambda}_{s+1}$  exceeds that of  $\hat{\Omega}_s$ .

Reference [17] provides a way of calculating the dimensionality of these Virasoro representations. We copy here Zamolodchikov's table for the results:

s	1	3	5	7	9	11	13	15	17	19	21
$\dim(\hat{\Lambda}_{s+1})$	1	1	1	2	2	3	4	5	7	9	11
$\dim(\hat{\Omega}_s)$	0	1	1	1	2	2	3	5	6	8	12

From which we can simply read off that we have nontrivial IOM for  $s = 1, 7, 11, 13, 17, 19$ . This is a curious list of numbers, with no obvious pattern. A quick query to the On-Line Encyclopedia of Integer Sequences (OEIS) [29] yields the following sequences that start with these numbers in this order:

- A007775: Numbers not divisible by 2, 3 or 5.
- A005776: Exponents associated to the Weyl group  $\mathcal{W}(E_8)$ .
- A154723: The triangle read by rows in which row n lists all the pairs of noncomposite numbers that are equidistant from n, or only n if there are no such pairs.
- A135776 (A135777): Numbers having number of divisors equal to number of digits in base 6 (7).

Where (A.....) refers to the index of the sequence in the OEIS. While none of these sequences were published in the OEIS at the time of his paper, Zamolodchikov still conjectured the list of IOM to continue indefinitely, making the field theory integrable [37]. This word integrable is notoriously vague. It captures the way in which the theory is solvable by certain techniques. In classical mechanics, it is defined as a property of the Hamiltonian dynamics, for particle physicists it is a property of the scattering matrix, and

in condensed matter and more abstract mathematics it is related to solutions of the Yang-Baxter equation. Zamolodchikov takes it to mean the presence of an infinite number of integrals of motion. In all of these situations, the crux is that everything one might want to know about the theory is constrained by symmetries and conserved quantities alone. Surprisingly perhaps, theories for which this happens can be highly nontrivial and physically relevant. Zamolodchikov, hoping to be confirmed in his suspicion that this magnetic Ising model was integrable, went on to investigate the scattering processes in this perturbed system.

## 3.2 S-matrix theory

In theories of interactions, one of the most fundamental objects is the scattering(S)-matrix. We often want to look at which processes are allowed to happen, regardless of anything else going on, and the S-matrix captures these elementary processes by defining in- and out-states. Given a configuration of a set of particles at  $t = -\infty$ , the S-matrix maps this to a set of outgoing particles at  $t = +\infty$  (or it equivalently might map an out-state to an in-state). Denoting a particle of type  $A_n$  with rapidity ( $= \log(\text{momentum})$ )  $\theta$  by  $A_n(\theta)$ , we will define the S-matrix by:

$$|A_1(\theta_1)\dots A_N(\theta_N)\rangle = \sum_{\{B_i, \theta'_i\}} S_{A_1\dots A_N}^{B_1\dots B_M} |B_1(\theta'_1)\dots B_M(\theta'_M)\rangle \quad (3.28)$$

In a previous section, we have found that the model we are interested in has a large, possibly infinite, amount of conserved quantities  $P_s$ . Let's in particular look at operators of the form  $e^{-iP_s}$  and what their action on in- and out-states does to a matrix element of  $S$ :

$$\langle \text{out} | e^{iP_s} S e^{-iP_s} | \text{in} \rangle \quad (3.29)$$

Now since  $P_s$  is conserved, it commutes with  $S$  and we get simply

$$= \langle \text{out} | S | \text{in} \rangle \quad (3.30)$$

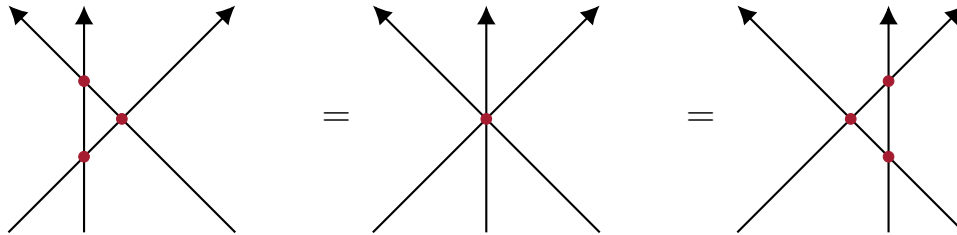


Figure 3.1: The effect of applying the translation operator to in- and out-states of a  $3 \rightarrow 3$  scattering process.

So applying the operator to our in- and out-states has no effect on the total amplitude of the scattering process. Now take one of the most commonly conserved quantities, momentum, the generator of translations, and look what this statement means for a  $3 \rightarrow 3$  scattering process. The fact that  $e^{iP}$  can freely translate the particles in space without changing the amplitude ensures that all processes in figure 3.1 should be considered equivalent. Most importantly, we see that we can write a 3-particle scattering as the product of three 2-particle scatterings.

This argument can be made much more rigorous, but all we need to do is convince ourselves that these conserved quantities result in an S-matrix that can be fully factorised in terms of separate 2-particle S-matrices. In fact, for any S-matrix in 1+1 dimensions that has this property of being 2-particle factorisable, we have the following [10]:

- Scattering processes allow no particles production.
- The set of momenta in the in-state is the same as the set of momenta in the out-state.

Now when we say that no particles are created, that is only true under the analytic S-matrix mapping from in- to out-states. It can happen that the S-matrix has poles. In the language of quantum field theory, the S-matrix can be seen as the propagator of a set of particles, so that its poles actually correspond to the propagator of a bound state of multiple particles, which, although it doesn't appear as an out-state, can survive for macroscopic times. It is therefore the structure of the poles of the S-matrix that carries the hidden information about the composite particles that the theory can contain. The key idea of the bootstrap procedure is to see if you can find any poles that correspond to bound states, then demand that this bound state's dynamics respect the conserved quantities, and see if there are new poles appearing as a result of this demand. One can repeat

this process until it consistently closes, and thus arrive at the full bound spectrum.

We start with the assumption that there are conserved charges like the one in equation (3.29), and that their eigenvalues are additive when the operator works on a multi-particle state:

$$P_s |A_a(\theta)\rangle = q_a^{(s)} e^{s\theta} |A_a(\theta)\rangle \quad (3.31)$$

$$P_s |A_a(\theta_a)A_b(\theta_b)\dots\rangle = (q_a^{(s)} e^{s\theta_a} + q_b^{(s)} e^{s\theta_b} + \dots) |A_a(\theta_a)A_b(\theta_b)\dots\rangle \quad (3.32)$$

When our 2-particle S-matrix has a pole, i.e. a bound state of type  $c$ , at fusion angle  $\theta_a - \theta_b = iU_{ab}^c$ , we can find constraints on the spin of possible conserved charges by demanding that the expectation value of the conserved charge are the same before and after the formation of the bound state. In the frame where the created bound state of type  $c$  is at rest, we get the demand:

$$q_c^{(s)} = q_a^{(s)} e^{-is(\pi - U_{ac}^b)} + q_b^{(s)} e^{is(\pi - U_{bc}^a)} \quad (3.33)$$

Zamolodchikov assumed that the effective Lagrangian of the  $\mathbb{Z}_2$ -perturbed system would contain a particle  $a$  that would interact with a  $\mathbb{Z}_2$ -breaking  $\phi^3$ -like interaction, so that there would be a version of (3.33) with all fusion angles the same. Since they have to add up to  $2\pi$ , we have  $U_{aa}^a = \frac{2\pi}{3}$ , leading to the constraint

$$2 \cos\left(\frac{s\pi}{3}\right) = 1 \quad (3.34)$$

which is solved by any  $s$  that has no common divisor with 6. The first of these solutions are  $s = 1, 5, 7, 11, 13, 17$ . These have some overlap with the spin values for conserved charges we found in the previous section, but we found a bit too many here, so let's tighten the constraints by adding another particle of type  $b$ . Furthermore, we assume that  $aa \rightarrow b$  and  $bb \rightarrow a$  are both possible. Defining  $x_1 = e^{iU_{11}^2}$  and  $x_2 = e^{iU_{22}^1}$ , we get the following two constraints:

$$x_1^s + x_1^{-s} = \frac{q_2^{(s)}}{q_1^{(s)}} \quad (3.35)$$

$$x_2^s + x_2^{-s} = \frac{q_1^{(s)}}{q_2^{(s)}} \quad (3.36)$$

Which we can combine into:

$$(x_1^s + x_1^{-s})(x_2^s + x_2^{-s}) = 1 \quad (3.37)$$

Now in fact, this last equation is so restricting that it will generally be overdetermined if there are more than two conserved charges. Nevertheless, Zamolodchikov found that it does admit a consistent solution provided that  $s$  has no common divisor with 5, and

$$x_1 = e^{\pi i/5} \quad (3.38)$$

$$x_2 = e^{2\pi i/5} \quad (3.39)$$

If we now look at the first conserved charge, i.e.  $s = 1$ , momentum, we see that its eigenvalue on a state  $|A_a(\theta)\rangle$  is  $q_a^1 e^\theta$ . Since  $\theta$  is a rapidity, this invites us to interpret  $q_a^1$  as its mass  $m_a$ , leading to an expression for the mass ratio of the two bound states:

$$\begin{aligned} \frac{m_b}{m_a} &= \frac{q_b^1}{q_a^1} = x_1 + x_1^{-1} = 2 \cos\left(\frac{\pi}{5}\right) \\ &= \phi \end{aligned} \quad (3.40)$$

Where  $\phi$  is the golden ratio 1.6180339...

If we now combine these results, we find that we have conserved charges for any  $s$  having no common divisor with 5 or 6, i.e. no common divisor with 30. These values of  $s$  now perfectly match those we found in the previous section based on the dimension counting. In this case however, it is much more clear that this pattern indeed continues ad infinitum.

Note that we have not yet deduced the existence of these particles, we have simply assumed their existence and then confirmed that it was consistent with the conserved charges we

found earlier. To deduce the existence of further particles, we need to look for poles in the S-matrix. Let's start in the lightest sector with  $S_{aa}$ . It needs to have poles at the fusion angles of a third  $a$ -particle ( $\theta = 2i\pi/3$ ) and a  $b$ -particle ( $\theta = 2i\pi/5$ ). It would thus be nice to construct our S-matrix from building blocks that independently can insert poles. Dorey [10] introduces the following building block to achieve just this, with the nice property that it already obeys unitarity:

$$(x)(\theta) = \frac{\text{sh}(\theta/2 + i\pi x/60)}{\text{sh}(\theta/2 - i\pi x/60)} \quad (3.41)$$

This has simple poles at  $\theta = i\pi x/30$ , and when we include both  $(x)(\theta)$  and  $(30 - x)(\theta)$ , the product immediately satisfies crossing symmetry. Our first guess for  $S_{11}$  will thus be:

$$S_{11} = (10)(12)(18)(20) \quad (3.42)$$

$$(3.43)$$

Where we dropped the dependence on  $\theta$ . However, can now write down the bootstrap equation for the  $11 \rightarrow 11$  S-matrix<sup>2</sup>:

$$S_{11}(\theta) = S_{11}(\theta - i\pi/3)S_{11}(\theta + i\pi/3) \quad (3.44)$$

And we see that our  $S_{11}$  only satisfies this when we add the blocks  $-(2)(28)$ , adding two poles that correspond to a third particle of mass  $m_c = 2m_a \cos(\pi/30)$ .

We could now continue bootstrapping our way through all the possible scatterings, each time adding blocks to have our S-matrix be consistent, and adding particles accordingly. We would find that the bootstrap closes and leaves us with an S-matrix with the following properties:

- 8 distinct particles

---

<sup>2</sup>This is fully analogous to the Yang-Baxter equation we discussed before: In an integrable model, a particle  $a$  interacting with  $b$  should be considered equivalent to a particle  $a$  interacting with particles  $c$  and  $d$  who together form  $b$ .

- 8 different mass ratios, each a component from the largest eigenvalue of the Cartan Matrix of  $E_8$ .
- Conserved charges for all  $s$  with no common divisor with 30, leading to the pattern that  $s \bmod 30$  is an exponent of the  $E_8$  Lie algebra.
- Higher spin charges that form the other eigenvectors of the  $E_8$  Cartan matrix.

# 4

## Affine Lie Algebraic Descriptions

In the previous chapters, we've seen mysterious numbers appearing in descriptions of a perturbation of the Ising model. More explicitly, we found that under some natural assumptions, the S-matrix bootstrap procedure closes after revealing the existence of eight particles whose masses (and higher spin charges) are related to each other by the Cartan eigenvectors of the Lie algebra  $E_8$ . Let's briefly revisit some of the concepts we will need in our description of Lie algebras to try and get a bit closer to what this means.

### 4.1 Lie algebras

This section is in no way a self contained introduction into the theory of Lie algebras, but simply serves as a reminder to the already familiar reader, and as a place to establish notation.

A Lie algebra  $\mathfrak{g}$  is a vector space endowed with a binary, bilinear, antisymmetric operation called the Lie bracket:

$$[ \ , \ ] : \mathfrak{g} \times \mathfrak{g} \rightarrow \mathfrak{g} \tag{4.1}$$

That satisfies the Jacobi identity:

$$[x, [y, z]] + [y, [z, x]] + [z, [x, y]] = 0 \tag{4.2}$$

A specific Lie algebra can be specified by the Lie bracket of a subset of its elements that forms a basis for the full vector space, called generators:

$$[J^a, J^b] = \sum_c i f_c^{ab} J^c \quad (4.3)$$

Where the  $f_c^{ab}$  are called the structure constants.

It could of course happen that there is a subset of generators  $\{L^a\}$  for which we have  $[L^a, J^b] \in \{L^a\}$ . We will call this set the ideal. A proper ideal is then a proper subset for which this holds. We will here be concerned with situations in which there is no such proper ideal (i.e. the only ideals of this algebra are the empty set and the full set), and we will call these Lie algebras simple (and will use the term semisimple for a direct sum of simple algebras).

Since we can capture our entire algebra  $\mathfrak{g}$  in terms of the commutator<sup>1</sup> of its generators, it would be nice to choose our basis of generators in a way that minimises these relations. This basis is called the Cartan-Weyl basis, and is constructed as follows. We take the maximal set  $\mathfrak{h}$  of commuting generators:

$$[H^i, H^j] = 0 \quad \forall H^i, H^j \in \mathfrak{h} \quad (4.4)$$

If this maximal set has  $r$  elements, we say that  $\text{rank}(\mathfrak{g}) = r$ . The rest of our algebra is now specified by the commutators of the Cartan subalgebra and the other generators, and the other generators amongst each other. To complete our Cartan-Weyl basis, we define our other generators  $E^\alpha$  (which we will refer to as ladder operators) so that they satisfy the following equation:

$$[H^i, E^\alpha] = \alpha_i E^\alpha \quad (4.5)$$

We call the vector  $\alpha$  a root of  $\mathfrak{g}$ , and it defines a map  $\alpha(H^i) (= \alpha_i) : \mathfrak{h} \rightarrow \mathbb{C}$ , so belongs to the vector space dual to  $\mathfrak{h}$ . Another way to look at the roots is by defining the adjoint

---

<sup>1</sup>I will often refer to the Lie bracket as a commutator since this is the one most familiar in physics where we usually only work with representations of algebras, and since it necessarily satisfies the Jacobi identity.

action of a generator:

$$\text{ad}(H^i) \cdot J^a := [H^i, J^a] \tag{4.6}$$

The roots are now simply the adjoint action of the Cartan subalgebra on the ladder operators.

Lastly, we need to find the commutator of the ladder operators amongst each other. The Jacobi identity implies:

$$[H^i, [E^\alpha, E^\beta]] = (\alpha^i + \beta^i)[E^\alpha, E^\beta] \tag{4.7}$$

so we see that if  $\alpha + \beta$  was one of our roots, then according to (4.5),  $[E^\alpha, E^\beta]$  has to be proportional to  $E^{\alpha+\beta}$ . If  $\alpha + \beta = 0$ , then apparently  $[E^\alpha, E^\beta]$  is proportional to some linear combination of elements of  $\mathfrak{h}$ . Equation (4.5) actually only defines our ladder operators up to normalisation, so we can just pick this linear combination and decide  $[E^\alpha, E^\beta] = \frac{2}{\alpha \cdot \alpha} \alpha \cdot H$ , where we define  $\cdot$  as the usual scalar product<sup>2</sup>  $\alpha \cdot \beta = \sum_i \alpha^i \beta^i$ . lastly, if  $\alpha + \beta$  is neither a root nor zero, then  $[E^\alpha, E^\beta]$  must be zero itself. Summarising:

$$[H^i, H^j] = 0 \tag{4.8}$$

$$[H^i, E^\alpha] = \alpha_i E^\alpha \tag{4.9}$$

$$[E^\alpha, E^\beta] \propto E^{\alpha+\beta} \quad \text{if } \alpha + \beta \text{ a root} \tag{4.10}$$

$$= \frac{2}{\alpha \cdot \alpha} \alpha \cdot H \quad \text{if } \alpha = -\beta \tag{4.11}$$

$$= 0 \quad \text{otherwise} \tag{4.12}$$

Let's now investigate those roots a bit further and look at the space they live in:  $\mathfrak{h}^*$ , dual to  $\mathfrak{h}$ . While  $\mathfrak{h}^*$  has the same dimension as  $\mathfrak{h}$ , namely  $\text{rank}(\mathfrak{g}) = r$ , the number of roots that we have is equal to the number of ladder operators, which is actually the dimension of our full algebra  $\mathfrak{g}$  minus the dimension of  $\mathfrak{h}$ . As soon as the dimension of our algebra is more than twice its rank, we will find roots that are linear combinations of each other. In our perpetual search for simplicity, we would of course like to be left with just  $r$  roots and the

---

<sup>2</sup>This scalar product on the root space is actually induced by the Killing form on  $\mathfrak{g}$ .

recipe for how to make linear combinations of them.

If we want to do any of this, we should first write our roots explicitly in a basis of  $\mathfrak{h}^*$ :

$$\alpha = \sum_i n_i \beta_i \tag{4.13}$$

In order to choose which roots we will use to express the others, we will have to use a quite arbitrary construction. Define a positive root as a root for which the first nonzero element of its  $n$ -vector is positive. This is a rather arbitrary definition, since it fully depends on both the basis we choose, and the ordering of this basis. Nevertheless, it gets the trick done since it allows us to define a simple root as a root that can not be written as the sum of two positive roots, and in the end, our most important results will again be independent of this choice of basis. Since these simple roots span  $\mathfrak{h}^*$ , there must be  $r$  of them, and we can define the following  $r \times r$  matrix:

$$A_{ij} = \frac{2\alpha_i \cdot \alpha_j}{\alpha_j \cdot \alpha_j} \tag{4.14}$$

Which we will call the Cartan matrix of our algebra  $\mathfrak{g}$ . Remarkably, this matrix is completely independent of our choice of basis for  $\mathfrak{h}^*$ , and uniquely specifies a Lie algebra.

Lastly, before we move on to bigger things, let's define the so-called weights to give some context to this construction.

We have defined our roots as a kind of eigenvalues of the operator  $\text{ad}(H^i)$ . However, What we have implicitly done is choose the vector space on which the elements of the algebra act to be the algebra itself. This adjoint representation gives us a very explicit expression for the action of the algebra, and allowed us to lift this action to the dual space so that the scalar product on  $\mathfrak{h}^*$  could be defined. However, this is in no way necessary, and we might just as well look at eigenvalues of the Cartan subalgebra in different representations:

$$\rho(H^i) |\lambda\rangle = \lambda^i |\lambda\rangle \tag{4.15}$$

Where  $\rho(H^i)$  is some representation of  $\mathfrak{h}$  and  $\{|\lambda\rangle\}$  a basis that diagonalises the representation  $\rho$ . The full  $r$ -vector  $\lambda$  induces the dual map:

$$\lambda(H^i)(= \lambda^i) : \mathfrak{h} \rightarrow \mathbb{C} \quad (4.16)$$

We will call these  $\lambda$  weights, and they obviously also live in  $\mathfrak{h}^*$ . In fact, if we choose  $\rho$  to be the adjoint representation, we get our usual roots back. Roots are thus the weights of the adjoint representation.

We now have the necessary terminology to tackle what we are really here for: affine extensions of these algebras, and their role in quantum field theories.

## 4.2 Affine extensions

Let  $\mathfrak{g}$  be a semisimple Lie algebra. We can then define the tensor product

$$\tilde{\mathfrak{g}} := \mathfrak{g} \otimes C^\infty(S^1) \quad (4.17)$$

of the Lie algebra  $\mathfrak{g}$  and the algebra of  $C^\infty$  functions on the circle with the bracket

$$[g \otimes \mu, h \otimes \nu] = [g, h] \otimes \mu \nu \quad \mu, \nu \in C^\infty(S^1), \text{ and } g, h \in \mathfrak{g} \quad (4.18)$$

Now, note that these functions are periodic and can be expanded in a Fourier series:

$$\mu(\theta) = \sum_n \mu_n e^{i\theta n} \quad (4.19)$$

Under the redefinition  $t = e^{i\theta}$ , it is now obvious that  $\tilde{\mathfrak{g}}$  can also be written as

$$\tilde{\mathfrak{g}} = \mathfrak{g} \otimes \mathbb{C}[t, t^{-1}] \quad (4.20)$$

Where  $\mathbb{C}[t, t^{-1}]$  is the algebra of Laurent polynomials in one variable. Here,  $\otimes$  is a tensor product in the sense that a vector space  $A \otimes B$  is spanned by elements  $a \otimes b$  with  $a \in A, b \in B$ . Which means that  $\tilde{\mathfrak{g}}$  is spanned by elements  $(g \in \mathfrak{g}) \otimes (\mu \in C^\infty(S^1) : S^1 \rightarrow \mathbb{C})$ , i.e.

(smooth) maps from  $S^1$  to  $\mathfrak{g}$ . Maps from the circle to some other space are called ‘loops’, so the algebra  $\tilde{\mathfrak{g}}$  is called the loop algebra.

Looking at the algebra of the new generators  $J_n^a := J^a \otimes t^n$ , we can add a central fully commuting element  $\hat{k}$  to their algebra:

$$[J_n^a, J_m^b] = \sum_c i f_c^{ab} J_{n+m}^c + \hat{k} n \delta_{a,b} \delta_{n+m,0}, \text{ with } [J_n^a, \hat{k}] = 0 \quad (4.21)$$

Let’s now look for the new Cartan subalgebra. The most obvious choice is just taking the Cartan subalgebra of  $\mathfrak{g}$  tensored with the  $t^0$  modes,  $\{H_0^1, \dots, H_0^r\}$ , and adding  $\hat{k}$  to it, since these obviously all commute.

However, let’s look at what this does to the roots of the algebra, defined by the adjoint action of the Cartan subalgebra on the rest of the algebra:

$$\text{ad}(H_0^i) E_n^\alpha = [H_0^i, E_n^\alpha] = \alpha_i E_n^\alpha \quad (4.22)$$

$$\text{ad}(\hat{k}) E_n^\alpha = [\hat{k}, E_n^\alpha] = 0 \quad (4.23)$$

$$(4.24)$$

This leads to the root  $(\alpha^1, \dots, \alpha^r, 0)$ , which is infinitely degenerate (i.e. independent of  $n$ ). We clearly need a kind of  $n$ -grading, which is efficiently implemented by the operator  $L_0 := -t \frac{d}{dt}$ :

$$\text{ad}(L_0) E_n^a = -n E_n^a \quad (4.25)$$

We thus have a grading that lifts the degeneracy of the roots, while still commuting with all the elements of  $\tilde{\mathfrak{h}}$  and  $\hat{k}$ . It thus leads us to a new algebra  $\hat{\mathfrak{g}} = \tilde{\mathfrak{g}} \oplus \mathbb{C} \hat{k} \oplus \mathbb{C} L_0$ , of which we can define a Cartan subalgebra as

$$\hat{\mathfrak{h}} = \{H_0^1, \dots, H_0^r, \hat{k}, L_0\} \quad (4.26)$$

Leaving us with the rest of the (now infinite dimensional) algebra as ladder operators:

$$E_n^\alpha \quad \forall n \quad \text{and} \quad H_n^i \quad \text{for } n \neq 0 \quad (4.27)$$

We call  $\hat{\mathfrak{g}}$  an affine Lie algebra.

Having now defined our full Cartan subalgebra, we can find a basis for our root space and define a Cartan matrix. A general affine root can be denoted by  $\hat{\alpha} = (\alpha, k_\alpha, n_\alpha)$ , where the entries are the eigenvalues of a ladder operator w.r.t. (respectively)  $H_0^i$ ,  $\hat{k}$ , and  $L_0$ . Since  $\hat{k}$  is emphatically chosen such that it commutes with every element of the algebra (i.e. adjoint action is zero), the root component  $k_\alpha$  is always zero and we need only  $r+1$  basis vectors to span the hyperplane on which the roots live. The root associated to  $H_n^i$  is thus  $(0, 0, n) := n\delta$ , such that the root associated to  $E_n^\alpha$  is  $(\alpha, 0, n) := \alpha + n\delta$  ( $n > 0$ ). We now need to find the  $r+1$  simple roots of this affine Lie algebra,  $r$  of which are simply the simple roots of our original Lie algebra, and it can be shown[8] that a sufficient addition to our basis of simple roots is  $\alpha_0 = -\theta + \delta$ , where  $\theta$  is the so-called highest root, i.e. the root of  $\mathfrak{g}$  that has the largest sum of components once it is written in the basis of our root space. Our full set of simple roots is now  $\{\alpha_i\}$ ,  $i = 0, \dots, r$ , and Cartan matrix can stay defined in the usual way.

### 4.3 WZW models and the coset construction

Now that we've established an understanding of Lie algebras, let's see how these constructions appear in field theories. Consider the following nonlinear  $\sigma$  model. It is a field theory with a Lie group valued target space (describing objects propagating over the group manifold), and has an explicit formulation in terms of an action:

$$S_\sigma = \frac{1}{4a^2} \int d^2x \text{Tr}'(\partial^\mu g^{-1} \partial_\mu g) \quad (4.28)$$

Where  $a$  is some dimensionless coupling constant,  $g$  is a group valued field, and  $\text{Tr}'$  is a trace that is made representation independent by normalisation. It is not exactly what we are looking for though. First of all, it turns out that while classically conformally invariant,

it actually loses this symmetry at the quantum level so it can't be a candidate for our Ising CFT. There is however a modification of the action that restores conformal invariance, and results in an interesting current algebra. The explicit derivation of this action is beyond the scope of this thesis, so we will just print the result from [8] here:

$$S^{WZW} = \frac{k}{16\pi} \int d^2x \operatorname{Tr}'(\partial^\mu g^{-1} \partial_\mu g) + k\Gamma \quad (4.29)$$

Where the first term is the standard nonlinear  $\sigma$  model term (with a rescaled coupling constant, now called  $k$ ), and  $\Gamma$  is the so-called Wess-Zumino term:

$$\Gamma = \frac{-i}{24\pi} \int_B d^3y \epsilon_{\alpha\beta\gamma} \operatorname{Tr}'(\tilde{g}^{-1} \partial^\alpha \tilde{g} \tilde{g}^{-1} \partial^\beta \tilde{g} \tilde{g}^{-1} \partial^\gamma \tilde{g}) \quad (4.30)$$

Where the integral goes over a manifold whose boundary is the compactification of our original base manifold, and the tildes indicate that the field has been extended over this new integration manifold (the question of uniqueness for this extension is interesting, but not relevant to our current discussion). That is, when our original base space was the complex plane, the boundary of  $B$  will be the Riemann sphere, so  $B$  is just a 3-ball. This new action comes with the conserved currents

$$J(z) = -k \partial_z g g^{-1} \quad (4.31)$$

$$\bar{J}(\bar{z}) = k g^{-1} \partial_{\bar{z}} g \quad (4.32)$$

Since these are still independently conserved, let's focus our attention on only the holomorphic part, and expand it in the algebra generators  $t^a$ :

$$J(z) = \sum_a J^a t^a \quad (4.33)$$

Leading to the following operator product expansion (OPE) [8]:

$$J^a(z)J^b(w) \sim \frac{k\delta_{ab}}{(z-w)^2} + \sum_c i f_{abc} \frac{J^c(w)}{(z-w)} \quad (4.34)$$

Where  $f_{abc}$  are the structure constants of our algebra, and  $\sim$  means equal up to non-singular terms.

Defining the current Laurent modes

$$J^a(z) = \sum_{n \in \mathbb{Z}} z^{-n-1} J_n^a \quad (4.35)$$

And inverting this to

$$J_n^a = \frac{1}{2\pi i} \oint dz z^n J^a(z) \quad (4.36)$$

We can now look at the commutator of two of current modes by the usual relation between the commutator and complex contour integrals:

$$[J_n^a, J_m^b] = \frac{1}{(2\pi i)^2} \left( \oint dw w^m \oint dz z^n - \oint dz z^n \oint dw w^m \right) \mathcal{R}(J^a(z)J^b(w)) \quad (4.37)$$

Where we can replace the radially ordered product  $\mathcal{R}(J^a(z)J^b(w))$  by the OPE (4.34). Fixing  $w$  temporarily, and noting that the difference between the  $z$  integrals amounts exactly to one  $z$  integral around the point  $z = w$ , we can write this as:

$$= \frac{1}{(2\pi i)^2} \oint_{w \approx 0} dw w^m \oint_{z \approx w} dz z^n \left( \frac{k\delta_{ab}}{(z-w)^2} + \sum_c i f_{abc} \frac{J^c(w)}{(z-w)} \right) \quad (4.38)$$

Expanding  $z$  around the point  $w$  as  $z = (w^n + (z - w)w^{n-1}n + \text{higher terms})$ , we get

$$= \frac{1}{2\pi i} \oint_{w \approx 0} dw \left( nw^{n+m-1}k\delta_{ab} + \sum_c i f^{abc} J^c w^{n+m} \right) \quad (4.39)$$

$$= nk\delta_{ab}\delta_{m+n,0} + \sum_c i f^{abc} J_{n+m}^c \quad (4.40)$$

$$(4.41)$$

Where we recognise exactly our original affine Lie algebra bracket with central element  $k$ .

**The Sugawara Construction** Up until now, while it's neat that our currents obey the affine extension of the algebra associated to our group manifold, it is not very clear why these WZW-models should be of any significance in our discussion, or even in the discussion of conformal field theory in general. The point that illustrates this is the following definition of the energy momentum tensor, referred to as the Sugawara construction.

$$T(z) = \frac{1}{2(k+g)} \sum_a : J^a J^a : (z) \quad (4.42)$$

Where the dots impose normal/radial ordering, and  $g$  is the dual Coxeter number of the finite Lie algebra associated to the group manifold. Recalling that the energy momentum tensor has an OPE with itself of the form:

$$T(z)T(w) \sim \frac{c/2}{(z-w)^2} + \frac{2T(w)}{(z-w)^2} + \frac{\partial T(w)}{(z-w)} \quad (4.43)$$

One finds[8]

$$c = \frac{k \dim(\mathfrak{g})}{k+g} \quad (4.44)$$

To see the Virasoro algebra that is indicative of a CFT, we expand  $T(z)$  in modes:

$$T(z) = \sum_n z^{-n-2} L_n \quad (4.45)$$

After which one can show that they obey the Virasoro algebra:

$$[L_n, L_m] = (n - m)L_{n+m} + \frac{c}{12}n(n^2 - 1)\delta_{n+m,0} \quad (4.46)$$

Thus in a sense, what the Sugawara construction provided us with, was an embedding of the Virasoro algebra in the original affine Lie algebra. Remarkably, the embedding is such, that the modules of highest weight representations of the affine Lie algebra overlap with modules of highest weight Virasoro representations (descending weights in the Virasoro representation match with descendants of primary fields in our WZW CFT). Still, the CFTs that can be described by these WZW-models all have a central charge bigger than 1 (in fact,  $\dim(E_8) = 248$ , so an affine  $E_8$  WZW model at level  $k = 1$  would have  $c = 248/31 = 8$ ). These are not the theories we are interested in, and we need another construction to take us home.

**Cosets** Let now  $\hat{\mathfrak{g}}$  be an affine Lie algebra at level  $k$ , and  $\mathfrak{f}$  a subalgebra of  $\hat{\mathfrak{g}}$  at level  $k'$ . We can construct an energy momentum tensor and associated modes for both of these through the Sugawara construction, resulting in  $L_n^{\hat{\mathfrak{g}}}$  and  $L_n^{\mathfrak{f}}$ . If we now define

$$L_n^{\hat{\mathfrak{g}}/\mathfrak{f}} := L_n^{\hat{\mathfrak{g}}} - L_n^{\mathfrak{f}}$$

We can look at the commutator

$$[L_n^{\hat{\mathfrak{g}}/\mathfrak{f}}, L_m^{\hat{\mathfrak{g}}/\mathfrak{f}}] = [L_n^{\hat{\mathfrak{g}}}, L_m^{\hat{\mathfrak{g}}}] - [L_n^{\mathfrak{f}}, L_m^{\mathfrak{f}}] \quad (4.47)$$

$$= (n - m)L_{n+m}^{\hat{\mathfrak{g}}/\mathfrak{f}} + (c(\hat{\mathfrak{g}}_k) - c(\mathfrak{f}_{k'}))n \frac{n^2 - 1}{12} \delta_{n+m,0} \quad (4.48)$$

From which we see that  $L_n^{\hat{\mathfrak{g}}/\mathfrak{f}}$  still obeys the Virasoro algebra, but with a different central charge, namely the difference between the central charges that the individual Virasoro

algebras would get:

$$c(\hat{\mathfrak{g}}/\mathfrak{f}) = \frac{k \dim \hat{\mathfrak{g}}}{k + g} - \frac{k' \dim \mathfrak{f}}{k' + g'} \quad (4.49)$$

Where  $g'$  is the dual Coxeter number of  $\mathfrak{f}$ .

These  $L_n^{\hat{\mathfrak{g}}/\mathfrak{f}}$  are therefore the modes of another Sugawara energy momentum tensor  $T^{\hat{\mathfrak{g}}/\mathfrak{f}} := T^{\hat{\mathfrak{g}}} - T^{\mathfrak{f}}$ .

Now if we recognise that the currents  $J_{\mathfrak{f}}^a$ , are weight 1 primaries w.r.t. both  $T^{\mathfrak{f}}$  and  $T^{\hat{\mathfrak{g}}}$ , then we can say:

$$T^{\mathfrak{f}} J_{\mathfrak{f}}^a \sim T^{\hat{\mathfrak{g}}} J_{\mathfrak{f}}^a \quad (4.50)$$

Such that

$$T^{\hat{\mathfrak{g}}/\mathfrak{f}} J_{\mathfrak{f}}^a = \left( T^{\hat{\mathfrak{g}}} - T^{\mathfrak{f}} \right) J_{\mathfrak{f}}^a \sim 0 \quad (4.51)$$

And since  $T^{\mathfrak{f}}$  is fully defined through the currents  $J_{\mathfrak{f}}^a$ , we can also conclude

$$T^{\hat{\mathfrak{g}}/\mathfrak{f}} T^{\mathfrak{f}} \sim T^{\hat{\mathfrak{g}}/\mathfrak{f}} J_{\mathfrak{f}}^a \sim 0 \quad (4.52)$$

The original  $T^{\hat{\mathfrak{g}}}$  can therefore be decomposed in two orthogonal (in the sense that their OPE vanishes) pieces:

$$T^{\hat{\mathfrak{g}}} = T^{\hat{\mathfrak{g}}/\mathfrak{f}} + T^{\mathfrak{f}} \quad (4.53)$$

With

$$[T^{\hat{\mathfrak{g}}/\mathfrak{f}}, T^{\mathfrak{f}}] = 0 \quad (4.54)$$

An especially interesting and simple case, is that of the diagonal cosets which we will write as:

$$\mathfrak{g}/\mathfrak{f} = \frac{\hat{\mathfrak{g}}_k \oplus \hat{\mathfrak{g}}_l}{\hat{\mathfrak{g}}_{k+l}} \quad (4.55)$$

Taking now  $\hat{\mathfrak{g}} = \hat{\mathfrak{su}}(2)$ , the affine extension of the  $\mathfrak{su}(2)$  algebra, and  $l = 1$ :

$$\mathfrak{g}/\mathfrak{f} = \frac{\hat{\mathfrak{su}}(2)_k \oplus \hat{\mathfrak{su}}(2)_1}{\hat{\mathfrak{su}}(2)_{k+1}} \quad (4.56)$$

We get a family of CFTs with central charges

$$c_{\mathfrak{g}/\mathfrak{f}} = 1 - \frac{6}{(k+2)(k+3)} \quad (4.57)$$

Which is exactly the series of central charges of minimal unitary models.

This leads us to a surprising conclusion: Every system that is described by a minimal unitary model has a description in terms of a field theory associated to a diagonal embedding of an affine Lie algebra.

**Operator Content** However, it would be nice if we could follow this description a bit further than just the central charge, and also find the correspondences between representations of the coset and the fields in the CFT (since as mentioned, the highest weight modules overlap). We first need to identify the representations of the coset. For this, we use again that the algebra splits into orthogonal components, and that we can decompose the representations according to (see [8] for more details)

$$\lambda = \bigoplus_{\mu} b_{\lambda\mu} \mu \quad (4.58)$$

Where  $\lambda$  is a representation of  $\mathfrak{g}$  and  $\mu$  of  $\mathfrak{f}$  (embedded in  $\mathfrak{g}$ ).

These branching functions  $b_{\lambda\mu}$  are then the natural candidates for the coset representation. There are subtleties with identifying fields and representations, since in practice this identification is done by comparing characters, but these cases are beyond the scope of this thesis, and I refer the interested reader to [8] and [18]. The key point to take away from this is not the technicalities in calculating the characters of representations, but rather

that we can make this identification between states in the Virasoro reps and the affine Lie algebra reps at all. It allows us to actually look at which primary fields the coset model contains, and thus which exact model it describes. There are different cosets that all lead to the same central charge. The  $c = \frac{1}{2}$  Ising CFT can for example be reached by taking  $k=1$  in a diagonal  $\hat{su}(2)_k$  coset:

$$\frac{\hat{su}(2)_1 \oplus \hat{su}(2)_1}{\hat{su}(2)_2} \quad (4.59)$$

But also, more relevant to our discussion, by a diagonal  $E_8$  coset at level 1:

$$\frac{(\hat{E}_8)_1 \oplus (\hat{E}_8)_1}{(\hat{E}_8)_2} \quad (4.60)$$

**Summary** The critical Ising model that we have been studying thus has a description in terms of a CFT with an affine Lie algebra as its current algebra. And remarkably, we can take as this algebra either the ‘most basic’ one,  $A_1(= su(2))$  or the ‘most exceptional’ one,  $E_8$ . We have thus found a point of contact between the Ising model and the algebra  $E_8$ .

## 4.4 Toda field theory

There is a second natural relation between CFTs, their deformations, and (affine) Lie algebra’s, namely in so-called Toda field theories. Starting from the classical Toda field equations which describe  $n$  scalar fields  $\tilde{\phi}_i$  self-interacting [19]:

$$\partial_\mu \partial^\mu \tilde{\phi}_i + \frac{m^2}{\beta} \sum_{j=1}^n A_{ij} e^{\beta \tilde{\phi}_j} = 0 \quad (4.61)$$

We can introduce new variables and make it describe fields taking values in the root-space of the Lie algebra  $\mathfrak{g}$  of which  $A_{ij}$  is the Cartan matrix:

$$\tilde{\phi}_i = \langle \alpha_i, \phi \rangle + \frac{1}{\beta} \log \frac{2n_i}{\langle \alpha_i, \alpha_i \rangle} \quad (4.62)$$

Where  $\langle \cdot, \cdot \rangle$  is the scalar product in the root space induced by the Killing form on  $\mathfrak{g}$ , and  $n_i$  is the  $i$ th Kac (or Coxeter) label, i.e. the projection of the highest root  $\theta$  on the  $i$ th basis vector of the root space. Our field equations are now the Euler-Lagrange equations of the following action:

$$S_{\text{TFT}} = \int d^2x \left( \frac{1}{2} \langle \partial_\mu \phi, \partial^\mu \phi \rangle - \frac{m^2}{\beta^2} \sum_{i=1}^r n_i e^{\beta \langle \alpha_i, \phi \rangle} \right) \quad (4.63)$$

Where the sum now goes up to  $\text{rank}(\mathfrak{g}) = r$ . It can be shown that these theories are actually conformally invariant, i.e. the sum of all marginal couplings stays exactly marginal. While interesting in their own right, what made people interested in Toda field theories is the fact that there is a very natural way to perturb them away from conformal invariance. This perturbation just needs to be an extra term in the potential that makes the total coupling marginally (ir)relevant, but the most interesting case would of course be an integrable<sup>3</sup> perturbation. It turns out that when adding a perturbation by adding a field  $\phi_{r+1}$ , and thus necessarily also a root  $\alpha_{r+1}$ , we get an integrable non-conformal theory as long as we take the new roots to be those of the affine extension of  $\mathfrak{g}$ , and  $n_{r+1} = 1$  [19]. We now write our potential as an explicit series in the fields  $\phi^i$ :

$$V(\phi) = \frac{m^2}{\beta^2} \sum_{i=1}^{r+1} n_i e^{\beta \langle \alpha_i, \phi \rangle} \quad (4.64)$$

$$= \frac{m^2}{\beta^2} \sum_{i=1}^{r+1} n_i \left( 1 + \beta \langle \alpha_i, \phi \rangle + \frac{1}{2} \beta^2 \langle \alpha_i, \phi \rangle \langle \alpha_i, \phi \rangle + \dots \right) \quad (4.65)$$

Now we are mainly interested in the term that is quadratic in our fields, since it is this term that will actually form our mass-squared matrix:

$$(M^2)_{ij} = m^2 \sum_{k=1}^{r+1} n_k (\alpha_k)_i (\alpha_k)_j \quad (4.66)$$

The eigenvalues of this operator will form the mass spectrum of our Toda theory. Up to a total normalisation, this matrix is fully specified given a Lie algebra  $\mathfrak{g}$ . In fact, for  $\mathfrak{g}$  a

---

<sup>3</sup>Integrable in the sense that the S-matrix factorises.

simply laced Lie algebra, it can be shown that the eigenvalues of this operator  $M^2$  will always be the components of the Perron-Frobenius eigenvector of the Cartan matrix of  $\mathfrak{g}$  [13]. For  $E_8$  we again get:

$$\begin{aligned}
 m_1 &= M & m_2 &= 2M \cos\left(\frac{\pi}{5}\right) \\
 m_3 &= 2M \cos\left(\frac{\pi}{30}\right) & m_4 &= 2m_2 \cos\left(\frac{7\pi}{30}\right) \\
 m_5 &= 2m_2 \cos\left(\frac{2\pi}{15}\right) & m_6 &= 2m_2 \cos\left(\frac{\pi}{30}\right) \\
 m_7 &= 4m_2 \cos\left(\frac{\pi}{5}\right) \cos\left(\frac{7\pi}{30}\right) & m_8 &= 4m_2 \cos\left(\frac{\pi}{5}\right) \cos\left(\frac{2\pi}{15}\right)
 \end{aligned}$$

The exact mass spectrum Zamolodchikov found through his S-matrix bootstrap procedure.

## 4.5 Hidden geometry

We will now show a striking, remarkably visual, correspondence between the scattering theory that Zamolodchikov proposed and geometry in the root space of  $E_8$ . This space is the 8-dimensional vector space in which the 240 roots of  $E_8$  live. A 2D projection is shown on the front page of this thesis. All of these roots have a squared length of 2, and with each root  $\alpha$  we can associate a reflection  $r_\alpha$  in a 7D hyperplane orthogonal to  $\alpha$  itself. Denoting the full set of roots by  $\Phi$ , we can look at the set  $\{r_\alpha\}, \alpha \in \Phi$ , endowed with the operation of successive reflection, which is referred to as the Weyl group  $\mathcal{W}$ . The action of an element  $r_\alpha$  is defined as

$$r_\alpha(x) = x - 2 \frac{\langle \alpha, x \rangle}{\langle \alpha, \alpha \rangle}, \text{ where } x \in \text{span}(\Phi) \quad (4.67)$$

and  $\langle \cdot, \cdot \rangle$  is the usual scalar product on the root space. Now since we can compose these reflections to make other reflections in  $\mathcal{W}$ , and since adding the simple roots together can generate all of  $\Phi$ , we can actually generate all of  $\mathcal{W}$  by just those  $r_\alpha$  where  $\alpha$  is a simple root. We thus arrive at the following set of generators for  $\mathcal{W}$ :  $\{r_1, r_2, \dots, r_8\}$ . Looking at the definition of the reflections, we see that the only information we need are mutual inner products of the simple roots, which are completely contained in both the Cartan matrix and the Dynkin diagram. So far, this whole construction could be followed for any Cartan

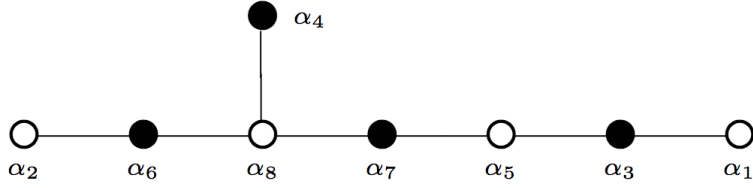


Figure 4.1: The Dynkin diagram of  $E_8$ . It is a bipartite graph that separates into a black and a white subgraph, that each contain only nodes (i.e. roots) that share no edge (i.e. are mutually orthogonal). Source: [10]

matrix, but we will now use a particular property of  $E_8$ , namely that the simple roots can be separated into two sets that each comprise only roots that are mutually orthogonal, the black roots and the white roots (see figure 4.1).

**Orbits** We can write down an element  $w \in \mathcal{W}$  in so-called Steinberg ordering, in which all reflections w.r.t. black roots are to the left of the reflections w.r.t. white roots. Since reflections in orthogonal planes commute, the only thing that matter is white first vs. black first, but this just amounts to switching from  $w$  to  $w^{-1}$ . Following the convention of Dorey [11], we will write  $w^{-1} = r_8 r_5 r_2 r_1 r_7 r_6 r_4 r_3$ . Note that since  $\Phi$  is finite, orbits of a particular element of  $\Phi$  must close under the repeated action of this element  $w^{-1}$ . Using the code from the appendix A.2, we look at these orbits, and track the coefficients of the simple roots over time. The results can be seen in figure 4.3.

Note that for all orbits, the recurrence time is exactly 30, i.e.  $w^{30}(\alpha) = \alpha, \forall \alpha \in \Phi$ . In fact, what can also be seen from the plots, and actually holds in general for  $E_8$ , is that  $w^{15} = -\mathbf{1}$ .

The relevance of this discussion is not immediately clear, but an inspection of the pole structure of Zamolodchikov’s S-matrix can reveal a pattern.

**Pole Structure** In our discussion of the S-matrix in the previous chapter, we found a way to write this matrix as a product of fundamental building blocks ( $x$ ). In particular, we found

$$S_{11} = -(2)(10)(12)(18)(20)(28) \tag{4.68}$$

If we identify the block (0) with a factor 1, and the block (30) with a factor of -1, then we

can actually simplify this expression by introducing the new block  $[x] = (x - 1)(x + 1)$ , so that we can  $S_{11}$  as:

$$S_{11} = [1][11][19][29] \tag{4.69}$$

This seems quite arbitrary, but it actually turns out that we can write all the sectors of  $S$  in this way. Two more examples are [10]:

$$S_{12} = [7][13][17][23] \tag{4.70}$$

$$S_{13} = [2][10][12][18][20][28] \tag{4.71}$$

Now these series of numbers don't really seem to mean a lot at first sight, they certainly don't show up in any of the same sequences in the OEIS (Online Encyclopedia of Integer Sequences). However, there is a hidden pattern here. If we draw a number line, and place a rectangle on top of the number  $x$ , ranging from  $i(x - 1)\pi/30$  to  $i(x + 1)\pi/30$ , we get the pattern in figure 4.2. The exact same pattern can be seen in the  $\alpha_1$  and  $\alpha_2$  coefficients in the orbit of  $\alpha_1$  under the Coxeter element. This is remarkable: The pole structure in the scattering theory of Zamolodchikov is actually completely determined by the reflections of the Weyl group of the simple  $E_8$  roots. In fact, this principle holds more generally: a particle of type  $i$  can form a bound state with one of type  $j$  at relative rapidity  $i(x - 1)\pi/30$  or  $i(x + 1)\pi/30$ , as long as  $w^x(\alpha_i)$  has a nonzero coefficient for root  $\alpha_j$ . The whole bootstrap procedure, a laborious and awkward exercise, is thus equivalent to simply calculating orbits of simple roots under the Coxeter element.

**Reflections on Reflections** We have now seen a number of ways in which  $E_8$  plays a role in the scattering theory of the scaling limit of the Ising model:

- Assuming a  $\mathbb{Z}_2$  perturbation, we included a cubic field interaction that allowed for a conserved bootstrap procedure to predict eight particles with masses related to each other by an eigenvector of the  $E_8$  Cartan matrix.
- We then constructed a CFT where the fields take values on the group manifold associated to the Lie algebra of the diagonal coset of the affine extension of  $E_8$ , and

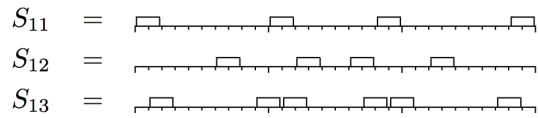


Figure 4.2: The distribution of blocks on the positive number line for the scattering sector of the first particle with the first three particles. Source: [10]

ended up with a theory with the same central charge and field content as the scaled critical Ising model.

- Starting from a conformally invariant Toda Field theory, we found that letting the fields take values in the root space of affine  $E_8$ , and having them interact with its simple roots through the Toda potential leads to the same spectrum of particles as Zamolodchikov found.
- The full pole structure, and thus the pattern of bound states, that emerges in the S-matrix of the perturbed Ising model is hidden in the mutual reflections of the simple roots of  $E_8$ .

While our understanding of the role of  $E_8$  has thus certainly increased since Zamolodchikov first found his S-matrix, all these leads are still very mysterious and leave a lot unexplained. Why does the affine extension correspond to a perturbation? Was there already an  $E_8$  structure present in the unperturbed Ising model? Do we actually need the full structure of  $E_8$  as a Lie algebra, or is everything we need the geometry of its eight simple roots? Most notably, none of these theories can actually tell us what those bound states are made of, and everything we have seen so far is only true in the scaling limit, while the model we were originally investigating, the Ising model, is fundamentally only defined on a discrete lattice. Puzzled but intrigued, hoping for more insight, we now leave continuous space behind us, and turn our attention to a very different kind of mathematical physics: discrete lattice models.

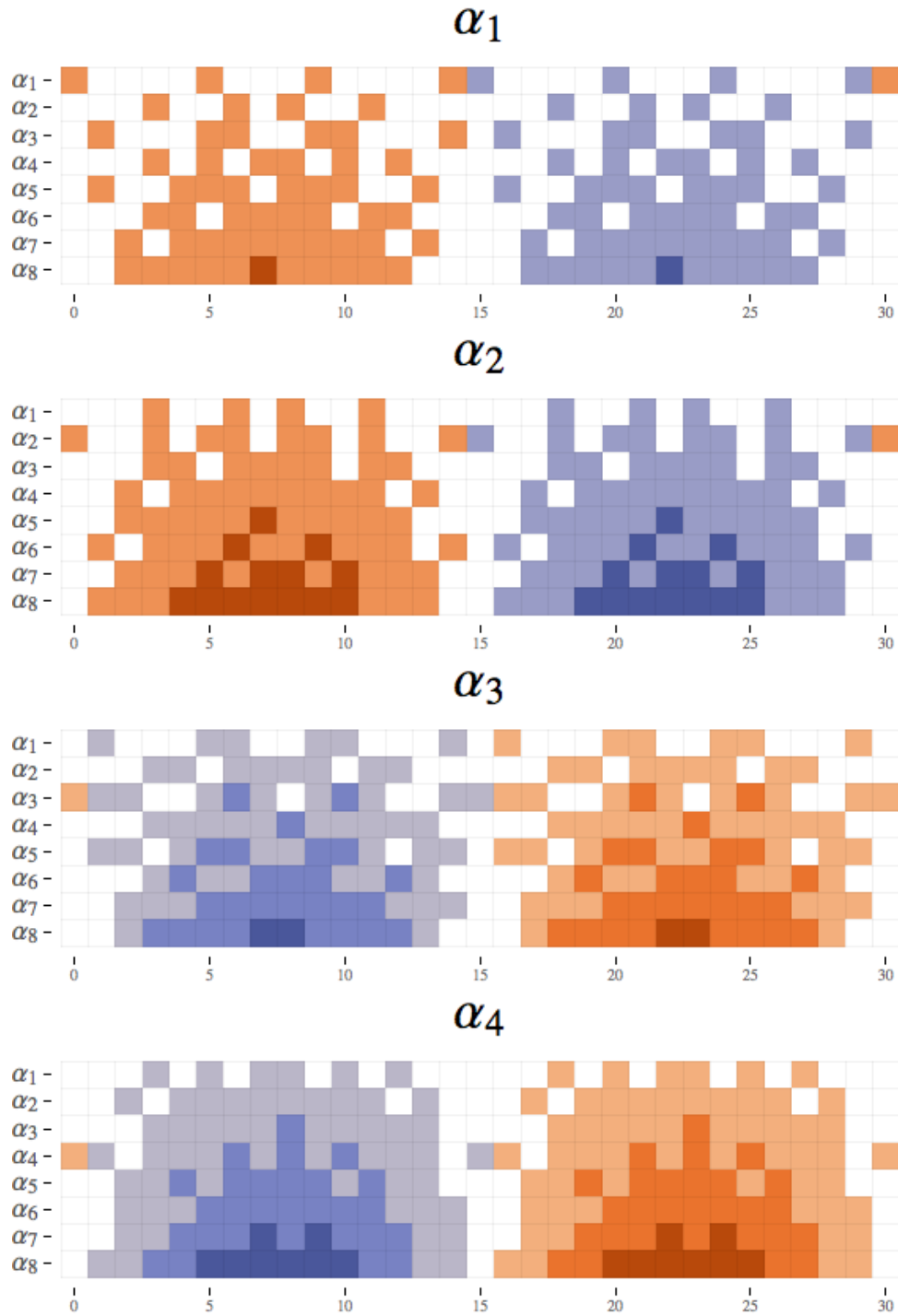


Figure 4.3: Plots of the orbits of all eight roots under the Coxeter element. on the x-axis there are the consecutive powers of  $w$ , on the y-axis there are the eight roots. Blue colours are negative coefficients, orange colours are positive, both normalised to the largest coefficient in the orbit.

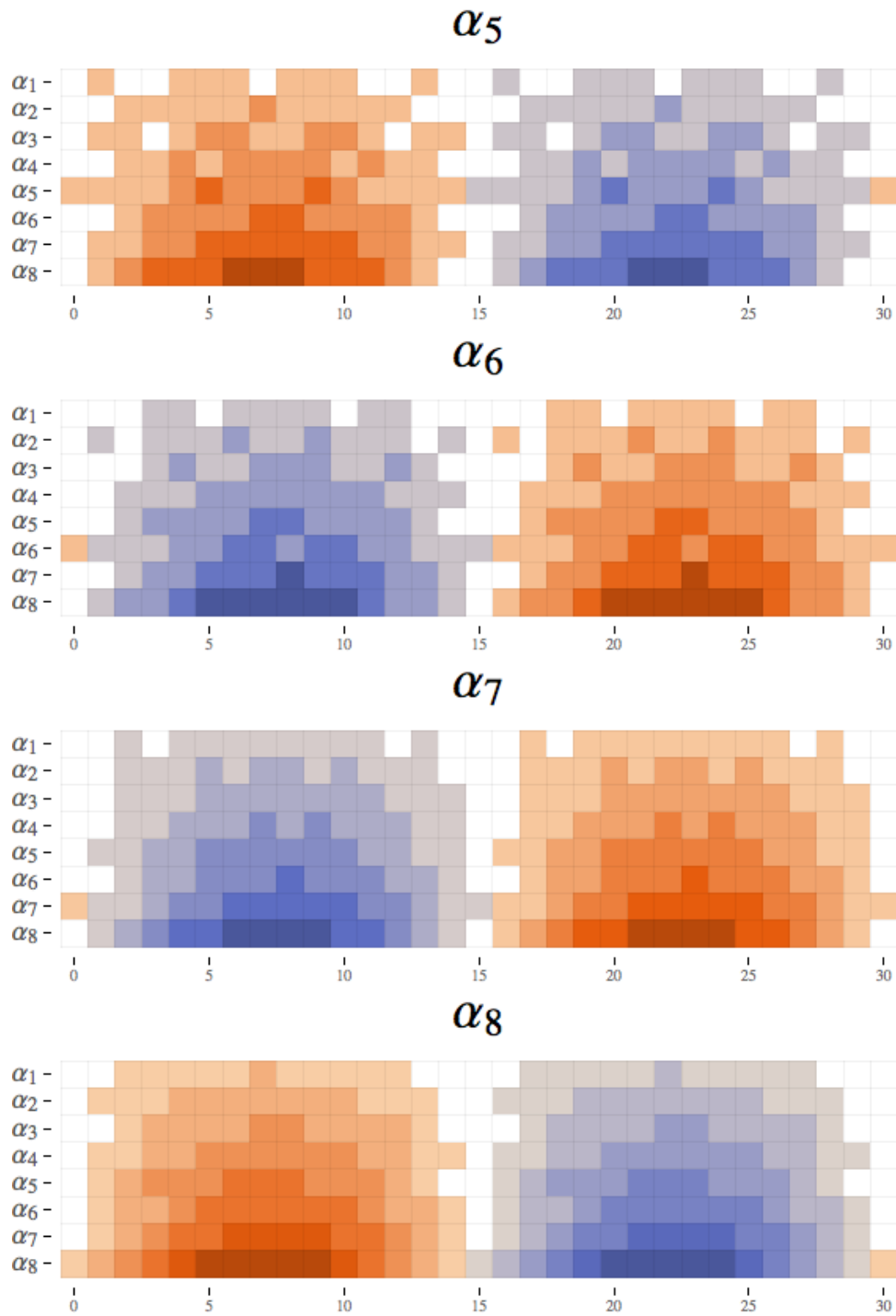


Figure 4.3: (Continued)

# 5

## Back to Lattice Models

*Statistical physics is the repeated translation of models into each other, until one arrives at a model that was solved by Baxter.* - Eytan Domany, 2017 [9]

In the previous chapters, we have explored a number of ways in which either the group  $E_8$ , its associated algebra, or just some properties of those can be linked to the magnetic perturbation of the Ising Model. In a sense though, Zamolodchikov's main point has still been unexplored. His main conjecture in the original paper was that there should be a solvable lattice model in the universality class of the magnetic Ising model that has these eight particles as excitations on its lattice. That is indeed the best thing we can hope for, since we do not have an exact solution to the magnetic Ising model itself. The previous chapters have certainly made this conjecture more plausible, but have not gotten us closer to the explicit version of this lattice model, nor explained what those eight particles actually are. There has been progress on this front, which we will review here in this second part of the thesis. Central will be the paper [3], by Bazhanov, Nienhuis and Warnaar, where they find that an integrable off-critical deformation of the dilute  $A_3$  model shows the same  $E_8$  structure in the the solutions of its (thermodynamic) Bethe Ansatz. These solutions are notoriously ambiguous though, and it is not very clear what these excitations are in terms of more natural quantum numbers. We know that this dilute  $A_3$  model lies in the same universality class as the Ising model, which leads us to the conjecture that it must also have a natural description in terms of the Ising free fermions. On top of that, it offers an off-critical integrable extension that reveals the eight excitations. If we manage to link these two descriptions, we could thus find a description of the eights particles in

terms of free fermion momentum occupation numbers. Throughout the rest of this thesis, this will be our main goal.

As inspiration, we first look at the critical spin- $\frac{1}{2}$  Ising model, which famously has a description in terms of its free fermions, but also allows for a translation to the integrable 6-vertex model and thus can be described by its own Bethe Ansatz. The steps needed to translate the critical Ising model into a Bethe Ansatz are very similar to those needed to arrive at the Bethe Ansatz of the dilute  $A_3$  model, so we first practice and review these steps in this simpler case. The main object of study will be the transfer matrix, since it is the main tool of the algebraic Bethe Ansatz, and all the translations fundamentally link partition sums, which can be canonically defined by the system's transfer matrix. Once we've successfully connected the free fermion Ising transfer matrix to the one of the six-vertex Bethe Ansatz (the top row in figure 5.1), we will, in the next chapter, turn our attention towards the dilute  $A_3$  model. With the Bethe Ansatz results from [3], we hope to establish, as we first did for the critical Ising model, a link between the transfer matrix eigenvalues of the dilute  $A_3$  model in terms of Bethe quantum numbers and those in terms of the more natural free fermion quantum numbers (corresponding to the path in the bottom row of figure 5.1).

## 5.1 Transfer matrix spectrum of a diagonal Ising model

It turns out that in the correspondence between the Ising model on a square lattice and a 6-vertex model, the original Ising lattice will be rotated by  $\pi/2$ , so to be able to treat the 6-vertex model on a normal square lattice, we will look at the Ising model on a square lattice, rotated by  $\pi/2$  (see figure 5.2).

We impose periodic boundary conditions, and get a bipartite lattice with two different transfer matrices  $D_1$  and  $D_2$ , both operators acting on a spin chain  $\phi = (\mu_1, \mu_2, \dots, \mu_M)^1$

---

<sup>1</sup>We take the lattice to be homogeneous and isotropic to simplify notation. All results generalise to the situation in which the horizontal and vertical couplings of the unrotated lattice take respective values  $J_h$  and  $J_v$ . Simply changing all functions  $f(2J)^2$  to be  $f(2J_h)f(2J_v)$  gives the inhomogeneous results.

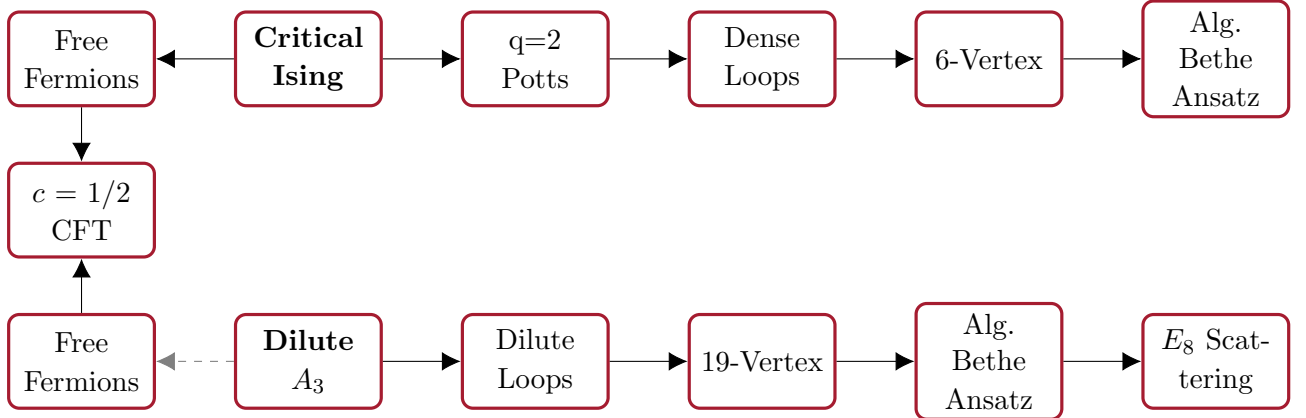


Figure 5.1: An overview of the different models we'll encounter in the next sections, and their mutual relations. Most of the words have not been defined yet, so this diagram mainly serves as a reference to come back to later. The key point is that we are going to start with the top row, and look at the link between critical Ising free fermions and its algebraic Bethe Ansatz through dense loops and the 6-vertex model. In a later chapter we will then cover the bottom row, where we go from the dilute  $A_3$  model to a Bethe Ansatz that contains the  $E_8$  scattering matrix. The link towards the free fermions in the bottom row is less exact, but this nuance will also be addressed later.

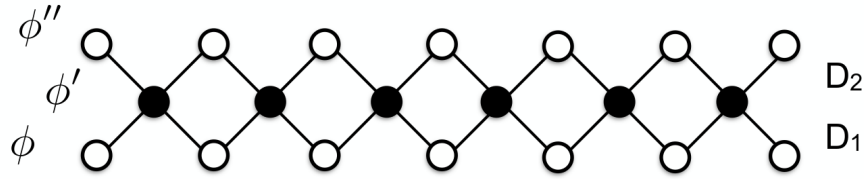


Figure 5.2: Three rows,  $\phi$ ,  $\phi'$  and  $\phi''$ , on a diagonal lattice. Source: [15]

$$(D_1)_{\phi, \phi'} = \exp\left(J \sum_{j=1}^M \mu_j \mu'_j + \mu_{j+1} \mu'_j\right) \quad (5.1)$$

$$(D_2)_{\phi', \phi''} = \exp\left(J \sum_{j=1}^M \mu'_j \mu''_j + \mu'_j \mu''_{j+1}\right) \quad (5.2)$$

However, we are interested in diagonalising the full transfer matrix  $T = D_1 D_2$ . It is shown in the appendix A.3 that both these matrices commute with another operator acting on the same chain: the 1D quantum Ising Hamiltonian:

$$H = \sum_{j=1}^M (\sigma_j^x + S \sigma_j^z \sigma_{j+1}^z)$$

Which, by identifying  $\sigma^x$  as the spin-flip Pauli operator, and  $\sigma^z$  as the diagonal Pauli spin matrix, we can also write in  $\mu$ -basis:

$$H_{\mu\mu'} = \sum_{j=1}^M (\delta_{\mu_1, \mu'_1} \delta_{\mu_2, \mu'_2} \dots \delta_{\mu_j, -\mu'_j} \dots \delta_{\mu_M, \mu'_M}) + S \mu_j \mu_{j+1} \delta_{\mu, \mu'}$$

Since both  $D_1$  and  $D_2$  commute with  $H$ , their product also does, and the full transfer matrix  $T$  and  $H$  can be simultaneously diagonalised.

In the appendix A.4 we write the Hamiltonian in terms of fermion operators in momentum space, using the diagonalisation of this operator as done in [35].

The total eigenvalue of the transfer matrix is  $\Lambda = \prod_{0 \leq q \leq \pi} \lambda(q)$ , where we have to make a choice for  $\lambda(q)$  for each factor in the product, since for every  $q \neq 0, \pi$  there are four options:  $q$  and  $-q$  are both occupied, either is, or neither are. These are respectively:

$$\lambda_{1,1}(q) = 2(\cosh^2 2J + R_q) \quad (5.3)$$

$$\lambda_{1,0}(q) = \lambda_{0,1}(-q) = 2 \sinh 2J (1 - e^{-iq}) \quad (5.4)$$

$$\lambda_{0,0}(q) = 2(\cosh^2 2J - R_q) \quad (5.5)$$

Where  $R_q = \sqrt{1 + S^2 + 2S \cos q}$  and  $S = \sinh^2 2J$

These different choices correspond to different fermion occupations, so every eigenvalue can thus be identified with a fermion occupation.

There is a nuance to address. Remember that  $q$  ranges in  $(-\pi, \pi]$ , and goes in steps of  $2\pi/N$ . We still should check exactly which values our boundary conditions impose. Our original boundary conditions in real space were periodic:  $\sigma_{M+1}^i = \sigma_1^i$ . These boundary conditions are more subtle however for fermionic operators, being dependant on the even/oddness of the number of fermions. Luckily, we can see from the definition of the Hamiltonian in terms of these operators that fermions can only be created or destroyed in pairs, so the overall parity of the fermion number is conserved, and the Hilbert space

decomposes in separate even and odd sectors as  $\mathcal{H} = \mathcal{E} \oplus \mathcal{O}$ . Defining  $\mathcal{P}$  as the projection operator on the even subspace  $\mathcal{E}$ , we can write  $c_{M+1}^{(\dagger)} = c_1^{(\dagger)}(1 - 2\mathcal{P})$ , and capture all boundary conditions.

Looking at the Fourier decomposition,

$$c_{M+1}^{(\dagger)} = \frac{1}{\sqrt{M}} e^{(-)ik(M+1)} c_k^{(\dagger)} \quad (5.6)$$

We demand this to be equal to  $c_1^{(\dagger)}(1 - 2\mathcal{P})$ , and can conclude that:

$$k = \frac{2\pi}{M} j \quad (5.7)$$

with

$$(5.8)$$

$$j \in \left(-\frac{M}{2}, \frac{M}{2}\right] \cap \mathbb{Z} + \frac{1}{2} \quad \text{in the sector } \mathcal{E} \quad (5.9)$$

$$j \in \left(-\frac{M}{2}, \frac{M}{2}\right] \cap \mathbb{Z} \quad \text{in the sector } \mathcal{O} \quad (5.10)$$

We have assumed our total number of lattice sites  $M$  here to be even. If  $M$  is odd, then the two sectors switch momentum values.

With this information, we are indeed able to identify a fermion momentum occupation with each eigenvalue of the transfer matrix. Tables of this for some small system sizes can be found in the appendix A.5. With this identification in hand, we can continue into the other direction (in fig. 5.1), and work towards the Bethe Ansatz, starting from a loop model.

## 5.2 From spin models to loop- and vertex-models

We start our discussion with the definition of the  $q$ -state Potts model on a lattice  $\mathcal{L}$ . This is not the model we are necessarily interested in, but a more general model of which our Ising model is a special case. Since it is not really more complicated to work with, we will

keep things as general as possible for a while. Each vertex has a spin  $\sigma$  that takes a value in  $\{1, 2, \dots, q\}$ . Any two vertices that are connected by an edge contribute an energy  $\epsilon$  if they are in the same spin-state. This leads to the following partition sum:

$$Z_q = \sum_{\text{spin cfg.}} \exp\left(\beta\epsilon \sum_{\langle i,j \rangle} \delta_{\sigma_i, \sigma_j}\right) \quad (5.11)$$

Where the sum over  $\langle i, j \rangle$  is over pairs of nearest neighbours  $(i, j) \in \mathcal{L}$ .

We now go back to our Ising model, and see that we can indeed write its partition sum in terms of the partition sum of this Potts model<sup>2</sup>:

$$Z_{\text{Ising}} = \sum_{\text{cfg.}} e^{\sum_{\langle i,j \rangle} K\sigma_i\sigma_j} \quad (5.12)$$

$$= \sum_{\text{cfg.}} e^{\sum_{\langle i,j \rangle} 2K\delta_{\sigma_i, \sigma_j} - K} \quad (5.13)$$

$$\propto \sum_{\text{cfg.}} e^{\sum_{\langle i,j \rangle} 2K\delta_{\sigma_i, \sigma_j}} \quad (5.14)$$

$$= Z_q \quad (5.15)$$

Where in the last equality we set  $q=2$ , and take the Potts coupling to be twice the Ising coupling.

This Potts sum can be rewritten if we define  $v := e^{\beta\epsilon} - 1$ :

$$Z_q = \sum_{\text{spin cfg.}} \prod_{\langle i,j \rangle} (1 + v\delta_{\sigma_i, \sigma_j})$$

This product consists of  $E$  binomial factors, where  $E$  is the number of edges in  $\mathcal{L}$ . If we were to fully write out this product, we would end up with  $2^E$  terms, each corresponding to a unique list of  $E$  choices between the first term (1), or the second term ( $v\delta_{\sigma_i, \sigma_j}$ ) in the factors. If we now take the vertices of  $\mathcal{L}$ , and only draw an edge between  $(i, j)$  if we took the ( $v\delta_{\sigma_i, \sigma_j}$ ) in the expansion of the product, we can associate a graph  $G$  on  $\mathcal{L}$  to each term in the expansion of the product (see figure 5.3).

If this graph contains  $l$  edges, the associated term in the expansion of the product has a

---

<sup>2</sup>One can understand this intuitively by recognising that the Ising model is basically a model of two different nearest neighbour configurations, with two different energies. The Potts model then just generalises this to  $q$  different configurations with two different energies.

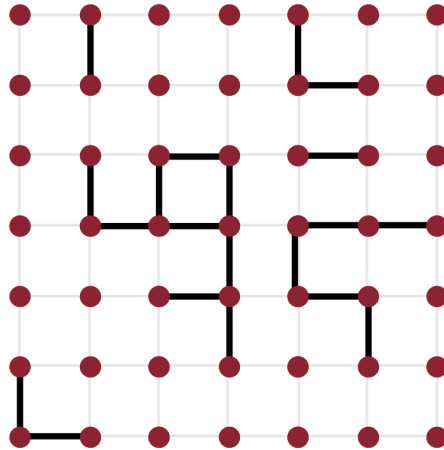


Figure 5.3: An example of clusters on the square lattice. This graph has 20 edges and  $6(+20)$  connected components, so will contribute a factor of  $q^{6+20}v^{20}$  to the partition sum.

weight  $v^l$ .

This representation of the Potts partition function is called the Fortuin-Kasteleyn cluster representation (introduced in [12]), where *cluster* refers to a connected component of the graph. What is left is the summation over all spin configurations. The delta functions, however, restrict clusters to have all vertices in the same spin-state, so summing over all possibilities amounts to an overall multiplicative factor:

$$Z = \sum_{G \in \mathcal{L}} q^C v^l$$

Where the sum is now over all possible graphs on  $\mathcal{L}$ .

So far we've considered all edges equivalent, but this is of course neither necessary nor realistic. Without making the energies  $q$ -dependent, we can already define multiple classes of edges on the lattice (e.g. horizontal and vertical edges on the square lattice). The partition sum is then generalised to:

$$Z = \sum_{G \in \mathcal{L}} q^C \prod_r v_r^{l_r}$$

where  $r$  labels the different classes of edges.

We now have a lattice with a (possibly disconnected) graph  $G$ . We can then look at the so-called 'medial' lattice  $\mathcal{L}'$  associated to  $\mathcal{L}$ . The construction of this lattice is explained in detail in [2], and we show an example for a general planar lattice in figure 5.4.

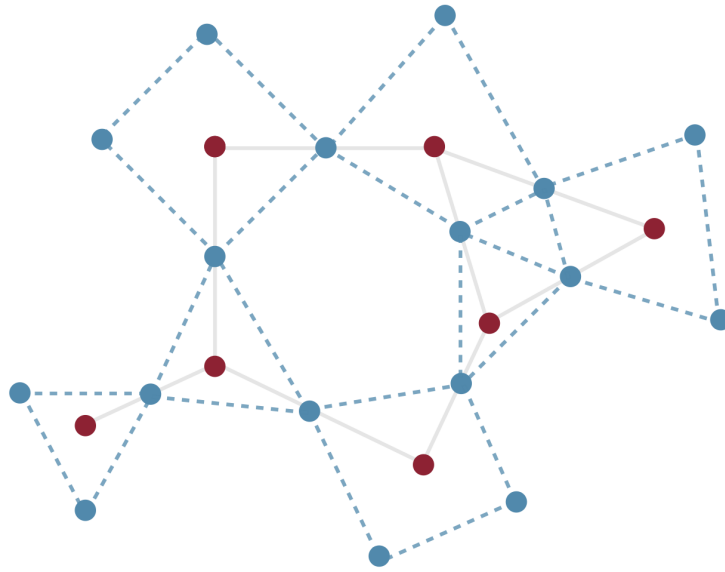


Figure 5.4: A planar lattice (red dots, solid lines) and its medial, or surrounding lattice (blue dots, dashed lines).

This medial lattice in a sense 'surrounds' the original lattice, and around every connected component of a graph  $G$  on  $\mathcal{L}$ , we can draw a polygon on  $\mathcal{L}'$  (we use the definition of polygon here where the interior of the shape is excluded). Components of  $G$  with cycles will be associated to two polygons on  $\mathcal{L}'$ , one surrounding, and one within the cycle (see figure 5.5).

Denoting the number of polygons on  $\mathcal{L}'$  by  $p$ , and the number of cycles in  $G$  by  $S$ ,  $\mathcal{L}'$  is decomposed into  $p = C + S$  polygons, and we can use the Euler characteristic for planar graphs:

$$v - e + f - C = 1$$

Where  $v$  is the number of vertices,  $e$  the numbers of edges,  $f$  the number of faces<sup>3</sup>, and  $C$  the number of connected components. In our case:

$$N - \sum_r l_r + (S + 1) - C = 1$$

---

<sup>3</sup>We include the exterior face here, and take the point of view where a connected graph corresponds to a stereographic projection of a polygon decomposition of the sphere (with Euler characteristic 2).

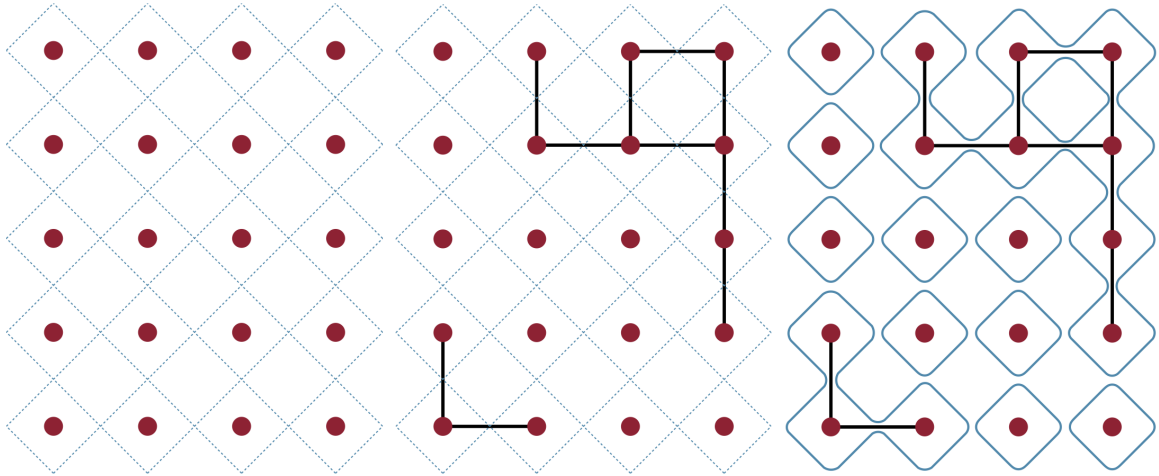


Figure 5.5: Here we see the individual steps in the construction of the polygons. We start with the square lattice (red dots) and generate the medial lattice (left). Then, we draw the Fortuin-Kasteleyn clusters corresponding to a term in the partition sum (middle). Finally, we draw loops on the medial lattice, in such a way that every connected component gets surrounded by a loop, and their cycles get filled in with loops (right).

Or equivalently

$$2C = N + p - \sum_r l_r$$

So that we can now rewrite the partition sum as:

$$Z = q^{N/2} \sum_{\mathcal{P} \in \mathcal{L}'} q^{p/2} \prod_r x_r^{l_r} \quad (5.16)$$

Where we have defined  $x_r := q^{-1/2}v_r$  and the summation is now over all polygon decompositions  $\mathcal{P}$  of the medial lattice  $\mathcal{L}'$ .

**Models on Diagrams** The construction we have just seen is an example of a more general procedure, introduced by Pasquier in the late 80s [25] [26]. He considered spin models on periodic lattices, where the spins take values on a graph (we will refer to these models as Pasquier models). This means the following:

- Take any graph  $\mathcal{G}$ .
- Sites of the lattice can be in either of  $r$  states, or heights, where  $r$  is the order of the graph  $\mathcal{G}$ , i.e. the number of nodes.

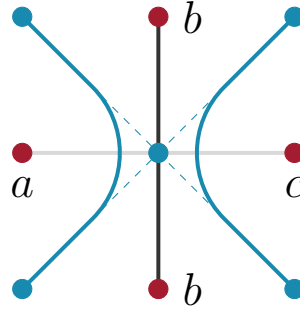


Figure 5.6: Our original (rotated) square lattice with vertices (red dots) in states  $a$ ,  $b$  and  $c$ . Two of the vertices are in the same state  $b$ , so they share a bond (black line), and create two domain walls (solid blue line) on the dual lattice (blue dots and dashes)

- Two connected (e.g. nearest neighbour) sites  $(\alpha, \beta)$  can be in states  $(a, b)$  if and only if the nodes  $a$  and  $b$  share an edge in  $\mathcal{G}$ .

These diagrams come with a so-called adjacency matrix  $A$ . We write  $a \sim b$  if nodes  $a$  and  $b$  share an edge in  $\mathcal{G}$ . The adjacency matrix is then defined as follows:

$$A_{ab} = \begin{cases} 1 & \text{if } a \sim b \\ 0 & \text{otherwise} \end{cases} \quad (5.17)$$

Since each vertex takes a value on the diagram, domain walls form between sites in states that share an edge in the diagram. These domain walls can then be naturally defined as running along the edges of the dual lattice (see fig. 5.6).

We give a local boundary between state  $a$  and  $b$  the following weight:

$$A_{ab} \left( \frac{S_a}{S_b} \right)^{1/4} \quad (5.18)$$

Resulting in the partition sum of local weights:

$$Z_{\mathcal{G}} = \sum_{\text{cfg.}} \prod_{\text{vert. } k} \left( W_k \prod_{\text{l.d.w.}} A_{ij} \left( \frac{S_j}{S_i} \right)^{1/4} \right) \quad (5.19)$$

The first sum is over all allowed height configurations of the lattice, where each configuration gets a weight that is the product over all vertices of some factor  $W_k$  that just depends

on the local geometry of the domain walls, and a product over the actual local domain walls (l.d.w.) present. Most importantly, since one always encounters four more turns clockwise than counterclockwise<sup>4</sup> (or the other way around), a full domain wall, a closed loop, will then always amount to

$$A_{ij} \left( \frac{S_a}{S_b} \right) \quad (5.20)$$

The trick now is to define the weights  $S_a$  in a clever way. If we define the vector of weights  $S$  to be the Perron-Frobenius eigenvector<sup>5</sup> of the matrix  $A$ , then summing over all allowed heights inside the loop, as we will invariably do when calculating the partition sum, will give the following weight to the loop:

$$W_{\text{loop}} = \sum_j A_{ij} \frac{S_j}{S_i} = \Lambda \quad (5.21)$$

Where  $\Lambda$  is the Perron-Frobenius eigenvalue of the matrix  $A$ .

Note, however, that when we impose periodic boundary conditions in at least one direction, loops can form that actually don't contribute  $\Lambda$ , but rather just  $A_{ab}$ , since their left- and right turns cancel to close in on themselves around the cylinder. The product over these weights is always 0 (if two adjacent domains are not in adjacent states on  $\mathcal{G}$ ) or 1. Their net effect is thus that we have to sum over all allowed configurations of a stack of slices of the cylinder/torus. On the torus, the last sum that has to be done is thus over all possible closed paths of  $N_w$  steps on the the diagram, where  $N_w$  is the number of domains that wind the periodic cycle. That number is simply the trace of  $A^{N_w}$ . The full partition sum is therefore:

$$Z = \sum_j \sum_{\text{cfg. vertices k}} \prod W_k \Lambda^{N_c} \lambda_j^{N_w} \quad (5.22)$$

---

<sup>4</sup>That is, as long as every bend along a domain wall is a quarter ( $\pi/2$ ) turn, one can generalise this to other lattices with bending angle  $\gamma$  by changing the exponent  $\frac{1}{4}$  to  $\frac{\gamma}{2\pi}$ .

<sup>5</sup>This is the vector whose existence is implied by the Perron-Frobenius theorem: A real, square, non-negative matrix will have a unique largest real eigenvalue, and there is a basis in which the components of the corresponding eigenvector are all nonnegative.

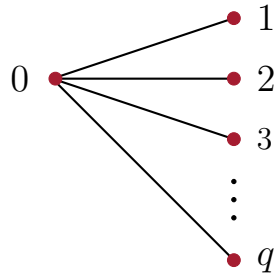


Figure 5.7: The diagram associated to the  $q$ -state Potts model. There are  $q$  nodes on the right, each connected to a ‘neutral’ node  $0$  on the left.

Where  $\lambda$  is the vector of eigenvalues of  $A$ .

What is left to specify are the weights  $W_k$ , that only depend on the geometry of the local domain walls. This depends on the algorithm we used to draw the domain walls. To arrive at the partition sum of the Potts model on a square lattice  $\mathcal{L}$ , we use the following construction:

- Take as sites of a new lattice  $\mathcal{L}'$  the sites of the union of  $\mathcal{L}$  and its dual, and connect these sites diagonally to their nearest neighbours (this is effectively a doubling of the square lattice, and a rotation by  $\pi/2$ ).
- The graph corresponding to the  $q$ -state Potts model is then the one in figure 5.7.
- Draw the Fortuin-Kasteleyn clusters of sites in the same states on the *original* lattice  $\mathcal{L}$  (effectively ignoring the neutral supercluster in state 0).
- Draw domain walls along the edges of the lattice dual to  $\mathcal{L}'$ .
- Take as local weights  $W_k$  either 1 or  $v$ , corresponding to a domain wall configuration that reflects respectively an open or closed edge in the Fortuin-Kasteleyn decomposition.

We effectively just doubled our lattice and introduced a neutral site to make neighbouring spins on our original lattice independent, rather than determined by an adjacency matrix. We also used that the medial square lattice and the dual of the union of the square lattice and its dual have the same sites. One can check that this indeed gives the exact same

loops, and the  $q \times q$  connectivity matrix of the diagram in figure 5.7 is:

$$A^{\text{Potts}} = \begin{pmatrix} 0 & 1 & \dots & 1 \\ 1 & & & \\ \vdots & & & \\ 1 & & & \end{pmatrix} \quad (5.23)$$

with eigenvalues

$$\lambda = \sqrt{q}, -\sqrt{q}, 0, \dots, 0 \quad (5.24)$$

We get the same loops, and the same loop weight, as in equation (5.16), but the added information that for loops around a periodic cycle, we have to sum over  $\sqrt{q}$  and  $-\sqrt{q}$  as weights for non-contractible loop. Our full partition sum for such a Pasquier model becomes:

$$Z = \sum_j \sum_{\mathcal{P} \in \mathcal{L}} \Lambda^{N_c} \lambda_j^{N_w} \prod_r v_r^{l_r} \quad (5.25)$$

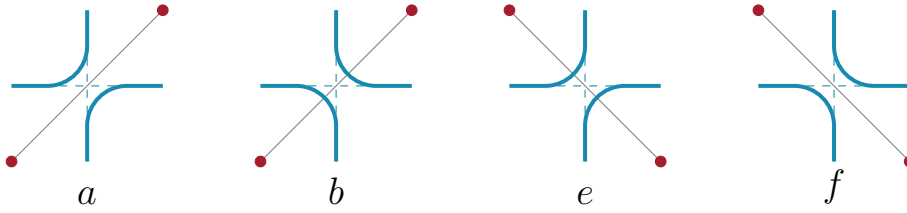
**An Example** To verify this, and see the translation in action, let's look at a simple case: an  $L = 1$  anisotropic Ising model with SW $\rightarrow$ NE coupling  $J_1$ , and SE $\rightarrow$ NW coupling  $J_2$ . It comes with the following transfer matrix:

$$T_{\text{Ising}} = \begin{pmatrix} e^{J_1+J_2} & e^{-J_1-J_2} \\ e^{-J_1-J_2} & e^{J_1+J_2} \end{pmatrix} \quad (5.26)$$

With eigenvalues:

$$\begin{bmatrix} 2 \operatorname{sh}(J_1 + J_2) \\ 2 \operatorname{ch}(J_1 - J_2) \end{bmatrix} \quad (5.27)$$

Once we've drawn the loops on the medial lattice, the following vertices appear:



Where we give the following weights according to the compatible Ising states:

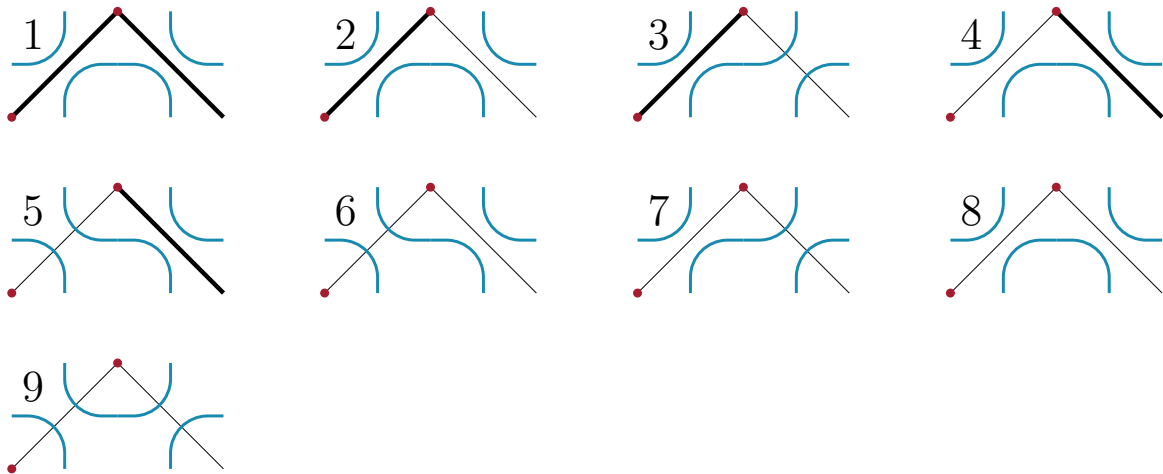
$$a = \frac{e^{J_1} - e^{-J_1}}{\sqrt{2}} \quad (5.28)$$

$$b = e^{-J_1} \quad (5.29)$$

$$e = \frac{e^{J_2} - e^{-J_2}}{\sqrt{2}} \quad (5.30)$$

$$f = e^{-J_2} \quad (5.31)$$

An  $L = 1$  Ising model thus corresponds to an  $L = 2$  loop model, and we get the following possible loop configurations (where we've also shown the Ising sites in red, and boldened the compatible FK-clusters):



We call two blue vertical edges that are directly connected *inside connected*, like the bottom ones in cfg. 1. Edges that are connected by crossing the periodicity, like the bottom ones in cfg. 9, are called *outside connected*. Edges that are not connected at all, like the ones in cfg. 3, shall be called *disconnected*. We can then write the transfer matrix as an operator

that maps different loop connectivity patterns into each other. In the basis where the inside connected state is  $(1, 0, 0)$ , outside connected =  $(0, 1, 0)$ , and disconnected =  $(0, 0, 1)$ , the transfer matrix then becomes:

$$T_{\text{loops}} = \begin{pmatrix} af w_c + ae + bf & af w_{n.c.} & af \\ be w_{n.c.} & be w_c + bf + ae & be \\ 0 & 0 & bf + ae \end{pmatrix} \quad (5.32)$$

Where  $w_c$  is the weight of a contractible loop, and  $w_{n.c.}$  that of a non-contractible loop. Equation (5.22) then tells us that to get all eigenvalues of the Ising model, the non-contractible loop weights have to take different values, namely all eigenvalues of the  $q = 2$  Potts connectivity matrix:  $(\sqrt{2}, -\sqrt{2}, 0)$ . That means we will get a total of  $3 \times 3 = 9$  eigenvalues.

$$\pm w_{n.c.} = w_c = \sqrt{2} \implies \begin{bmatrix} \sqrt{2} (\text{ch}J_2 \text{sh}J_1 + (\text{ch}J_1 - 2\text{sh}J_1) \text{sh}J_2) \\ \sqrt{2} (\text{ch}J_2 \text{sh}J_1 + (\text{ch}J_1 - 2\text{sh}J_1) \text{sh}J_2) \\ \sqrt{2} \text{ch}(J_1 + J_2) \end{bmatrix} \quad (5.33)$$

$$w_{n.c.} = 0, \quad w_c = \sqrt{2} \implies \begin{bmatrix} \sqrt{2} (\text{ch}J_2 \text{sh}J_1 + (\text{ch}J_1 - 2\text{sh}J_1) \text{sh}J_2) \\ \sqrt{2} \text{ch}(J_1 - J_2) \\ \sqrt{2} \text{sh}(J_1 + J_2) \end{bmatrix} \quad (5.34)$$

So we see that we indeed had to take different weights for the non-contractible loops to find all original Ising eigenvalues (up to an irrelevant factor  $\sqrt{q}$ ). Note also that we greatly increased our Hilbert space in this representation of our model, and we get way too many eigenvalues. However, throughout all these translations, we only pick up constant factors, and the original eigenvalues can still be identified by their mutual ratios. It is thus still possible to accomplish our original goal of identifying certain eigenvalues with those of free

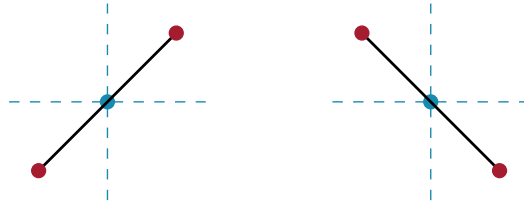


Figure 5.8: Vertices on the medial square lattice (blue) come in two flavours: those lying on vertical edges of the original (rotated by  $\pi/2$  ccw) lattice (left), and those lying on horizontal edges (right).

fermions.

**Locality Lost** Note that we started with a model wherein  $q$  emphatically had to take integer values. In this loop representation however, it just appears as a regular parameter, and nothing is stopping us from letting it take arbitrary values. This freedom did come at a steep price though: we were forced to introduce non-local contributions of loops. We will now redefine our statistical ensemble so that all weights will be local again.

We start by giving each loop an orientation, either clockwise or anticlockwise. At each vertex in  $\mathcal{L}'$ , there will then be two oriented loop elements, where the path bends an angle  $\alpha$  resp.  $\beta$  to the right (bending to the left just counts as a negative angle to the right). There are eight of these local loop configurations (see bottom of figure 5.9). We assign a weight  $z^{\alpha+\beta}$  to each such vertex. On top of that, note that there are two possibilities for a vertex in  $\mathcal{L}'$  (as seen in figure 5.5): either it lies inside a loop (i.e. on an edge of an FK cluster in  $\mathcal{L}$ ), or it lies just outside it (i.e. an empty edge in  $\mathcal{L}$ ). To each vertex inside a loop we assign an extra weight  $x_r$  if it corresponds to an edge of type  $r$ . If we now restrict our analysis to the square lattice,  $\mathcal{L}'$  is actually a bipartite lattice, with a sublattice with only vertices that are on vertical edges of  $\mathcal{L}$ , and one with only vertices that are on its horizontal edges (see figure 5.8). If the vertex was on a vertical (horizontal) edge, we only assign a weight  $x_r$  if local loop configurations connect points vertically (horizontally).

To find out which value of  $z$  corresponds to our original weights, note that by summing over loop orientations, and multiplying vertices, every contractible loop<sup>6</sup> now contributes  $z^{2\pi} + z^{-2\pi}$  to the total partition sum, since the sum of all bends around a loop must equal  $2\pi$ . The full partition sum then becomes:

<sup>6</sup>We will cover the case of non-contractible loops in the next section.

$$Z = \sum_{\mathcal{P} \in \mathcal{L}'} \left( (z^{2\pi} + z^{-2\pi})^p \prod_r x_r^{l_r} \right) \quad (5.35)$$

To relate our new degree of freedom  $z$  to our Potts parameter  $q$ , we introduce an auxiliary parameter  $\theta$ , and define the following:

$$z = e^{\theta/2\pi} \quad (5.36)$$

$$q^{1/2} = 2 \cosh \theta \quad (5.37)$$

We get our original partition sum (5.16) back<sup>7</sup>, and each contractible loop again contributes  $\sqrt{q}$ .

As seen in figure 5.9, there are four local loop configurations that are together associated to only two different arrow configurations. Since we're summing over all configurations anyway, we might just as well take the top six vertices as our elementary weights  $\omega_{1-6}$ , and simply take the sum of allowed loop vertices as the weight for the arrow configuration. We thus get a description of the square lattice Potts model in terms of six local arrow configurations with partition sum:

$$Z_{6V} = \sum_{cfg.} \prod_{r=1}^6 (\omega_r^{(h)})^{n_r^{(h)}} (\omega_r^{(v)})^{n_r^{(v)}} \quad (5.38)$$

Where the sum is over all arrow configurations, the indices  $(h)$  and  $(v)$  refer respectively to the horizontal and vertical sublattice,  $n_i$  counts the number of vertices of type  $i$ , and

$$\omega^{(h)} = \{1, 1, x_h, x_h, e^{-\theta/2} + e^{\theta/2}x_h, e^{\theta/2} + e^{-\theta/2}x_h\} \quad (5.39)$$

$$\omega^{(v)} = \{x_v, x_v, 1, 1, e^{\theta/2} + e^{-\theta/2}x_v, e^{-\theta/2} + e^{\theta/2}x_h\} \quad (5.40)$$

This set of configurations was first investigated as a model for the residual entropy of frozen water, and is therefore also known as the *ice-rule*. It contains a rich algebraic structure that we will further discuss in the context of the Bethe Ansatz.

---

<sup>7</sup>Up to an irrelevant global factor of  $q^{N/2}$ .

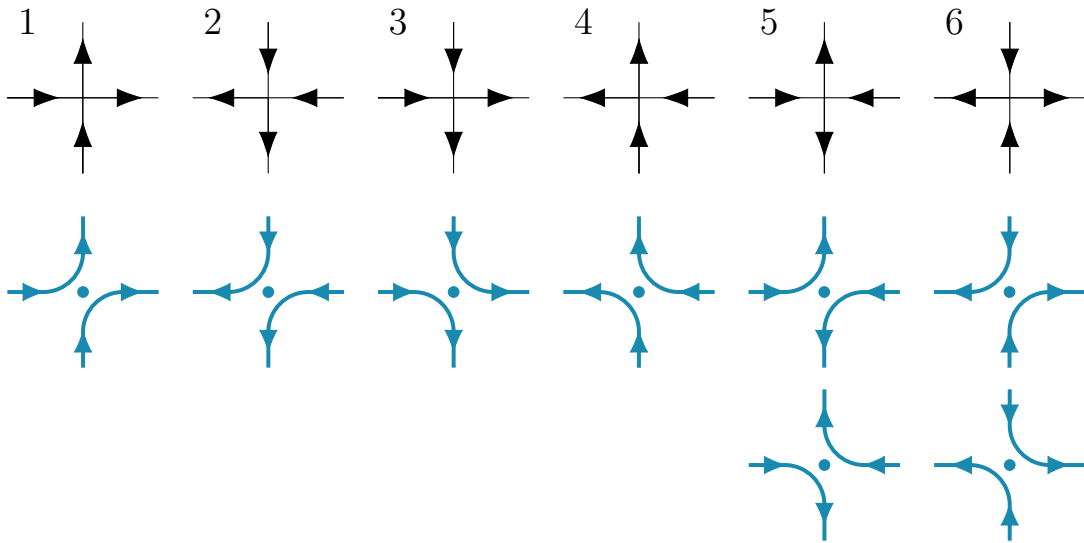


Figure 5.9: The six arrow configurations obeying the ice-rule (top), and their corresponding local loop configurations (bottom)

**Duality** The weights we have defined for our vertices can still be arbitrarily anisotropic. While nicely general, it would be nicer (in fact *much* nicer, as will become clear when discussing the Bethe Ansatz), to only have to deal with one set of weights. Setting  $x_h = x_v$  doesn't solve this problem, and we are also emphatically interested in the critical Ising model, not the homogeneous.

When we demand the Potts model to be critical (i.e.  $x_h x_v = 1$  or equivalently  $J_2 = \log \coth(J_1/2)$ ), the weights  $\omega_i^{(v)}$  in (5.40) can all be written as  $x_h \omega_i^{(h)}$ . These extra factors  $x_h$  can be taken outside of the product and the sum and just scale the partition sum by an irrelevant factor, leaving us with just one set of weights. The critical Ising model thus corresponds to a homogeneous vertex model, which will turn out to be very nice.

**A Twist** So far, we've acted like our lattice was infinite and not considered loops around a periodic cycle. If instead we choose our lattice to be bounded and periodic in one direction, the obvious choice is to impose fully periodic boundary conditions on the cycle, effectively wrapping our lattice around a cylinder<sup>8</sup>. This reintroduces the complication we've seen before, since this new topology allows for polygons whose edges don't have angles that

<sup>8</sup>This leaves the other boundary conditions unspecified. We will keep using our results from earlier on the torus, but effectively set one cycle to be so long that no loops span it, which is harmless since we can interpret one of the cycles as (imaginary) time anyway.

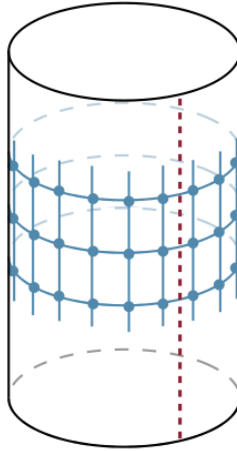


Figure 5.10: A six vertex model on a lattice (in blue), with a seam (red dashed) running along the cylinder through the edges. Arrows crossing the seam get an extra factor in their Boltzmann weight.

sum to  $\pm 2\pi$ . This situation is solved by adjusting the boundary conditions. We introduce a ‘seam’ along the side of the cylinder, as if cutting it open back into a plane (see figure 5.10). We then give every arrow pointing to the right (left) through this seam an extra weight  $e^\theta$  ( $e^{-\theta}$ ). A polygon that loops around the cylinder will now contribute a total of  $e^\theta + e^{-\theta} = 2 \cosh(\theta) = q^{1/2}$  to the partition sum, whereas a polygon that crosses the seam but doesn’t wrap the cylinder gets an extra factor  $e^\theta e^{-\theta} = 1$ , since it will necessarily cross the seam twice, in different directions. These are now fully consistent with our previous calculation, and the system is again described by equation (5.38), but with this extra weight added for edges that cross the seam. The exponentiated parameter  $\theta$  is referred to as the *twist* in these twisted boundary conditions. We’ve seen before that the corresponding loop model actually demands summing over different weights for the non-contractible loops, which now just translates to summing over different twists.

### 5.3 The twisted algebraic Bethe Ansatz

The reason for writing the Potts model as a six-vertex model is that the six-vertex model is particularly well suited for analytic treatment with the Algebraic Bethe Ansatz (ABA). The key problem is the diagonalisation of the transfer matrix and the resulting expression for the spectrum. This spectral problem is generally hard and has no systematic treatment,

so the ABA uses the technique of commuting transfer matrices. By defining a whole one-parameter family of transfer matrices that all commute with the original transfer matrix, we could maybe exploit this extra degree of freedom, since once we can diagonalise just one of these matrices, their intercommutativity ensures that all are diagonal. We will use a bit of physical intuition from the quantum-classical mapping and refer to the vertical direction of our 2D classical lattice as the *quantum* space, and while we will call the horizontal the *auxiliary* space.

What we are looking for is thus a one parameter family of transfer matrices  $\tau(\lambda) \in \text{End}(\mathcal{H})$ , where  $\mathcal{H}$  is the quantum Hilbert space of a row in our lattice, such that

$$[\tau(\lambda), \tau(\mu)] = 0 \quad \forall \lambda, \mu \in \mathbb{C} \quad (5.41)$$

The second important step is to define a transfer matrix as a partial trace over the auxiliary space  $\mathcal{A}$  of an object  $T(\lambda)$  acting in a larger space  $\mathcal{A} \otimes \mathcal{H}$ :

$$\tau(\lambda) = \text{Tr}_{\mathcal{A}}(T(\lambda)) \quad (5.42)$$

We will call this object  $T(\lambda)$  the monodromy matrix. We can graphically represent a matrix element of  $T(\lambda)$  as:

$$T_j^i(\lambda) = \begin{array}{c} | \\ \text{i} \text{---} \bullet \text{---} \text{j} \\ | \end{array}$$

Where  $i$  and  $j$  are states on the horizontal edges, and the vertical line now represents the Hilbert space of our full quantum chain. From this, we see that tracing over the horizontal direction corresponds to a transfer matrix of a quantum chain with periodic boundary conditions.

The commutator (5.41) then becomes:

$$[\text{Tr}_{\mathcal{A}}T(\lambda), \text{Tr}_{\mathcal{A}}T(\mu)] = 0 \quad (5.43)$$

If we add a second auxiliary space and define operators in the space  $\mathcal{A}_1 \otimes \mathcal{A}_2 \otimes \mathcal{H}$  as

$$T_1(\lambda) = T(\lambda) \otimes \text{id}_2 \quad \text{and} \quad T_2(\lambda) = \text{id}_1 \otimes T(\lambda) \quad (5.44)$$

So that  $\text{Tr}_{\mathcal{A}_1} T_2(\lambda) = T(\lambda)$  etc., we can write the commutator as

$$[\text{Tr}_{\mathcal{A}_2} T_1(\lambda), \text{Tr}_{\mathcal{A}_1} T_2(\lambda)] = \text{Tr}_{\mathcal{A}_1 \otimes \mathcal{A}_2} [T_1(\lambda), T_2(\mu)] \quad (5.45)$$

Writing out the commutator, we get the expression:

$$\text{Tr}_{\mathcal{A}_1 \otimes \mathcal{A}_2} (T_1(\lambda) T_2(\mu)) = \text{Tr}_{\mathcal{A}_1 \otimes \mathcal{A}_2} (T_2(\mu) T_1(\lambda)) \quad (5.46)$$

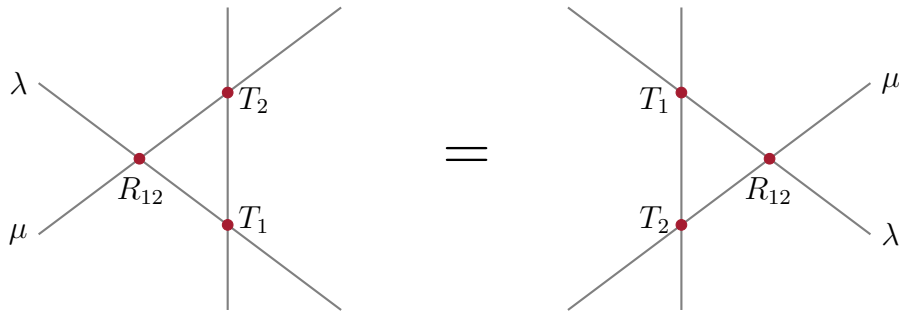
Where the trace only enjoys its cyclic property in the space that is being traced out, making this a non-trivial statement. We can, however, still exploit this cyclicity since (5.46) certainly holds if there is a winding matrix  $R_{12}(\lambda, \mu)$  that flips the order of the monodromy matrices around by acting only in the space  $\mathcal{A}_1 \otimes \mathcal{A}_2$ :

$$R_{12}(\lambda - \mu) T_1(\lambda) T_2(\mu) R_{12}(\lambda - \mu)^{-1} = T_2(\mu) T_1(\lambda) \quad (5.47)$$

Pictorially, we can represent the product  $T_1(\lambda) T_2(\mu)$  as:

$$T_1(\lambda) T_2(\mu) = \begin{array}{c} | \\ \text{---} \bullet T_2(\mu) \\ | \\ \text{---} \bullet T_1(\lambda) \\ | \end{array}$$

Note that we now look at the whole monodromy matrix so we don't specify edge states. Equation (5.47) can now be represented by:



This is a version of the Yang-Baxter equation and finding matrices  $T$  and  $R$  that satisfy it is equivalent to identifying an integrable model. This statement maybe sounds deeper than it is, since satisfying this equation is often taken as the definition of integrability.

We can now start specifying our spaces a bit more. The most insightful (and in our case sufficient) choice for an auxiliary space is to choose  $\mathcal{A}_1 \simeq \mathcal{A}_2 \simeq \mathbb{C}^2$ , where  $\simeq$  denotes an isomorphism. Note that if the vertical quantum space per site is also  $\mathbb{C}^2$ , which corresponds to binary complex states on sites, we get a representation of the Yang-Baxter algebra that looks a lot like something we've seen before. In our discussion of Lie algebras, we saw that we can form the adjoint representation of an algebra by its structure constants, taking as the vector space in which the algebra acts the algebra itself. We here do something similar by taking the horizontal and vertical spaces the same, so we will call this the adjoint representation of the Yang-Baxter algebra<sup>9</sup>.

This invites us to write our monodromy matrix as a  $2 \times 2$  matrix, with entries taking operator values in  $\mathcal{H}$ .

$$T(\lambda) = \begin{pmatrix} A(\lambda) & B(\lambda) \\ C(\lambda) & D(\lambda) \end{pmatrix} \quad (5.48)$$

Denoting our binary  $\mathbb{C}^2$ -spanning states by 0 and 1, we can represent these operators as:

---

<sup>9</sup>This is a very natural representation to work in, since interpreting the two directions as simply the two directions of a classical 2D lattice model (instead of space and time of a quantum chain), then both directions should be treated on equal footing; Generating the partition sum by multiplying vertical or horizontal transfer matrices should both be allowed and lead to the same result.

$$\begin{array}{cc}
 A(\lambda) = 0 \text{ --- } \bullet \text{ --- } 0 & B(\lambda) = 1 \text{ --- } \bullet \text{ --- } 0 \\
 \begin{array}{c} | \\ \hline \\ | \end{array} & \begin{array}{c} | \\ \hline \\ | \end{array} \\
 \\
 C(\lambda) = 0 \text{ --- } \bullet \text{ --- } 1 & D(\lambda) = 1 \text{ --- } \bullet \text{ --- } 1 \\
 \begin{array}{c} | \\ \hline \\ | \end{array} & \begin{array}{c} | \\ \hline \\ | \end{array}
 \end{array}$$

Having this more or less explicit form for  $T(\lambda)$ , we can now try to find matrices  $R(\lambda)$  so that the pair  $(R, T)$  will satisfy the Yang-Baxter equation (5.47). One can write out the tensor products and would find that the following  $R$ -matrix suffices:

$$R(\lambda) = \begin{pmatrix} a(\lambda) & 0 & 0 & 0 \\ 0 & b(\lambda) & c(\lambda) & 0 \\ 0 & c(\lambda) & b(\lambda) & 0 \\ 0 & 0 & 0 & a(\lambda) \end{pmatrix} \quad (5.49)$$

Note that we've cheated a little bit by calling each direction just  $\mathbb{C}^2$ , acting as if our chain is only one site long. In general, for a chain of length  $L$ , we need a way to extend the action of the monodromy matrix over  $L$  sites. We can do this by defining an extra product  $\Delta$  on the Yang-Baxter algebra, called a co-product:  $\Delta : \mathcal{A} \otimes \mathcal{H} \rightarrow (\mathcal{A} \otimes \mathcal{H}) \otimes (\mathcal{A} \otimes \mathcal{H})$ . It works on our monodromy matrix as follows:

$$\Delta T(\lambda)_j^i = \sum_k T_k^i(\lambda) \otimes T_j^k(\lambda) \quad (5.50)$$

It thus extends the operator so that it can act on a longer chain, summing over all internal states of the horizontal direction:

$$\Delta \left( i \text{ --- } \bullet \text{ --- } j \right) = \sum_k \left( i \text{ --- } \bullet \text{ --- } k \text{ --- } \bullet \text{ --- } j \right)$$

To fully define the Yang-Baxter algebra as a bialgebra and use this co-product to iteratively define our operators on the full chain, we would have to show some more properties of the algebra. Fortunately, we are physicists and we can get away with some useful abuse of notation. Reassured by the fact that there is a way to define these operators along the whole chain, we simply decompose our Hilbert space as  $\mathcal{H} = \otimes_{j=1}^N \mathcal{H}_j$  and write our full monodromy matrix as a product over local matrices  $L_i$ :

$$T(\lambda) = L_N(\lambda)L_{N-1}\dots L_1(\lambda) \tag{5.51}$$

Each  $L_i$  now acts in one separate copy of  $\mathbb{C}^2$ .

**Gauge Freedom** In the adjoint representation, we then have  $L_i(\lambda) = R(\lambda)$ , which might worry the attentive reader, since we now have only three free parameters ( $a, b$  and  $c$ ) to define our local weights, whereas we previously needed four different ones (see eq. (5.39)) to define the weights of the homogeneous 6-vertex model, which is what we're trying to solve after all. Recall, however, that we have implicitly been imposing periodic boundary conditions by tracing over all these local operators to get our transfer matrix. On a periodic lattice, the ice-rule actually has an interesting consequence: the total number of arrows pointing north and the number pointing south is conserved along each row of vertical edges. This means that there are as many 'sources' as 'sinks' per row of vertices, which are respectively  $\omega_5$  and  $\omega_6$  in eq. (5.39). So say that we have two different weights, parametrised by some factor  $k$ :  $\omega_5 = ck, \omega_6 = c/k$ , then we only get terms in our partition sum in which there are as many  $\omega_5$  as  $\omega_6$ , and the factors of  $k$  and  $1/k$  exactly cancel. We thus get a kind of 'gauge'-freedom in defining our weights  $\omega_5$  and  $\omega_6$ . Taking  $c = e^{-\theta/2}\sqrt{e^\theta + x}\sqrt{1 + e^\theta x}$  and  $k = -\sqrt{1 + e^\theta x} (\sqrt{e^\theta + x})^{-1}$ , we find back the weights in equation (5.39) for  $\omega_5 = ck$  and  $\omega_6 = c/k$ . We can thus get away with only three free parameters in our  $L$ -matrix.

**Let's Twist Again** Another nuance to address are the boundary conditions. Recall that

the six-vertex model we're trying to solve actually had a twist in its boundary conditions, depending on the arrow configurations on a seam along the cylinder. Now that we have this local formulation of the monodromy matrix, this can be neatly implemented by an additional twist operator, often referred to in the literature as the Sklyanin K-matrix, that modifies one of the local operators. If we choose to place the seam between the Nth and the first spin, we can write the following:

$$T(\lambda) = \tilde{L}_N(\lambda)L_{N-1}(\lambda)\dots L_1(\lambda) \quad (5.52)$$

With

$$\tilde{L}_N(\lambda) = L_N(\lambda)K(\theta) \quad (5.53)$$

Where we introduced the twist matrix  $K(\theta)$ , an operator in  $\mathcal{A} \otimes \mathcal{H}_N$  that acts in the auxiliary space  $\mathcal{A}$  as a 2x2 matrix:

$$K(\theta) = \begin{pmatrix} e^\theta & 0 \\ 0 & e^{-\theta} \end{pmatrix} \otimes id_{\mathcal{H}} \quad (5.54)$$

Explicitly writing out the tensor product:

$$L_N(\lambda) = \left( \begin{array}{cc} \begin{array}{c} \rightarrow \bullet \rightarrow \\ \leftarrow \bullet \leftarrow \end{array} & \begin{array}{c} \rightarrow \bullet \leftarrow \\ \leftarrow \bullet \leftarrow \end{array} \\ \begin{array}{c} \leftarrow \bullet \rightarrow \\ \leftarrow \bullet \leftarrow \end{array} & \begin{array}{c} \leftarrow \bullet \leftarrow \\ \leftarrow \bullet \leftarrow \end{array} \end{array} \right) \otimes \left( \begin{array}{cc} \begin{array}{c} \uparrow \\ \bullet \\ \uparrow \end{array} & \begin{array}{c} \downarrow \\ \bullet \\ \downarrow \end{array} \\ \begin{array}{c} \uparrow \\ \bullet \\ \downarrow \end{array} & \begin{array}{c} \downarrow \\ \bullet \\ \downarrow \end{array} \end{array} \right) \quad (5.55)$$

And imposing the ice-rule, we indeed get a matrix in the form of  $R(\lambda)$ , and  $\tilde{L}_N(\lambda)$  gets exactly the right twisted weights.

We will denote operators on chains with twisted boundary conditions with tildes, and thus write:

$$\tilde{T}(\lambda) = \begin{pmatrix} \tilde{A}(\lambda) & \tilde{B}(\lambda) \\ \tilde{C}(\lambda) & \tilde{D}(\lambda) \end{pmatrix} = \begin{pmatrix} A(\lambda)e^\theta & B(\lambda)e^{-\theta} \\ C(\lambda)e^\theta & D(\lambda)e^{-\theta} \end{pmatrix} \quad (5.56)$$

Looking at the shape of  $\tilde{T}(\lambda)$ , it is now tempting to think of  $\tilde{B}(\lambda)$  and  $\tilde{C}(\lambda)$  as respectively raising and lowering operators. We start by defining the vacuum. It should have the properties that it diagonalises  $\tilde{A}(\lambda)$  and  $\tilde{D}(\lambda)$ <sup>10</sup>, and that it is annihilated by the lowering operator:

$$\tilde{A}(\lambda) |0\rangle = e^\theta a(\lambda)^L |0\rangle \quad (5.57)$$

$$\tilde{D}(\lambda) |0\rangle = e^{-\theta} d(\lambda)^L |0\rangle \quad (5.58)$$

$$\tilde{C}(\lambda) |0\rangle = 0 \quad (5.59)$$

Where we take the  $L$ th power since these operators should we understood as co-products extended over the whole chain:  $\tilde{A}(\lambda) = e^\theta \Delta^{L-1} A(\lambda)$ .

We can now look at ‘excited’ states that still diagonalise the transfer matrix by demanding that  $\tilde{B}(\lambda)$  excitations are still eigenstates of  $\tilde{A}(\lambda) + \tilde{D}(\lambda)$ :

$$\left( \tilde{A}(\lambda) + \tilde{D}(\lambda) \right) \prod_{j=1}^M \tilde{B}(\lambda_j) |0\rangle = \Lambda_\tau(\lambda | \{\lambda_j\}_M) \prod_{j=1}^M \tilde{B}(\lambda_j) |0\rangle \quad (5.60)$$

Where we can now use the results from normal untwisted ABA for the six-vertex model to look at how these states behave. A more detailed derivation is given in appendix A.6. The main idea is that we use the Yang-Baxter relation for the R-intertwining of our monodromy matrices to derive a set of commutation relations that allow us to commute the  $A(\lambda)$  and  $D(\lambda)$  operators through the  $B(\lambda)$ s. Demanding that these excitations are still eigenstates of  $\tilde{\tau}(\lambda)$  gives us the twisted Bethe equations:

---

<sup>10</sup>This is a sufficient condition to diagonalise the transfer matrix  $\tilde{\tau}(\lambda) = \tilde{A}(\lambda) + \tilde{D}(\lambda)$

$$e^{2\theta} \left( \frac{a(\lambda_i)}{b(\lambda_i)} \right)^L = \prod_{k \neq i}^M \frac{a(\lambda_i - \lambda_k) b(\lambda_k - \lambda_i)}{b(\lambda_i - \lambda_k) a(\lambda_k - \lambda_i)} \quad (5.61)$$

Note that we have so far only chosen the shape of our R-matrix, and not its actual parametrisation in terms of the spectral parameter. There is still a number of different options that all satisfy the correct algebra and we will continue now with the hyperbolic trigonometric parametrisation, giving us:

$$R(\lambda) = \begin{pmatrix} 1 & 0 & 0 & 0 \\ 0 & \frac{\sinh \lambda}{\sinh \lambda + \eta} & \frac{\sinh \eta}{\sinh \lambda + \eta} & 0 \\ 0 & \frac{\sinh \eta}{\sinh \lambda + \eta} & \frac{\sinh \lambda}{\sinh \lambda + \eta} & 0 \\ 0 & 0 & 0 & 1 \end{pmatrix} \quad (5.62)$$

Resulting in the Bethe equations:

$$\left( \frac{\sinh(\lambda_i)}{\sinh(\lambda_i + \eta)} \right)^L \prod_{k \neq i}^M \frac{\sinh(\lambda_i - \lambda_k - \eta)}{\sinh(\lambda_i - \lambda_k + \eta)} = e^{-2\theta} \quad (5.63)$$

Given such a set  $\{\lambda_j\}$  that satisfy the Bethe equations, we can then look at the spectrum of eigenvalues of the transfer matrix:

$$\Lambda_\tau(\lambda | \{\lambda_i\}_M) = e^\theta \prod_{i=1}^M \frac{\sinh(\lambda_i - \lambda + \eta)}{\sinh(\lambda_i - \lambda)} + e^{-\theta} \left( \frac{\sinh(\lambda)}{\sinh(\lambda + \eta)} \right)^L \prod_{i=1}^M \frac{\sinh(\lambda - \lambda_i + \eta)}{\sinh(\lambda - \lambda_i)} \quad (5.64)$$

Note how such a radical change in our system, twisting the boundary conditions and losing translational invariance<sup>11</sup>, in fact only resulted in very minor changes in our Bethe Ansatz

---

<sup>11</sup>Actually, one could "smear out" the twist over all vertices and give each vertex on a chain of length  $L$  an extra weight that is the  $L$ th root of the twist we put at the seam. While leading to the exact same partition sum, this actually restores translational invariance.

equations and the eigenvalues of the transfer matrix. We now have a set of quantum numbers  $\{\lambda_j\}$  that specify a certain eigenvalue of the transfer matrix  $\tilde{\tau}(\lambda)$ . We can tune  $\lambda$  so that it corresponds to our original critical weights  $J_1$  and  $J_2$  and find a one-to-one correspondence between eigenvalues. However, one usually rewrites the BAEs in their logarithmic form by simply taking the logarithm of both sides, after which new quantum numbers appear that account for the multivaluedness of the complex logarithm. Since these logarithmic BAEs are usually numerically more stable, these are the conventional Bethe quantum numbers most commonly seen in the literature<sup>12</sup>.

---

<sup>12</sup>The uniqueness of a set  $\{\lambda_j\}$  given the Bethe quantum numbers is a very subtle point, and will not be addressed here, but rather assumed.

# 6

## A Path Forward

### 6.1 The dilute $A_3$ model

In the previous sections, we have seen how a series of equivalent partition sums can allow for a translation between a free fermionic description of a spin model, and a description in terms of Bethe quantum numbers. This way, eigenvalues of the free fermion transfer matrix (section 5.1) can be directly identified with eigenvalues that correspond to certain Bethe quantum numbers. We have shown such a translation in the context of a critical spin- $\frac{1}{2}$  Ising model (i.e. self-dual  $q=2$  Potts model), but the actual model of interest here is the dilute  $A_3$  model in [3], where the S-matrix from Zamolodchikov [37] was found in the (thermodynamic) Bethe Ansatz. We will first define this model and its Bethe Ansatz, and then describe how the authors made the link with  $E_8$ .

**ADE models** It has been shown that the Pasquier models are critical whenever the largest eigenvalue of the adjacency matrix is smaller than or equal to two [32]. The graphs for which this is the case have been thoroughly categorised; They are the family of simply laced Dynkin diagrams (those of type  $A_n$ ,  $D_n$  and  $E_n$  in the classification of Lie algebras, and their affine extensions). Not only are these theories critical, it is actually possible to choose the Boltzmann weights of the configurations in figure 6.1 such that they satisfy the Yang-Baxter equation and the whole system becomes integrable [32]. Recall that to specify a Pasquier model, we need the graph that encodes its rules, but we also need to independently specify the local weights  $W_k$ . When constructing it to emphatically correspond to a Potts model, we found that we needed two of these local weights, 1 or  $v$ , corresponding to the



Figure 6.1: The nine possibilities of domain wall geometry around a vertex of the dual square lattice.

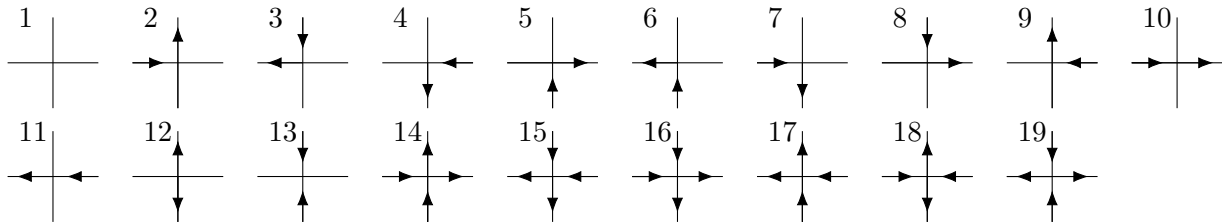


Figure 6.2: The 19 possible vertex configurations.

two possible edges in the Fortuin-Kasteleyn cluster construction, either an edge or no edge. This leads to two loop configurations at every vertex, making the loops *dense*. However, nothing restricts us to this. We can consider the more general case in which there are for example nine possible local geometries, as shown in figure 6.1. Where we previously only gave the rightmost two geometries a nonzero weight, we can now allow them all to appear, leading to loop configurations where vertices can also contain just one or even zero local loop configurations. This leads to global loop configurations that we will call *dilute*.

The dilute  $A_3$  model is then defined as the model in which we take the diagram to be the  $A_3$  Dynkin diagram, and we have nine independent local weights for each vertex in figure 6.1. We can then follow the same procedure as before, and orient the loops to arrive at the corresponding vertex model and its Bethe Ansatz.

**The Izergin-Korepin Vertex Model** Recall from earlier that a loop model can be rewritten in terms of a vertex model to restore the locality of the weights. We take the 9 vertices in fig. 6.1 of the dilute loop model, and put arrows as we did in the case of the dense loop model. The extra possibilities now give us 19 allowed vertices where we had 6 before (see figure 6.2).

These 19 vertices can again be given weights that satisfy the Yang-Baxter equation, and lead to the following Bethe Ansatz equation [33] [34]:

$$\left( \frac{\cosh(u_j - \frac{1}{2}i\theta)}{\cosh(u_j - \frac{1}{2}i\theta)} \right)^L = -s \prod_{k=1}^M \frac{\sinh(u_j - u_k - i\theta) \cosh(u_j - u_k + \frac{1}{2}i\theta)}{\sinh(u_j - u_k + i\theta) \cosh(u_j - u_k - \frac{1}{2}i\theta)} \quad (6.1)$$

With eigenvalues of the transfer matrix:

$$\Lambda(\lambda) = \left( \sin(\lambda + \frac{3}{4}\theta) \cos(\lambda + \frac{1}{4}\theta) \right)^L s \prod_{j=1}^M \frac{\sinh(u_j - \frac{5}{4}i\theta + i\lambda)}{\sinh(u_j - \frac{1}{4}i\theta + i\lambda)} \quad (6.2)$$

$$+ \left( \sin(\lambda + \frac{3}{4}\theta) \cos(\lambda - \frac{3}{4}\theta) \right)^L s \prod_{j=1}^M \frac{\sinh(u_j + \frac{3}{4}i\theta + i\lambda) \cosh(u_j - \frac{3}{4}i\theta + i\lambda)}{\sinh(u_j - \frac{1}{4}i\theta + i\lambda) \cosh(u_j + \frac{1}{4}i\theta + i\lambda)} \quad (6.3)$$

$$+ \left( \sin(\lambda - \frac{1}{4}i\theta) \cos(\lambda - \frac{3}{4}\theta) \right)^L s^{-1} \prod_{j=1}^M \frac{\cosh(u_j + \frac{5}{4}i\theta + i\lambda)}{\cosh(u_j + \frac{1}{4}i\theta + i\lambda)} \quad (6.4)$$

Using the following identities:

$$\cosh(x + iy) = \cosh x \cos y + i \sinh x \sin y \quad (6.5)$$

$$\sinh(x + iy) = \sinh x \cos y + i \cosh x \sin y \quad (6.6)$$

$$\log \left( \frac{x + iy}{x - iy} \right) = 2i \arctan \frac{y}{x} \quad (6.7)$$

We can rewrite these equations into their numerically more stable logarithmic form:

$$-2iL \arctan \left( \tan \frac{\theta}{2} \tanh u_j \right) = \quad (6.8)$$

$$\log s + 2i \sum_{k=1}^M \left( \arctan \left( \frac{\tanh(u_j - u_k)}{\tan \theta} \right) + \arctan \left( \tan \frac{\theta}{2} \tanh(u_j - u_k) \right) \right) + \left( \frac{M+1}{2} + \tilde{I}_j \right) 2\pi i$$

Where  $s$  is the value of the extra weight arrows pick up when crossing the seam, and  $\tilde{I}_j$  is an integer to account for the multivaluedness of the complex logarithm. We can now

define our Bethe quantum numbers  $I_j := \frac{M+1}{2} + \tilde{I}_j$ , and see that they are integers (half odd integers) for  $M$  odd (even). We have thus arrived at an explicit way to calculate the eigenvalues of the critical dilute  $A_3$  model and link each of these to a set of Bethe quantum numbers.

**An Off-critical Extension** This is of course good news for anyone who likes to solve critical models, but we are actually interested in an off-critical model, namely a magnetic perturbation of a critical model. This is where the real magic happens. It turns out that the dilute  $A_n$  models with odd  $n$  allow for off-critical  $\mathbb{Z}_2$ -odd perturbations that leave the system integrable. The effect of this perturbation can be captured by a modification of the parametrisation of the weights in terms of elliptic functions, still allowing one to write down the full Bethe Ansatz equations (BAEs). The simplest nontrivial case is  $n = 3$ , and it is this model that caught the interest of Bazhanov, Nienhuis and Warnaar in [3]. Another reason to consider this model in relation to the Ising model is the fact that the Dynkin diagram  $A_3$  is actually identical to the  $q=2$  Potts diagram (see figure 5.7).

For the explicit form of the elliptic parametrisation, I refer the interested reader to [3]. The key point is that one can write down the weights in terms of elliptic Jacobi  $\theta$  functions of two variables:

$$\theta_1(z, q) = \sum_{n=-\infty}^{\infty} (-1)^{n-1/2} q^{(n+1/2)^2} e^{(2n+1)iz} \quad (6.9)$$

The variable  $z$  takes on the role of spectral parameter, while the variable  $q$  corresponds to the perturbation. Setting  $q$  to zero brings us back to the original critical weights, while varying it breaks the  $\mathbb{Z}_2$  symmetry. It can thus be identified with an external magnetic field. The BAEs can be rewritten in terms of these generalised weights, and lead to an expression for the eigenvalues of the transfer matrix, again in terms of Bethe quantum numbers. However, these equations are generally hard to solve, and the authors of [3] started by looking at the thermodynamic limit where  $L \rightarrow \infty$ .

Motivated by a numerical study of this limit, they claim that solutions to the BAEs come in only nine different types, called strings. A string (of type  $t$ ) is defined as a set of complex numbers  $\{\alpha_{j,k}\}$  in the complex plane of Bethe roots, parametrised as:

$$\alpha_{j,k}^{(t)} = \alpha_j^{(t)} + i(\Delta_k^{(t)} + \epsilon^{(t)}r) , \quad k = (1, \dots, n^{(t)}) \quad (6.10)$$

A string is thus a set of  $n^{(t)}$  numbers that all lie on a vertical line in the complex plane, around the real number  $\alpha_j^{(t)}$ , with vertical spacings  $(\Delta_k^{(t)} + \epsilon^{(t)}r)^1$ .

In the thermodynamic limit, the roots start to form a continuum along the real axis, and the only string states that survive are the following nine:

$\alpha_{j,k}^{(t)} = \alpha_j^{(t)} + i(\Delta_k^{(t)} + \epsilon^{(t)}r) , \quad k = (1, \dots, n^{(t)})$			
$t$	$n^{(t)}$	$\Delta^{(t)}/5$	$\epsilon^{(t)}$
0	1	(0)	0
1	2	(-1, 1)	1
2	4	(-4, -2, 2, 4)	0
3	6	(-7, -5, -1, 1, 5, 7)	1
4	8	(-10, -8, -4, -2, 2, 4, 8, 10)	0
5	10	(-13, -11, -7, -5, -1, 1, 5, 7, 11, 13)	1
6	7	(-14, -6, -2, 0, 2, 6, 14)	1
7	4	(-3, -1, 1, 3)	0
8	5	(-12, -8, 0, 8, 12)	1

The BAEs then become integral equations for the density of these strings. Note that eight out of nine string states (all except the trivial one-string) are composed of complex numbers. Complex roots, or rapidities, cause the Bethe wave function of a string to be exponentially suppressed in the separation of its components, and as such correspond to bound states. It is therefore a promising sign that we find exactly eight bound states in the thermodynamic spectrum. In fact, our suspicions are confirmed when looking at the S-matrix of these bound states. Remarkably, the authors find the exact same S-matrix as Zamolodchikov in [37]. The conjecture by Zamolodchikov has been confirmed: There is

---

<sup>1</sup>The parameter  $r$  is determined by the choice of vertex weights and in our case of dilute  $A_3$  we have  $r = 16$ .

indeed a solvable lattice model in the universality class of the magnetically perturbed Ising model that contains the same  $E_8$  S-matrix. It is the integrable off-critical  $\mathbb{Z}_2$  breaking extension of the dilute  $A_3$  model. Finding this put a lot of minds at ease, but also left a big question on the table: What *are* these excitations on the lattice that somehow know about structure of  $E_8$ ?

**Summary** We want to understand the excitations of the magnetically perturbed Ising model, but unfortunately we have no explicit solution to this model. However, the authors of [3] found a different model, one that we can solve with the Bethe Ansatz, that apparently lies in the same universality class in the sense that it shares its thermodynamic excitation spectrum with the magnetically perturbed Ising model around the critical point. They were able to explicitly identify these eight particles in terms of string solutions to the thermodynamic Bethe Ansatz of this dilute  $A_3$  model. In light of our previous discussion on the relationship between the 6-vertex Bethe Ansatz and the critical Ising free fermions, we are now naturally lead to the question: Can we link the eight excitations of the off-critical dilute  $A_3$  model to some simpler description of the model, for example in terms of its own free fermions? To immediately focus on this off-critical extension would be a bit hubristic, so lets again start with a simpler case and begin with the critical dilute  $A_3$  model.

## 6.2 Free fermions in the critical dilute $A_3$ model

The dilute  $A_3$  model lies in the universality class of the Ising model. Its critical behaviour should be thermodynamically the same, but also at finite system size we expect there to be a one-to-one mapping between the eigenvalues of the transfer matrix of the magnetic Ising model, and those of the dilute  $A_3$  model. A numerical investigation showed that the dilute  $A_3$  spectrum did not have an exact free fermion character, but this is simply a finite size effect, and we can still associate an eigenvalue to the free fermion state it would thermodynamically become.

We will use the following three characteristics of each eigenvalue and its state to identify these correspondences:

1. The (approximate) numerical eigenvalue.

2. The total momentum of the corresponding eigenstate.
3. The conformal sector to which the state belongs.

These turn out to be sufficient in most cases, and determining these three characteristics for both the Ising eigenvalues and the  $A_3$  eigenvalues then allows us to identify the free fermions in the  $A_3$  model.

Determining the first property, the numerical value, is trivial, it is the very act of diagonalising the Hamiltonian<sup>2</sup> matrix. To determine the total momentum, we actually diagonalise the following operator:

$$H = \mathcal{H} + i\mathcal{S}_L + i\mathcal{S}_R \tag{6.11}$$

Where  $\mathcal{S}_{(L)R}$  is the (left) right shift operator along the chain. This operator has eigenvalues:

$$\Lambda_H = E + i \cos(p) \tag{6.12}$$

Where  $p$  is the total momentum of the state. We can do this for both the Ising model and the dilute  $A_3$  model, and identify the actual eigenvalues as the real part of  $\Lambda_H$ , while we have that  $\cos(p)$  is the imaginary part, so that  $p$  is indeed uniquely defined on the interval  $[0, \pi]$  (as opposed to on  $[\pi/2, -\pi/2]$  had we chosen to diagonalise  $\mathcal{H} + \mathcal{S}_L - \mathcal{S}_R$ ).

**Conformal Sectors** Now the last identification, an eigenvalue's conformal sector, is a bit more tricky. As mentioned before, the Ising CFT has three primary fields in its Kac table: the identity  $\mathbb{1}$ , the energy operator  $\epsilon$ , and a spin operator  $\sigma$ . All states in the corresponding theory are thus, through the operator-state correspondence, a certain descendant of one of these operators. And since the CFT is connected to the finite, non-conformal theory by a continuous scaling, we expect this identification to still be possible in the finite size Ising model. This correspondence teaches us that any such descendant eigenstate will have an extensive eigenvalue, plus some finite size corrections.

---

<sup>2</sup>We will actually work in the Hamiltonian limit of the transfer matrix, since the Hamiltonian operator will generally be more sparse than the transfer matrix, which is useful for numerical investigation.

We define a state  $|\psi\rangle$  on a chain of length  $L$  as:

$$|\psi\rangle = \sum_s \psi_s |s\rangle, \quad s = \{s_1, \dots, s_L\}, \quad s_i \in \{+1, -1\} \quad (6.13)$$

Its eigenvalue will generally be of the shape [5][36]

$$E_\psi = LE_\psi + \frac{\pi c}{6L} - \frac{2\pi}{L} \Delta_j + \mathcal{O}(L^{-1}) \quad (6.14)$$

Where  $c = 1/2$ ,  $E$  is the energy of the operator in the scaling limit, and  $\Delta_j$  is the conformal dimension of the state  $|\psi\rangle$ . Each state is a descendant of one of the three primaries, so their  $\Delta_j$  will differ an integer from either 0, 1, or  $\frac{1}{8}$ , corresponding to descendants of resp.  $\mathbb{1}$ ,  $\epsilon$ , or  $\sigma$ . However, it turns out that these extra  $\mathcal{O}(L^{-1})$  terms will generally grow as we get deeper in the spectrum (larger  $\Delta_j$ ), so accurately determining  $\Delta_j$ , and thus the conformal sector, will become impossible there for both mathematical and numerical reasons.

We will therefore use another trick, based on the fact that descendants will inherit the symmetry properties of their primaries. For a state  $|\psi\rangle \in \text{des}(\sigma)$  (i.e. a  $\sigma$  descendant), its components  $\psi_s$  in definition (6.13) should have the property that they are antisymmetric under a global spin flip  $s \rightarrow -s$ , e.g.  $\psi_{++++} = -\psi_{----}$ , while the other descendants are symmetric under this spin flip. If we thus have an eigenstate  $|\psi\rangle$ , and we see that its components satisfy  $\psi_s = -\psi_{-s}$ , then we know that it is a descendant of the primary  $\sigma$ .

There are still two sectors left:  $\text{des}(\mathbb{1})$  and  $\text{des}(\epsilon)$ . Under the order-disorder duality of the Ising model, the sign of a state's energy is effectively switched. Interpreting order as fixed boundary conditions, and disorder as summing over them, motivates us to define a disorder transformation  $D$  on a component as:

$$D_{s_1} \psi_s : \psi_{s_1, s_2, \dots, s_L} \rightarrow \psi_{0, s_2, \dots, s_L} := \frac{1}{\sqrt{2}} (\psi_{+, s_2, \dots, s_L} + \psi_{-, s_2, \dots, s_L}) \quad (6.15)$$

We can then look at how components transform under  $D$ . It turns out that in all cases we checked, the components satisfy exact relations like  $\psi_{00+++} = \pm \psi_{++---$ , that is, the states are exactly symmetric or antisymmetric under this disorder transformation. States

that are  $D$ -symmetric can be identified with descendants of the identity, while states that are  $D$ -antisymmetric are descendants of  $\epsilon$ .

We now have a way to assign a conformal sector to each of the ‘brute force’ eigenvalues of the Ising model. Since there can also be numerical errors or degeneracies in its free fermion description, we also want to identify the three properties of each free fermion state. Again, the first two are trivial (numerical value and momentum), but the conformal sector requires some attention. It turns out that we can make the following identifications:

- The number of fermions is even in  $\text{des}(\mathbb{1})$  and  $\text{des}(\epsilon)$ , and odd in  $\text{des}(\sigma)$ .
- The number of fermions with positive momentum is even in  $\text{des}(\mathbb{1})$  and odd in  $\text{des}(\epsilon)$ .

This gives us a way to uniquely assign a free fermion state to a conformal sector.

Ok, we’re almost there now. Remember that we are making these identifications so that we can link  $A_3$  eigenvalues to Ising eigenvalues. We thus also need to also assign eigenvalues of the  $A_3$  model to a particular conformal sector (we already found their numerical value and momentum earlier). Luckily, it can be done in a very similar manner. The key difference is the fact that this dilute  $A_3$  model actually has three local state possibilities (once the loops are oriented, each edge is oriented in either direction, or empty). We thus get states of the form:

$$|\psi\rangle = \sum_s \psi_s |s\rangle, \quad s = \{s_1, \dots, s_L\}, \quad s_i \in \{+1, -1, 0\} \quad (6.16)$$

Since the unoccupied state 0 is invariant under global arrow-flip, we can still use that  $\psi_s$  is antisymmetric under  $s \rightarrow -s$  iff  $|\psi\rangle \in \text{des}(\sigma)$ . The disorder operation now comes with the complication that we already have a ‘neutral’ state 0. However, it turns out that to identify the states, it is sufficient to look at the way the components without any minuses transform under the same disorder that we defined before, e.g.  $\psi_{00+++} = \pm\psi_{++000}$ . Again, we assign states that are symmetric under this transformation to  $\text{des}(\mathbb{1})$ , and states that are antisymmetric to  $\text{des}(\epsilon)$ .

**Summary** For each eigenvalue in the Ising model, its free fermion formulation, and the dilute  $A_3$  model, we have now assigned a numerical value, a momentum, and a conformal

sector. We could try to find further properties of these eigenstates, like for example which exact descendant they are, but the three we have already identified turn out to suffice. We can fully identify a unique free fermion character to each of the eigenvalues of the dilute  $A_3$  model.

### 6.3 Next steps

In theory, we now have a description of the dilute  $A_3$  model in terms of both the Bethe Ansatz and free fermions, so we should be able to reach our original goal of associating free fermion states to the  $E_8$  particles, or at least the critical spectrum. However, the BAEs in equation (6.1) are hard to solve, even numerically, and we were unable to generate enough stable solutions to really make explicit connections. This is not to say it is impossible. Equations like the ones in (6.1) can be solved with more advanced numerical techniques and clever assumptions about the patterns of solutions on the complex plane. The authors of [14] for example mention their numerical study of even the off-critical version of (6.1), and they indeed find indication for the eight particles.

The next step is thus obvious: a proper numerical investigation of these Bethe equations. Using the results from this thesis, these solutions could then shine light on the fermionic nature of the  $E_8$  particles. This last step is unfortunately out of my reach for now, but I hope that somebody else will be inspired by the progress and finish this ambitious project.

# 7

## Conclusion

*In theory, there is no difference between theory and practice. But, in practice, there is.* - Jan L.A. van de Snepscheut

In this thesis, we followed a historic line of research that was inspired by a famous paper by Alexander Zamolodchikov [37]. In his paper, Zamolodchikov studied the physics of the Ising model under a magnetic perturbation, and found a number of conserved quantities and excitations. We are now almost 40 years of research later, but nothing new has been discovered about its physics. There are still eight particles and the conserved quantities haven't changed. This is partly due to the fact that the original paper already included basically everything one might want to say about the system, but also due to the fact that the further research has not really been motivated by the promise of new physics. Rather, the fact that there seemed to be rich algebraic structures hidden in the physics motivated people to study it, not to exploit these mathematical structures, but rather to appreciate and enjoy them. Following this process of inquiry, we've seen many faces of a particular object called  $E_8$ . It is many things indeed. Its first appearance was as a Lie algebra: the eight particles have masses that have their mutual ratios encoded in the Cartan matrix of the Lie algebra  $E_8$ . We've also seen the associated Lie group appear as the target space manifold of an Ising ( $c = 1/2$ ) conformal field theory (a diagonal  $E_8$  coset WZW model). At the same time, we've seen quantum field theories ((affine)  $E_8$  Toda field theories) that describe the Ising model where we only needed the discrete eight-dimensional  $E_8$  lattice or its Dynkin diagram. It is not clear which of these is most fundamental, and perhaps that question doesn't even mean anything, but we set out to gain more understanding of the

role  $E_8$  plays in the Ising model.

Our hope was to get closer to its actual appearance in the physics. We took the descriptions of the eight particles in terms of the Bethe Ansatz, and tried to find a translation from their confusing and opaque Bethe quantum numbers into clear and simple free fermion momentum occupation quantum numbers, in the hope that such an identification would shine light on what those particles actually are in terms of excitations on the lattice. We practised such a translation first in the simpler case of the critical Ising model and the Bethe Ansatz for the six-vertex model, and afterwards set out on the journey to generalise this to the dilute  $A_3$ -model that contains the eight particles in its 19-vertex Bethe Ansatz. We ended up theoretically solving this problem by identifying the free fermion states of the dilute  $A_3$ -model as well as writing down its corresponding Bethe Ansatz. However, numerically solving the Bethe Ansatz equation turned out to be beyond the scope of this thesis.

The mystery thus persists, we don't know why and how the most complex semisimple Lie algebra we know appears in a perturbation of arguably the simplest nontrivial system in all of physics. As inspiration, we might remember that there are more places in physics where Lie algebraic symmetries lead to particles. Most famous are the Lie group symmetries of the Standard Model that generate the force-carrying gauge-bosons. There, demanding invariance under a symmetry transformation, fields transform under representations of the corresponding group, and demanding the theory to be invariant forces you to add a new field or particle. While this is somewhat reminiscent of the conserved charge bootstrap procedure that predicted the eight particles, the latter doesn't need an a priori specification of the algebraic structure, so the way in which the algebra appears is fundamentally very different. In fact, the same bootstrap calculation can be done by looking at reflections in the Weyl group of  $E_8$ , so it is not clear if we even need the full algebraic structure.

I don't doubt that there will be further research on this topic. The Ising model is so ubiquitous throughout the mathematical sciences, and  $E_8$  is such a mythical object in mathematics, that many more people will be gripped by its mysterious appearance. This thesis will hopefully aid research into a better understanding of the nature of the particles on the lattice, or inspire people to take a completely different approach altogether.

# Bibliography

- [1] D. J. Amit, H. Gutfreund, and H. Sompolinsky. Spin-glass models of neural networks. *Phys. Rev. A*, 32:1007–1018, Aug 1985. doi: 10.1103/PhysRevA.32.1007. URL <https://link.aps.org/doi/10.1103/PhysRevA.32.1007>.
- [2] R. J. Baxter, S. B. Kelland, and F. Y. Wu. Equivalence of the Potts model or Whitney polynomial with an ice-type model. *Journal of Physics A Mathematical General*, 9: 397–406, Mar. 1976. doi: 10.1088/0305-4470/9/3/009.
- [3] V. Bazhanov, B. Nienhuis, and S. Warnaar. Lattice ising model in a field: E8 scattering theory. *Physics Letters B*, 322(3):198 – 206, 1994. ISSN 0370-2693. doi: [https://doi.org/10.1016/0370-2693\(94\)91107-X](https://doi.org/10.1016/0370-2693(94)91107-X). URL <http://www.sciencedirect.com/science/article/pii/037026939491107X>.
- [4] W. Bialek, A. Cavagna, I. Giardina, T. Mora, E. Silvestri, M. Viale, and A. M. Walczak. Statistical mechanics for natural flocks of birds. *Proceedings of the National Academy of Sciences*, 109(13):4786–4791, 2012. ISSN 0027-8424. doi: 10.1073/pnas.1118633109. URL <http://www.pnas.org/content/109/13/4786>.
- [5] H. W. J. Bloete, J. L. Cardy, and M. P. Nightingale. Conformal Invariance, the Central Charge, and Universal Finite Size Amplitudes at Criticality. *Phys. Rev. Lett.*, 56:742–745, 1986. doi: 10.1103/PhysRevLett.56.742.
- [6] S. T. Carr and A. M. Tsvelik. Spectrum and correlation functions of a quasi-one-dimensional quantum ising model. *Physical review letters*, 90(17):177206, 2003.
- [7] R. Coldea, D. Tennant, E. Wheeler, E. Wawrzynska, D. Prabhakaran, M. Telling, K. Habicht, P. Smeibidl, and K. Kiefer. Quantum criticality in an ising chain: experimental evidence for emergent e8 symmetry. *Science*, 327(5962):177–180, 2010.
- [8] P. Di Francesco, P. Mathieu, and D. Senechal. *Conformal Field Theory*. Graduate Texts in Contemporary Physics. Springer-Verlag, New York, 1997. ISBN 9780387947853, 9781461274759. doi: 10.1007/978-1-4612-2256-9. URL <http://www-spines.fnal.gov/spines/find/books/www?cl=QC174.52.C66D5::1997>.

## BIBLIOGRAPHY

---

- [9] E. Domany, 2017. Said at the symposium ‘Ingenuity and Integrability in Statistical Mechanics’ at the University of Amsterdam.
- [10] P. Dorey. Exact s-matrices. In Z. Horváth and L. Palla, editors, *Conformal Field Theories and Integrable Models*, pages 85–125, Berlin, Heidelberg, 1997. Springer Berlin Heidelberg. ISBN 978-3-540-69613-1.
- [11] P. G. Dorey. Hidden geometrical structures in integrable models. 1993.
- [12] C. Fortuin and P. Kasteleyn. On the random-cluster model: I. introduction and relation to other models. *Physica*, 57(4):536 – 564, 1972. ISSN 0031-8914. doi: [https://doi.org/10.1016/0031-8914\(72\)90045-6](https://doi.org/10.1016/0031-8914(72)90045-6). URL <http://www.sciencedirect.com/science/article/pii/0031891472900456>.
- [13] M. Freeman. On the mass spectrum of affine toda field theory. *Physics Letters B*, 261(1-2):57–61, 1991.
- [14] U. Grimm and B. Nienhuis. Scaling limit of the Ising model in a field. *Phys. Rev. E*, 55:5011–5025, May 1997. doi: 10.1103/PhysRevE.55.5011.
- [15] C.-Y. Huang, T.-C. Wei, and R. Orus. Holographic encoding of universality in corner spectra. *Phys. Rev.*, B95(19):195170, 2017. doi: 10.1103/PhysRevB.95.195170.
- [16] E. Ising. Beitrag zur theorie des ferromagnetismus. *Zeitschrift für Physik*, 31(1):253–258, Feb 1925. ISSN 0044-3328. doi: 10.1007/BF02980577. URL <https://doi.org/10.1007/BF02980577>.
- [17] C. Itzykson, H. Saleur, and J. B. Zuber. *Conformal invariance and applications to statistical mechanics*. World Scientific Pub., 1988. ISBN 9971506068.
- [18] S. Ketov. *Conformal Field Theory*. World Scientific Pub., 1995. ISBN 9789810216085. URL <https://books.google.nl/books?id=xMt6QgAACAAJ>.
- [19] C. Korff. Lie algebraic structures in integrable models, affine toda field theory, July 2000.
- [20] J. Miekisz and P. Szymaska. On spins and genes. *Mathematica Applicanda*, 40, 08 2012.

## BIBLIOGRAPHY

---

- [21] P. Mognini. Eth theoretisches proseminar. Notes from a seminar at the ETH Zurich, March 2013.
- [22] C. M. Morris, R. Valdés Aguilar, A. Ghosh, S. M. Koochpayeh, J. Krizan, R. J. Cava, O. Tchernyshyov, T. M. McQueen, and N. P. Armitage. Hierarchy of bound states in the one-dimensional ferromagnetic ising chain  $\text{CoNb}_2\text{O}_6$  investigated by high-resolution time-domain terahertz spectroscopy. *Phys. Rev. Lett.*, 112:137403, Apr 2014. doi: 10.1103/PhysRevLett.112.137403. URL <https://link.aps.org/doi/10.1103/PhysRevLett.112.137403>.
- [23] G. Mussardo. *Statistical Field Theory*. Oxford University Press, 2010. ISBN 9780199547586.
- [24] M. Niss. History of the lenz-ising model 1920–1950: From ferromagnetic to cooperative phenomena. *Archive for History of Exact Sciences*, 59(3):267–318, Mar 2005. ISSN 1432-0657. doi: 10.1007/s00407-004-0088-3. URL <https://doi.org/10.1007/s00407-004-0088-3>.
- [25] V. Pasquier. Two-dimensional critical systems labelled by dynkin diagrams. *Nuclear Physics B*, 285:162 – 172, 1987. ISSN 0550-3213. doi: [https://doi.org/10.1016/0550-3213\(87\)90332-4](https://doi.org/10.1016/0550-3213(87)90332-4). URL <http://www.sciencedirect.com/science/article/pii/0550321387903324>.
- [26] V. Pasquier. Lattice derivation of modular invariant partition functions on the torus. *Journal of Physics A: Mathematical and General*, 20(18):L1229, 1987. URL <http://stacks.iop.org/0305-4470/20/i=18/a=003>.
- [27] S. Schaveling. The two dimensional ising model. Master’s thesis, University of Amsterdam, February 2016.
- [28] T. D. Schultz, D. C. Mattis, and E. H. Lieb. Two-dimensional ising model as a soluble problem of many fermions. *Rev. Mod. Phys.*, 36:856–871, Jul 1964. doi: 10.1103/RevModPhys.36.856. URL <https://link.aps.org/doi/10.1103/RevModPhys.36.856>.
- [29] N. Sloane. The on-line encyclopedia of integer sequences, 2018. URL [www.oeis.org](http://www.oeis.org).

## BIBLIOGRAPHY

---

- [30] D. Stauffer. Social applications of two-dimensional ising models. *American Journal of Physics*, 76(4):470–473, 2008. doi: 10.1119/1.2779882. URL <https://doi.org/10.1119/1.2779882>.
- [31] E. Verheijden. Traversable wormholes, shock waves and de sitter space. Master’s thesis, University of Amsterdam, July 2018.
- [32] S. O. Warnaar and B. Nienhuis. Solvable lattice models labelled by dynkin diagrams. *Journal of Physics A: Mathematical and General*, 26(10):2301, 1993. URL <http://stacks.iop.org/0305-4470/26/i=10/a=005>.
- [33] S. O. Warnaar, M. T. Batchelor, and B. Nienhuis. Critical properties of the izergin-korepin and solvable  $o(n)$  models and their related quantum spin chains. *Journal of Physics A: Mathematical and General*, 25(11):3077, 1992. URL <http://stacks.iop.org/0305-4470/25/i=11/a=016>.
- [34] S. O. Warnaar, B. Nienhuis, and K. A. Seaton. A critical ising model in a magnetic field. *International Journal of Modern Physics B*, 07(20n21):3727–3736, 1993. doi: 10.1142/S0217979293003474. URL <https://www.worldscientific.com/doi/abs/10.1142/S0217979293003474>.
- [35] W. F. Wolff and J. Zittartz. Inhomogeneous ising models with diagonal structure on a square lattice. *Zeitschrift für Physik B Condensed Matter*, 44(1):109–119, Mar 1981. ISSN 1431-584X. doi: 10.1007/BF01292658. URL <https://doi.org/10.1007/BF01292658>.
- [36] A. Zamolodchikov. Thermodynamic bethe ansatz in relativistic models: Scaling 3-state potts and lee-yang models. *Nuclear Physics B*, 342(3):695 – 720, 1990. ISSN 0550-3213. doi: [https://doi.org/10.1016/0550-3213\(90\)90333-9](https://doi.org/10.1016/0550-3213(90)90333-9). URL <http://www.sciencedirect.com/science/article/pii/0550321390903339>.
- [37] A. B. Zamolodchikov. Integrals of Motion and S Matrix of the (Scaled)  $T=T(c)$  Ising Model with Magnetic Field. *Int. J. Mod. Phys.*, A4:4235, 1989. doi: 10.1142/S0217751X8900176X.
- [38] J. B. Zuber and C. Itzykson. Quantum field theory and the two-dimensional ising

## BIBLIOGRAPHY

---

model. *Phys. Rev. D*, 15:2875–2884, May 1977. doi: 10.1103/PhysRevD.15.2875.  
URL <https://link.aps.org/doi/10.1103/PhysRevD.15.2875>.

# A

## Appendix

### A.1 The Experiment

Even though the Ising model was of course introduced to describe a part of reality, we have mostly been interested in the 1D-quantum and 2D-classical versions, which are quite difficult to realise in our notoriously 3-dimensional (quantum mechanical) universe. In fact, the 1D quantum chain we have been looking at does rely on the three Pauli matrices, corresponding to three spatial directions. This paradoxical dimensionality is why Zamolodchikov's prediction remained largely a mathematical exercise through the 90's and 00's.

This changed in 2010 when a group of experimentalists in Germany and the UK were able to examine a system that shared some of the essential features of this 1D magnetically perturbed Ising model [7]. They looked at the insulating quasi-1D Ising ferromagnet  $\text{CoNb}_2\text{O}_6$ . They call this quasi-1D because one can grow long chains of this crystal in which the  $\text{Co}^{2+}$  atoms will align along a zigzagging axis (see fig. A.1).

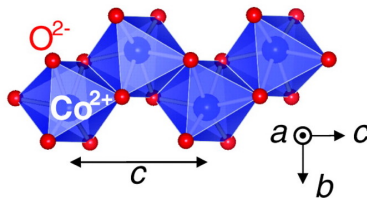


Figure A.1: Part of the  $\text{CoNb}_2\text{O}_6$ -chain, where the  $c$ -axis is defined to go along the chain. Source: [7]

There is, however, the question whether the individual chains in the 3D crystal will not affect each other too much to destroy the 1D characteristics. This matter is addressed theoretically in [6], and it is shown that the effect of nearby chains can to first order be described by a longitudinal field  $g_z$  on the 1D chain:

$$\mathcal{H} = -K(\sigma_j^z \sigma_{j+1}^z + h_x \sigma_j^x + g_z \sigma_j^z)$$

To verify that  $\text{CoNb}_2\text{O}_6$  crystals in the experiment indeed preserve these 1D dynamics, the researchers first examined the crystal with  $h_x = 0$ , and used that one dimensional spin chains contain some unique dynamics. In the ferromagnetic phase, there are the two  $\mathbb{Z}_2$  ground states, and a kink is a local deformation of the chain that interpolates between the two, schematically shown in figure A.2.

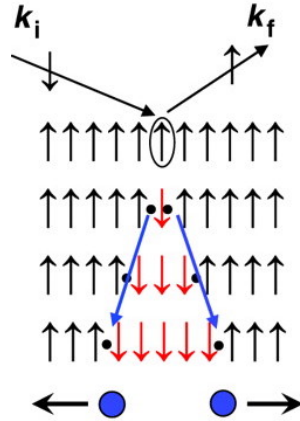


Figure A.2: A local spin-flip, caused by a neutron scattering, can spontaneously flip its neighbors and propagate the new groundstate in both directions. Time goes down the page. Source: [7]

Now the cost of such a kink propagating is actually zero, since at every moment in time, the domain wall, which is the part that costs energy, is the same size<sup>1</sup>. This results in a continuum spectrum when the crystal is examined by neutron spectroscopy. Note that

<sup>1</sup>There is a more subtle effect going on among different chains that actually does suppress pairs of kinks propagating far, since these large new domains also cost energy when next to a chain in a different ground state. This leads to an effect called kink confinement, and its precise character is later used to verify the model.

this is inherently a one dimensional effect. In higher dimensions, surface area actually scales with volume, and larger domains will cost more energy. Only in 1D we see a constant surface area for a growing domain, and these kinks can propagate at no cost. When going through the critical point by increasing the transverse magnetic field, we enter the paramagnetic phase, where there are no longer two degenerate ground states, and a sharp excitation peak is expected where a spin is flipped against the preferred direction of the transverse field. The experimenters use exactly these properties to verify that the crystal they investigate is indeed acting as a one-dimensional quantum Ising chain, and found good indication that it did.

Now cooling the crystal too 40 mK and coming from low transverse field, deeply in its ordered phase,  $h_x$  can be tuned to approach the quantum phase transition. At this point, it is precisely the longitudinal field induced by the inter-chain interaction that serves as the magnetic perturbation that predicts the spectrum of eight particles.

Bombarding the crystal with incoming neutrons, what the experiment showed was that as the transverse field approached the critical value, the ratio between the lightest two excitations indeed approached the golden ratio, as predicted by Zamolodchikov nearly two decades earlier (see figure A.3).

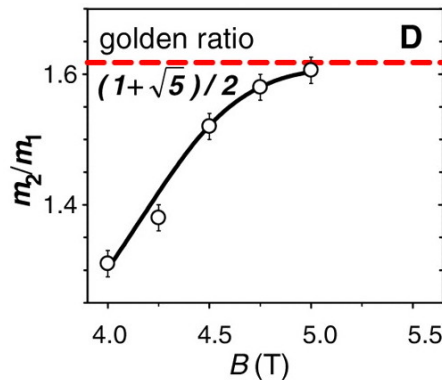


Figure A.3: As the magnetic field approaches the critical value of 5.5T, the ratio of the first two masses approaches  $\phi$ . Source: [7]

A full plot of excitation intensities (fig. A.4) shows two clear peaks for the lightest particles, but then evolves into a noisy plateau with little interesting detail.

This is due to the fact that the third particle weighs about  $2m_1$ , and all higher excita-

tion peaks get overshadowed by the continuum of producing multiple, or combinations of, lighter particles (see fig.A.5). This makes further identification of the eight predicted particles impossible, but the experimenters make the claim that they have conclusively identified the lightest two.

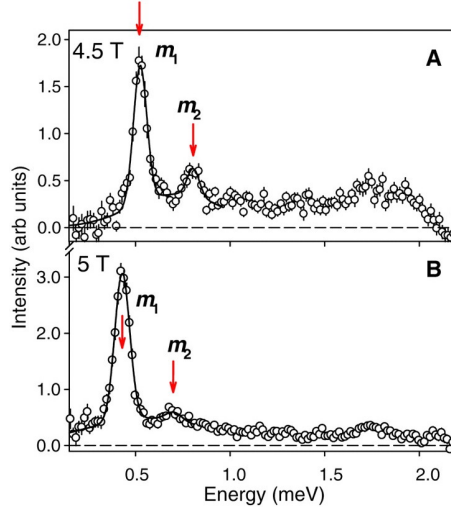


Figure A.4: Two spectra at different magnetic fields. Source: [7]

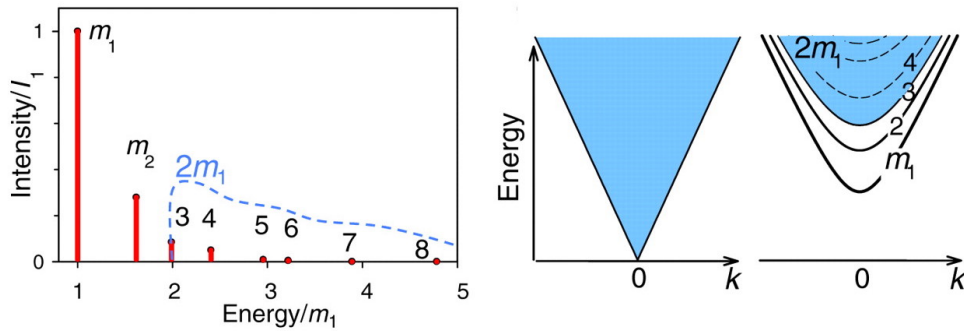


Figure A.5: (left) Relative contributions of the higher excitations to the spectrum, with overlay of the  $2m_1$  continuum (dashed line). (right) Effect on the critical spectrum of a longitudinal field: it introduces a gap, and creates two distinct energy levels, and a continuum above them. Source: [7]

**Addendum** After writing this thesis, it was brought to my attention that a similar experiment has been conducted in 2014, showing even more promising results [22]. Instead of using neutron scattering, the authors investigated the  $\text{CoNb}_2\text{O}_6$  with terahertz spectroscopy, i.e. electromagnetic radiation. This technique offers a much higher absorption

resolution, and the authors find even stronger evidence that the material is adequately described by 1D physics. Like [7], they do this by looking at bound states at zero transverse magnetic field ( $h_x = 0$ , so not in the vicinity of the critical point). Where [7] found five peaks to verify the 1D model, [22] found nine, and even an extra peak just below the  $2m_1$  threshold. They attribute this extra peak to a bound state between two interacting chains. However, in spite of the increased resolution, in the vicinity of the critical point, they still only report on the lowest two  $E_8$  states, the rest still hiding in the  $2m_1$  continuum. I'd like to thank Neil J. Robinson for bringing this experiment to my attention.

## A.2 Coxeter orbit code

```
Cart = [[2, -1, 0, 0, 0, 0, 0, 0], [-1, 2, -1, 0, 0, 0, 0, 0],
[0, -1, 2, -1, 0, 0, 0, 0], [0, 0, -1, 2, -1, 0, 0, 0],
[0, 0, 0, -1, 2, -1, 0, -1], [0, 0, 0, 0, -1, 2, -1, 0],
[0, 0, 0, 0, 0, -1, 2, 0], [0, 0, 0, 0, -1, 0, 0, 2]]
```

```
def r(i, rootVec):
    tempVec = [0, 0, 0, 0, 0, 0, 0, 0]

    for j in range(len(rootVec)):
        if rootVec[j] != 0:
            tempVec[j] += rootVec[j]
            tempVec[i] -= rootVec[j] * Cart[i][j]

    rootVec = tempVec
    return rootVec

def coxE1(rootVec):
    return r(6, r(4, r(2, r(0, r(7, r(5, r(3, r(1, rootVec))))))))

#The vector to compute the orbit of:
```

```
orbitVec = [1, 0, 0, 0, 0, 0, 0, 0]
```

```
for i in range(31):
    print [orbitVec[0], orbitVec[6],
          orbitVec[1], orbitVec[7],
          orbitVec[2], orbitVec[5],
          orbitVec[3], orbitVec[4]]
    orbitVec = coxE1(orbitVec)
```

### A.3 Commutator of diagonal transfer matrix and 1D quantum Ising Hamiltonian

For the paper that these calculations are based on, we refer the reader to [35].

We want to look at  $[H, D_1]$  where

$$(D_1)_{\mu\mu'} = \exp\left(\sum_{i=1}^M J(\mu_i\mu'_i + \mu_{i+1}\mu'_i)\right) \quad (\text{A.1})$$

$$H_{\mu\mu'} = \sum_{j=1}^N \left( \delta_{\mu_1\mu'_1} \delta_{\mu_2\mu'_2} \dots \delta_{\mu_j-\mu'_j} \dots \delta_{\mu_N\mu'_N} + S\mu_j\mu_{j+1}\delta_{\mu\mu'} \right) \quad (\text{A.2})$$

$$(\text{A.3})$$

Letting these operators now work on the same spin chain of length  $N$ , we can look at their commutator:

$$[H, D_1] = \sum_{\lambda} \left( H_{\mu\lambda}(D_1)_{\lambda\mu'} - (D_1)_{\mu\lambda}H_{\lambda\mu'} \right) \quad (\text{A.4})$$

Evaluating both terms individually:

$$\begin{aligned} \sum_{\lambda} H_{\mu\lambda}(D_1)_{\lambda\mu'} &= \sum_{\lambda} \left( \sum_{j=1}^N \left( \delta_{\mu_1\lambda_1} \delta_{\mu_2\lambda_2} \dots \delta_{\mu_j-\lambda_j} \dots \delta_{\mu_N\lambda_N} + S\mu_j\mu_{j+1}\delta_{\mu\lambda} \right) \exp\left( \sum_{i=1}^N J(\lambda_i\mu'_i + \lambda_{i+1}\mu'_i) \right) \right) \\ &= \sum_j \exp\left( \sum_i J(\mu_i\mu'_i + \mu_{i+1}\mu'_i) \right) \exp\left( -2J(\mu_j\mu'_j + \mu_j\mu'_{j-1}) \right) \end{aligned} \quad (\text{A.5})$$

$$+ \sum_j \exp\left( \sum_i J(\mu_i\mu'_i + \mu_{i+1}\mu'_i) \right) S\mu_j\mu_{j+1} \quad (\text{A.6})$$

$$= \sum_j \exp\left( \sum_i J(\mu_i\mu'_i + \mu_{i+1}\mu'_i) \right) \left( \exp\left( -2J(\mu_j\mu'_j + \mu_j\mu'_{j-1}) \right) + S\mu_j\mu_{j+1} \right) \quad (\text{A.7})$$

$$\begin{aligned} \sum_{\lambda} (D_1)_{\mu\lambda} H_{\lambda\mu'} &= \sum_{\lambda} \left( \exp\left( \sum_{i=1}^N J(\mu_i\lambda_i + \mu_{i+1}\lambda_i) \right) \sum_{j=1}^N \left( \delta_{\lambda_1\mu'_1} \delta_{\lambda_2\mu'_2} \dots \delta_{\lambda_j-\mu'_j} \dots \delta_{\lambda_N\mu'_N} + S\lambda_j\lambda_{j+1}\delta_{\lambda\mu'} \right) \right) \\ &= \sum_j \exp\left( \sum_i J(\mu_i\mu'_i + \mu_{i+1}\mu'_i) \right) \exp\left( -2J(\mu_j\mu'_j + \mu_{j+1}\mu'_j) \right) \end{aligned} \quad (\text{A.8})$$

$$+ \sum_j \exp\left( \sum_i J(\mu_i\mu'_i + \mu_{i+1}\mu'_i) \right) S\mu'_j\mu'_{j+1} \quad (\text{A.9})$$

$$= \sum_j \exp\left( \sum_i J(\mu_i\mu'_i + \mu_{i+1}\mu'_i) \right) \left( \exp\left( -2J(\mu_j\mu'_j + \mu_{j+1}\mu'_j) \right) + S\mu'_j\mu'_{j+1} \right) \quad (\text{A.10})$$

Assuming  $\exp\left( \sum_i J(\mu_i\mu'_i + \mu_{i+1}\mu'_i) \right) \neq 0$ , demanding the full commutator be zero amounts to demanding:

$$\sum_j \left( e^{-2J\mu_j\mu'_j} (e^{-2J\mu_{j+1}\mu'_j} - e^{-2J\mu_j\mu'_{j-1}}) + S(\mu'_j\mu'_{j+1} - \mu_j\mu_{j+1}) \right) = 0 \quad (\text{A.11})$$

Since we know that  $\mu_i\mu'_j$  can only be +1 or -1, we can simplify this demand by defining  $p$  and  $q$  by

$$p + q = e^{-2J} \tag{A.12}$$

$$p - q = e^{2J} \tag{A.13}$$

$$\implies e^{-2J\mu_i\mu'_j} = p + q(\mu_i\mu'_j) \tag{A.14}$$

Where

$$p = \cosh(-2J) \tag{A.15}$$

$$q = \sinh(-2J) \tag{A.16}$$

Our demand then becomes:

$$\implies \sum_j (p + q(\mu_j\mu'_j)) (p + q(\mu_{j+1}\mu'_j) - p - q(\mu_j\mu_{j-1})) = -S \sum_j (\mu'_j\mu'_{j+1} - \mu_j\mu_{j+1})$$

Assuming (in the general case)

$$\sum_j (\mu'_j\mu'_{j+1} - \mu_j\mu_{j+1}) \neq 0 :$$

We can conclude

$$(pq) \frac{\sum_j (\mu_{j+1}\mu'_j - \mu_j\mu'_{j-1})}{\sum_j (\mu'_j\mu'_{j+1} - \mu_j\mu_{j+1})} + q^2 \frac{\sum_j (\mu_j\mu'_j(\mu_{j+1}\mu'_j - \mu_j\mu'_{j-1}))}{\sum_j (\mu'_j\mu'_{j+1} - \mu_j\mu_{j+1})} = -S \tag{A.17}$$

Since in the numerator of the first term we may (because of periodicity) just as well relabel the second sum by an index  $\tilde{j} = j - 1$ , we see that the numerator sums to zero, and we should only evaluate the  $\propto q^2$  fraction.

$$-S = q^2 \frac{\sum_j (\mu_j \mu'_j (\mu_{j+1} \mu'_j - \mu_j \mu'_{j-1}))}{\sum_j (\mu'_j \mu'_{j+1} - \mu_j \mu_{j+1})} \quad (\text{A.18})$$

$$= q^2 \frac{\sum_j (\mu_j \mu_{j+1} (\mu'_j)^2 - \mu'_j \mu'_{j-1} (\mu_j)^2)}{\sum_j (\mu'_j \mu'_{j+1} - \mu_j \mu_{j+1})} \quad (\text{A.19})$$

$$= q^2 \frac{\sum_j (\mu_j \mu_{j+1} - \mu'_j \mu'_{j-1})}{\sum_j (\mu'_j \mu'_{j+1} - \mu_j \mu_{j+1})} \quad (\text{A.20})$$

$$= -q^2 \frac{\sum_j (\mu_j \mu_{j+1} - \mu'_j \mu'_{j-1})}{\sum_j (\mu_j \mu_{j+1} - \mu'_j \mu'_{j+1})} \quad (\text{A.21})$$

$$(\text{A.22})$$

Where we can again relabel the second sum in the numerator by an index  $\tilde{j} = j - 1$  so that the total fraction becomes one and we can immediately conclude that

$$[H, D_1] = 0 \text{ for } S = q^2 = \sinh^2(-2J) = \sinh^2(2J)$$

The calculation for  $D_2$  is fully analogous, and too similar to justify printing it here. It leads to exactly the same constraint:  $S = q^2$ , so both transfer matrices and the Hamiltonian can be simultaneously diagonalised.

## A.4 The diagonal Ising transfer matrix in fermion basis.

We start from the expression for the eigenvalues of the transfer matrix in Paulion-basis (B.5 in [35]):

$$\lambda \langle 0 | \Phi \rangle = 2^{-N/2} \sum_{\mu'} \langle \mu' | \prod_{j=1}^N A e^{B \sigma_j^3 \sigma_{j+1}^3} | \Phi \rangle \quad (\text{A.23})$$

Where  $|\Phi\rangle$  is an eigenstate of the transfer matrix. We then first do the Jordan-Wigner transformation to go from these Pauli operators (whose creation and annihilation operators obey mixed commutation relations) to proper fermion operators:

$$\sigma_j^1 = 2c_j^\dagger c_j - 1 \quad (\text{A.24})$$

$$\sigma_j^3 = (-1)^{\sum_{i=1}^{j-1} c_i^\dagger c_i} (c_j^\dagger + c_j) \quad (\text{A.25})$$

$$\sigma_j^2 = i\sigma_j^1 \sigma_j^3 \quad (\text{A.26})$$

So that we can rewrite the exponent with:

$$\sigma_j^3 \sigma_{j+1}^3 = (-1)^{\sum_{i=1}^{j-1} c_i^\dagger c_i} (c_j^\dagger + c_j) (-1)^{\sum_{i'=1}^{j-1} c_{i'}^\dagger c_{i'}} (c_{j+1}^\dagger + c_{j+1}) \quad (\text{A.27})$$

$$= (-1)^{2\sum_{i=1}^{j-1} c_i^\dagger c_i} (c_j^\dagger + c_j) (-1)^{c_j^\dagger c_j} (c_{j+1}^\dagger + c_{j+1}) \quad (\text{A.28})$$

$$= (c_j^\dagger - c_j)(c_{j+1}^\dagger + c_{j+1}) \quad (\text{A.29})$$

Going back to the original expression, we see that we should evaluate the sum over  $j$  of this operator. We can do this by Fourier transforming the fermion operators:

$$c_j^\dagger = \frac{1}{\sqrt{N}} \sum_k e^{-ikj} c_k^\dagger \quad (\text{A.30})$$

$$c_j = \frac{1}{\sqrt{N}} \sum_k e^{ikj} c_k \quad (\text{A.31})$$

Where  $k$  ranges in  $(-\pi, \pi]$ , and goes in steps of  $2\pi/N$ . We will now evaluate the full

operator term by term:

$$\sum_j c_j^\dagger c_{j+1}^\dagger = \sum_j \frac{1}{N} \sum_{k,l} c_k^\dagger c_l^\dagger e^{-(k+l)j} e^{-il} \quad (\text{A.32})$$

$$= \frac{1}{N} \sum_{k,l} c_k^\dagger c_l^\dagger (N \delta_{k,-l}) e^{-il} \quad (\text{A.33})$$

$$= \frac{1}{2} \left( \sum_k c_k^\dagger c_{-k}^\dagger e^{ik} + \sum_l c_{-l}^\dagger c_l^\dagger e^{-il} \right) \quad (\text{A.34})$$

$$= -i \sum_k c_{-k}^\dagger c_k^\dagger \sin k \quad (\text{A.35})$$

$$\sum_j c_j^\dagger c_{j+1} = \sum_j \frac{1}{N} \sum_{k,l} c_k^\dagger c_l^\dagger e^{-(k-l)j} e^{il} \quad (\text{A.36})$$

$$= \frac{1}{N} \sum_{k,l} c_k^\dagger c_l^\dagger (N \delta_{k,l}) e^{il} \quad (\text{A.37})$$

$$= \sum_k c_k^\dagger c_k e^{ik} \quad (\text{A.38})$$

And we now note that the other two terms are just the Hermitian conjugates of these, leading to the full expression:

$$\sigma_j^3 \sigma_{j+1}^3 = \sum_k -i \sin k (c_{-k} c_k + c_{-k}^\dagger c_k^\dagger) + c_k^\dagger c_k e^{ik} - c_k c_k^\dagger e^{-ik} \quad (\text{A.39})$$

$$= \sum_k 2 \cos k \left( c_k^\dagger c_k - \frac{1}{2} \right) + i \sin k (c_k^\dagger c_{-k}^\dagger + c_k c_{-k}) \quad (\text{A.40})$$

Where we've used that an anti-symmetric sum over  $k$  of  $\sin(k)$  equals zero, and cancelled the oddness in  $k$  of  $\sin(k)$  against the anticommutation of fermion operators. Since the summand is even in  $k$ , it is now tempting to write the full sum as twice the sum over  $k \geq 0$ . But recall that the  $k$ -interval is actually only *almost* antisymmetric, in the sense that there are two  $k$ 's that don't share an absolute value with another  $k$  in the sum:  $0$  and  $\pi$  (note that this does not mess up our earlier argument based on the antisymmetry of the  $k$ -interval, since  $\sin(0) = \sin(\pi) = 0$ ). When doubling the sum, these two values for  $k$  should not be counted twice, and have to be treated separately, leading to:

$$\begin{aligned}
 & \sigma_j^3 \sigma_{j+1}^3 = \\
 2(c_0^\dagger c_0 - \frac{1}{2}) - 2(c_\pi^\dagger c_\pi - \frac{1}{2}) + 2 \sum_{0 < k < \pi} 2 \cos k (c_k^\dagger c_k - \frac{1}{2}) + i \sin k (c_k^\dagger c_{-k}^\dagger + c_k c_{-k}) \quad (A.41)
 \end{aligned}$$

We thus get that we can rewrite the eigenvalues from position basis into momentum basis as:

$$\lambda \langle 0 | \Phi \rangle = 2^{-N/2} \sum_{\mu'} \langle \mu' | \prod_{j=1}^N A e^{B \sigma_j^3 \sigma_{j+1}^3} | \Phi \rangle \quad (A.42)$$

$$= \langle 0 | A e^{2\tilde{B}(c_0^\dagger c_0 - \frac{1}{2})} A e^{-2\tilde{B}(c_\pi^\dagger c_\pi - \frac{1}{2})} \prod_{0 < q < \pi} A^2 e^{2\tilde{B}(\tau_q^3 \cos(q) + \tau_q^1 \sin(q))} | \Phi \rangle \quad (A.43)$$

Where we defined as in [35]:

$$\tau_q^1 = i(c_q^\dagger c_{-q}^\dagger + c_q c_{-q}) \quad (A.44)$$

$$\tau_q^3 = c_q^\dagger c_q + c_{-q}^\dagger c_{-q} - 1 \quad (A.45)$$

$$A = 2 \sqrt{\cosh(J_1)^2 \cosh(J_2)^2 - \sinh(J_1)^2 \sinh(J_2)^2} \quad (A.46)$$

$$B = \text{acosh}(2 \cosh(J_1) \cosh(J_2) / A) \quad (A.47)$$

## A.5 Wolff-Zittartz eigenvalues

Eigenvalues and their momentum occupation, $L=3$ , $J_1 = J_2 = 1$				
Eigenvalue	$q = 0$	$\frac{\pi}{3}$	$\frac{2\pi}{3}$	$\pi$
22.1277	1		0	
403.877	1		2	
6.85568		0		0
403.824	0		1	
7.25372 - 12.5638i		(-1)		1
7.25372 + 12.5638i		1		1
0	1		(-1)	
0	1		1	

Eigenvalues and their momentum occupation, $L=4$ , $J_1 = J_2 = 1$					
Eigenvalue	$q = 0$	$\frac{\pi}{4}$	$\frac{\pi}{2}$	$\frac{3\pi}{4}$	$\pi$
2985.13		2		2	
2985.1	1		2		0
189.173		2		0	
109.16 + 109.16i	0		1		0
109.16 - 109.16i	0		(-1)		0
105.016	0		0		1
74.4109i		1		1	
-74.4109i		(-1)		(-1)	
52.6165 + 52.6165i		1		(-1)	
52.6165 - 52.6165i		1		1	
29.2694		0		2	
1.85486		0		0	
0	0		2		1
0	0		0		1
0	1		(-1)		1
0	1		1		1

## A.6 Derivation of the twisted Bethe equations

We start with the relation that defines our Yang-Baxter algebra:



$$\begin{aligned}
 \tilde{T}_2(\mu)\tilde{T}_1(\lambda)R_{12}(\lambda - \mu) = & \begin{pmatrix} a(\lambda-\mu)\tilde{A}(\mu)\tilde{A}(\lambda) & b(\lambda-\mu)\tilde{B}(\mu)\tilde{A}(\lambda)+c(\lambda-\mu)\tilde{A}(\mu)\tilde{B}(\lambda) \\ a(\lambda-\mu)\tilde{C}(\mu)\tilde{A}(\lambda) & c(\lambda-\mu)\tilde{C}(\mu)\tilde{B}(\lambda)+b(\lambda-\mu)\tilde{D}(\mu)\tilde{A}(\lambda) \\ a(\lambda-\mu)\tilde{A}(\mu)\tilde{C}(\lambda) & b(\lambda-\mu)\tilde{B}(\mu)\tilde{C}(\lambda)+c(\lambda-\mu)\tilde{A}(\mu)\tilde{D}(\lambda) \\ a(\lambda-\mu)\tilde{C}(\mu)\tilde{C}(\lambda) & c(\lambda-\mu)\tilde{C}(\mu)\tilde{D}(\lambda)+b(\lambda-\mu)\tilde{D}(\mu)\tilde{C}(\lambda) \end{pmatrix} \\
 & \begin{pmatrix} b(\lambda-\mu)\tilde{A}(\mu)\tilde{B}(\lambda)+c(\lambda-\mu)\tilde{B}(\mu)\tilde{A}(\lambda) & a(\lambda-\mu)\tilde{B}(\mu)\tilde{B}(\lambda) \\ b(\lambda-\mu)\tilde{C}(\mu)\tilde{B}(\lambda)+c(\lambda-\mu)\tilde{D}(\mu)\tilde{A}(\lambda) & a(\lambda-\mu)\tilde{D}(\mu)\tilde{B}(\lambda) \\ c(\lambda-\mu)\tilde{B}(\mu)\tilde{C}(\lambda)+b(\lambda-\mu)\tilde{A}(\mu)\tilde{D}(\lambda) & a(\lambda-\mu)\tilde{B}(\mu)\tilde{D}(\lambda) \\ b(\lambda-\mu)\tilde{C}(\mu)\tilde{D}(\lambda)+c(\lambda-\mu)\tilde{D}(\mu)\tilde{C}(\lambda) & a(\lambda-\mu)\tilde{D}(\mu)\tilde{D}(\lambda) \end{pmatrix} \quad (\text{A.54})
 \end{aligned}$$

From this we see that (A.48) actually encodes a set of commutation relations for our operators.

Our goal is to find out under what circumstances our  $\tilde{B}$ -excited states are still eigenvectors of our transfer matrix  $\tau(\lambda) = \tilde{A}(\lambda) + \tilde{D}(\lambda)$ . We write

$$\tilde{A}(\lambda) \prod_{j=1}^M \tilde{B}(\lambda_j) |0\rangle = \Lambda_{\tilde{A}} \prod_{j=1}^M \tilde{B}(\lambda_j) |0\rangle + \text{unwanted terms} \quad (\text{A.55})$$

$$\tilde{D}(\lambda) \prod_{j=1}^M \tilde{B}(\lambda_j) |0\rangle = \Lambda_{\tilde{D}} \prod_{j=1}^M \tilde{B}(\lambda_j) |0\rangle + \text{unwanted terms} \quad (\text{A.56})$$

The commutations relations that follow from (A.53) and (A.54) can now be used to commute the operators  $\tilde{A}$  and  $\tilde{D}$  through all the  $\tilde{B}$ s, so that we can evaluate their action. We use the following commutation relations:

$$[\tilde{B}(\lambda), \tilde{B}(\mu)] = 0 \quad (\text{A.57})$$

$$\tilde{A}(\lambda)\tilde{B}(\mu) = \frac{a(\mu - \lambda)}{b(\mu - \lambda)}\tilde{B}(\mu)\tilde{A}(\lambda) - \frac{c(\mu - \lambda)}{b(\mu - \lambda)}\tilde{B}(\lambda)\tilde{A}(\mu) \quad (\text{A.58})$$

$$\tilde{D}(\lambda)\tilde{B}(\mu) = \frac{a(\lambda - \mu)}{b(\lambda - \mu)}\tilde{B}(\mu)\tilde{D}(\lambda) - \frac{c(\lambda - \mu)}{b(\lambda - \mu)}\tilde{B}(\lambda)\tilde{D}(\mu) \quad (\text{A.59})$$

The first one just means that the order of  $\tilde{B}$ -excitations in equations (A.55) and (A.56) doesn't matter, while the bottom ones allow us to actually commute the operators through. Let's focus on computing (A.55) first. Every time we push the  $\tilde{A}(\lambda)$  operator through a  $\tilde{B}(\lambda_i)$ , we get two terms, so that once we've brought  $\tilde{A}(\lambda)$  fully to the vacuum state, we end up with  $2^M$  terms. In one of these terms, we just picked up a factor  $\frac{a(\lambda_i - \lambda)}{b(\lambda_i - \lambda)}$  for each

commutation, leaving the spectral parameters alone, making the whole state an eigenstate of  $\tilde{A}(\lambda)$ . We will call this one term the wanted term, and the other ones the unwanted terms  $U$ :

$$\tilde{A}(\lambda) \prod_{j=1}^M \tilde{B}(\lambda_j) |0\rangle = \left( e^{\theta a(\lambda)^L} \prod_i^M \frac{a(\lambda_i - \lambda)}{b(\lambda_i - \lambda)} \right) \prod_{j=1}^M \tilde{B}(\lambda_j) |0\rangle + U_{\tilde{A}} \quad (\text{A.60})$$

And similarly for the  $\tilde{D}$ -operator:

$$\tilde{D}(\lambda) \prod_{j=1}^M \tilde{B}(\lambda_j) |0\rangle = \left( e^{-\theta b(\lambda)^L} \prod_i^M \frac{a(\lambda - \lambda_i)}{b(\lambda - \lambda_i)} \right) \prod_{j=1}^M \tilde{B}(\lambda_j) |0\rangle + U_{\tilde{D}} \quad (\text{A.61})$$

From this, we can immediately conclude that the eigenvalues of the transfer matrix will turn out to be:

$$\Lambda_{\tau}(\lambda|\{\lambda_j\}_M) = e^{\theta a(\lambda)^L} \prod_i^M \frac{a(\lambda_i - \lambda)}{b(\lambda_i - \lambda)} + e^{-\theta b(\lambda)^L} \prod_i^M \frac{a(\lambda - \lambda_i)}{b(\lambda - \lambda_i)} \quad (\text{A.62})$$

However, this is only true if the unwanted terms of  $\tilde{A}(\lambda)$  and  $\tilde{D}(\lambda)$  will indeed cancel. The constraints on the  $\lambda_i$  that make this happen determine the spectrum of the transfer matrix and are known as the Bethe Ansatz equations (BAEs).

Every term of the remaining  $2^M - 1$  terms will have the  $\tilde{A}$  operator exchange its spectral parameter with one of the  $\lambda_i$  in the  $\tilde{B}$  product. The sum of these unwanted terms takes the general form:

$$U_{\tilde{A}} = \sum_{i=1}^M \left( \prod_{j \neq i}^M \tilde{B}(\lambda_j) \right) \alpha_i \tilde{A}(\lambda_i) |0\rangle \quad (\text{A.63})$$

$$= \sum_{i=1}^M \alpha_i e^{\theta a(\lambda_i)^L} \left( \prod_{j \neq i}^M \tilde{B}(\lambda_j) \right) |0\rangle \quad (\text{A.64})$$

And for the  $\tilde{D}$ -operator:

$$U_{\tilde{D}} = \sum_{i=1}^M \left( \prod_{j \neq i}^M \tilde{B}(\lambda_j) \right) \delta_i \tilde{D}(\lambda_i) |0\rangle \quad (\text{A.65})$$

$$= \sum_{i=1}^M \delta_i e^{-\theta b(\lambda_i)L} \left( \prod_{j \neq i}^M \tilde{B}(\lambda_j) \right) |0\rangle \quad (\text{A.66})$$

The key now is to figure out what the coefficients  $\alpha_i$  and  $\delta_i$  are that capture the factor picked up by the total commutation, and all exchanges of the spectral parameter. A smart and simple trick can help us. Recall that one of the commutation relations told us that  $[B(\lambda), B(\mu)] = 0$ . We can thus rewrite the excited state as:

$$\prod_{j=1}^M \tilde{B}(\lambda_j) |0\rangle = \tilde{B}(\lambda_i) \prod_{j \neq i}^M \tilde{B}(\lambda_j) |0\rangle \quad (\text{A.67})$$

We now see that the total effect of ending up with an  $\tilde{A}(\lambda_i) |0\rangle$  term must be the same as when the spectral parameter exchange happens directly and only with  $\tilde{B}(\lambda_i)$ . We can thus write:

$$\alpha_i = -\frac{c(\lambda_i - \lambda)}{b(\lambda_i - \lambda)} \prod_{k \neq i}^M \frac{a(\lambda_k - \lambda_i)}{b(\lambda_k - \lambda_i)} \quad (\text{A.68})$$

$$\delta_i = -\frac{c(\lambda - \lambda_i)}{b(\lambda - \lambda_i)} \prod_{k \neq i}^M \frac{a(\lambda_i - \lambda_k)}{b(\lambda_i - \lambda_k)} \quad (\text{A.69})$$

Now we need to use some symmetry properties of our functions. As will be shown in the main text of this thesis, we will choose our weights such that  $\frac{c(\lambda - \lambda_i)}{b(\lambda - \lambda_i)} = -\frac{c(\lambda_i - \lambda)}{b(\lambda_i - \lambda)}$ , so that the demand that  $U_{\tilde{A}} + U_{\tilde{D}} = 0$  term-by-term amounts to:

$$\alpha_i e^{\theta} a(\lambda_i)^L = -\delta_i e^{-\theta} b(\lambda_i)^L \quad (\text{A.70})$$

$$\implies e^{2\theta} \left( \frac{a(\lambda_i)}{b(\lambda_i)} \right)^L = \prod_{k \neq i}^M \frac{a(\lambda_i - \lambda_k) b(\lambda_k - \lambda_i)}{b(\lambda_i - \lambda_k) a(\lambda_k - \lambda_i)} \quad (\text{A.71})$$

Where we have finally arrived at our twisted Bethe equations as the conditions that the transfer matrix has eigenvalues of the form (A.62).